FRACTALS and Applications

Maciej J. Ogorzałek
Department of Information Technologies
Faculty of Physics, Astronomy and Applied Computer Science
Jagiellonian University,
Kraków, Poland

PLVS RATIO QVAM VIS

- Remember the fine structures of the attractors?
- How can we measure the attracting limit set?

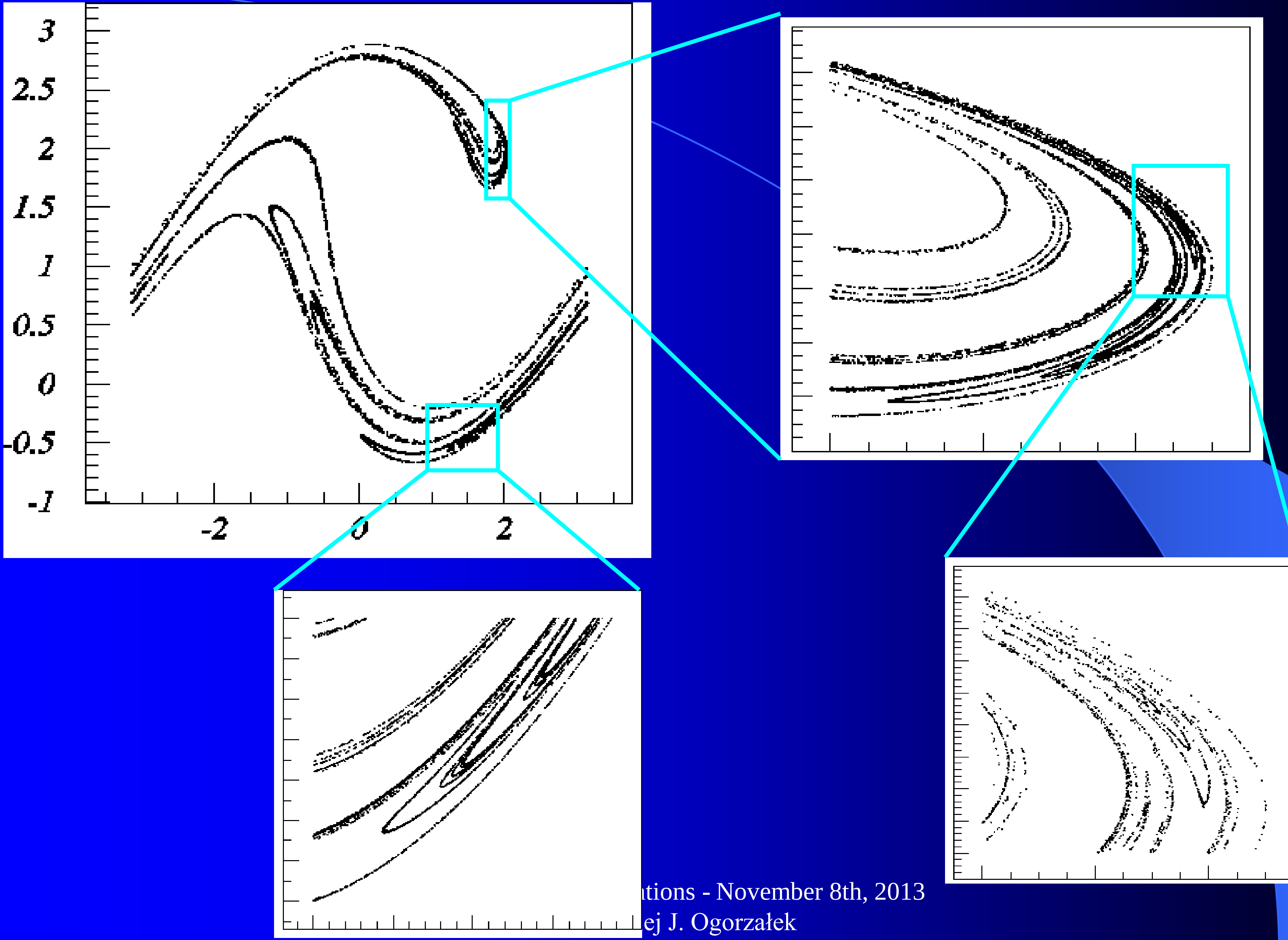
3
2.5
2
1.5
1
0.5
0
-0.5
-1
-2
0
2

Fractal – “broken, fragmented, irregular”

“I coined *fractal* from the Latin adjective *fractus*. The corresponding Latin verb *frangere* means "to break" to create irregular fragments. It is therefore sensible - and how appropriate for our need ! - that, in addition to "fragmented" (as in *fraction* or *refraction*), *fractus* should also mean "irregular", both meanings being preserved in *fragment*.”

B. Mandelbrot :

The fractal Geometry of Nature, 1982

Fractal geometry: the language of nature

- Euclid geometry: cold and dry
- Nature: complex, irregular, fragmented

"Clouds are not spheres, mountains are not cones, coastlines are not circles, and bark is not smooth, nor does lightning travel in a straight line."

Notion of length

- **Fractal geometry generalizes ordinary notions of length, scale, and dimension in interesting and subtle ways.**
  - For length, classical example is coastline length of a given country or border.
    - Result depends on fineness of *scale* used—as scale goes down, length goes up.
    - Ratio of scale to length gives rise to new notions of dimension.
  - Spirals provide another excellent example countering intuition about length.
    - *Example:* Smooth polygonal spiral can have finite or infinite length depending on method of construction.

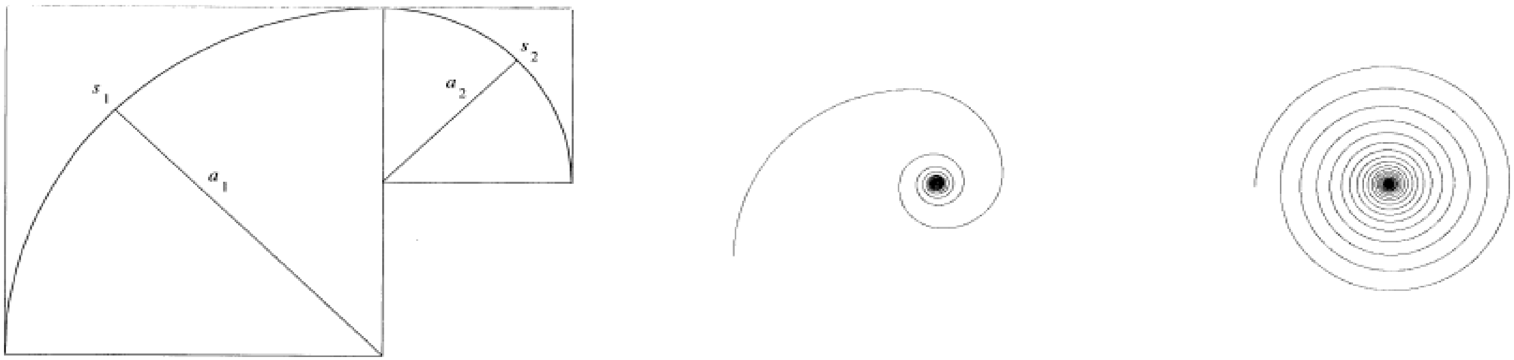

Construction Method — Infinite length ($a_k = 1/k$) — Finite length ($a_k = 0.95^{k-1}$)

Spiral 1 is infinitely long but Spiral 2 isn't.

- Quarter circles of progressively decreasing radius.
- $s_1 = \pi a_1/2$
- $s_2 = \pi a_2/2$

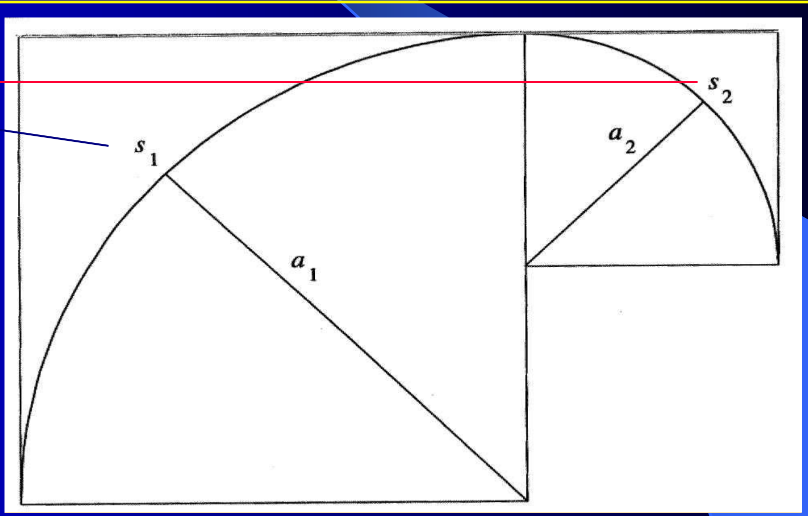

- Length = $$\frac{\pi}{2}\sum_{i=1}^{\infty} a_i$$

- If $a_i = 1, q, q^2, q^3, \ldots, q^{i-1}, \ldots$, then length is finite (right one, q=0.95).
- If $a_i = 1, 1/2, 1/3, 1/4, \ldots, 1/i, \ldots$, then length is infinite (left one).

Definition: Self-similarity

- A geometric shape that has the property of self-similarity, that is, each part of the shape is a smaller version of the whole shape.

Examples:

In nature – snow-flakes

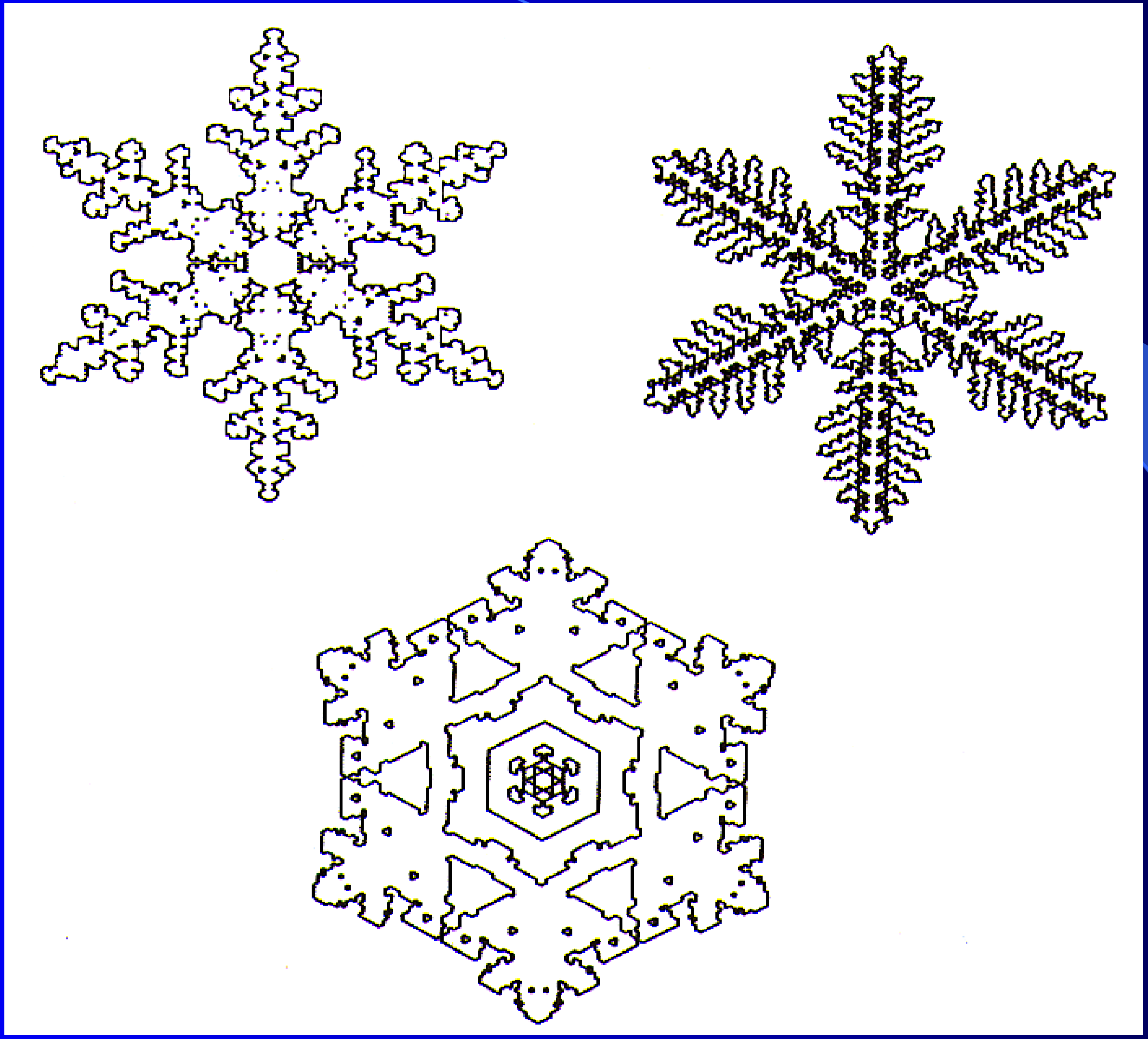

Another example: Cantor Set

- The oldest, simplest, most famous fractal

1 We begin with the closed interval [0,1].

2 Now we remove the open interval (1/3,2/3); leaving two closed intervals behind.

3 We repeat the procedure, removing the "open middle third" of each of these intervals

4 And continue infinitely.

- Fractal dimension:

  D = log 2 / log 3 = 0.63…

- Uncountable points, zero length

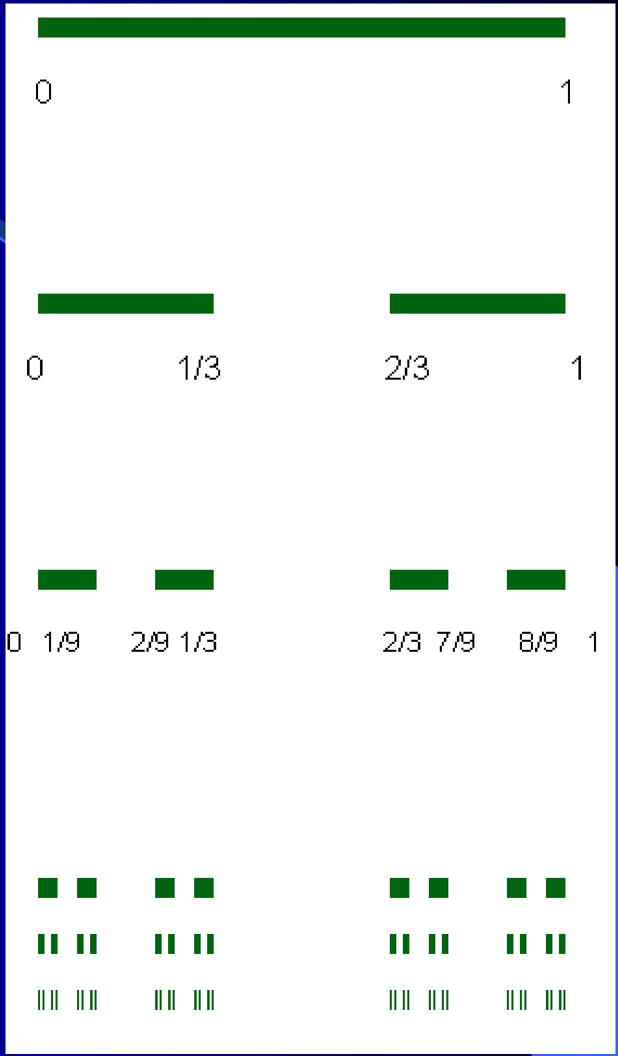

The Cantor set

- German mathematician Georg Cantor (1845-1918)
- The Cantor set— a perfect, nowhere dense subset
  - Start with a unit interval
  - Take away the open middle third
  - Take away the open middle third from each remaining segment
  - Repeat indefinitely

0 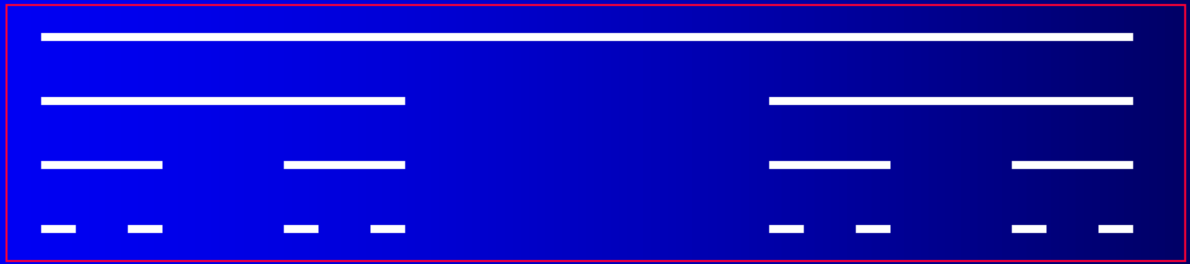 1

  - The final invariant set is the Cantor set.

- G. Cantor, *über unendliche, lineare Punktmannigfaltigkeiten V,* Mathematische Annalen 21 (1883) 545–591.

The Cantor set

- Triadic expansion
  - The Cantor set is the set of points in [0,1] for which there is a triadic expansion that does not contain the digit ‘1’.
  - e.g., 1/3 is 0.02222222…, 2/3 is 0.2, etc.
  - The triadic number 0.0200222000202022200022002 is in the Cantor set.
- Address
  - Let L denote the left middle third, and R denote the right middle third. We can represent every segment of the Cantor set by an address like LR, LL, LLR, etc.

- L R
- LL LR RL RR
- LLL LLR LRL LRR RLL RLR RRL RRR

Zero length but infinitely many points

- **Having as many points as the interval [0,1]**
- Every point in [0,1] can be represented as a binary number, e.g., 0[illegible]001110101.
- For each number in [0,1] in binary form, we replace symbolwise 1 by 2. E.g., 0.001 (binary) $\rightarrow$ 0.002 (triadic). Then,
  - Each point in [0,1] corresponds to a point in the Cantor set.
  - The Cantor set has as many points as the interval [0,1] has.

- **But zero length**
- The length of the Cantor set is $\lim_{n\to\infty}(2/3)^n = 0$.

Sierpinski Gasket

- Start with a solid triangle. Mark the midpoint of each side. Then, join them to partition 4 triangles.
- Remove the middle one.
- Repeat the process infinitely.
- The invariant set is the Sierpinski Gasket.

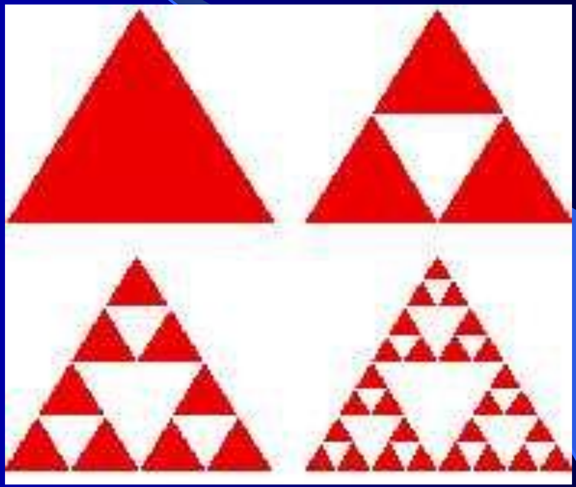

- AREA = 0
- Infinitely many points

Koch curve

- Helge von Koch (Sweden, 1904) introduced a curve which is infinitely long but can be drawn in finite area.

- CONSTRUCTION:
- Start with a unit interval.
- Replace middle third by two segments of equal length
- Repeat infinitely.

- Length=$\lim_{n\to\infty}(4/3)^n=\infty$

mathematical fractal: Koch Snowflake

- Step One.
  Start with a large equilateral triangle.
- Step Two.
  Make a Star.

1. Divide one side of the triangle into three parts and remove the middle section.
2. Replace it with two lines the same length as the section you removed.
3. Do this to all three sides of the triangle.

- Repeat this process infinitely.

- The snowflake has a finite area bounded by a perimeter of infinite length!

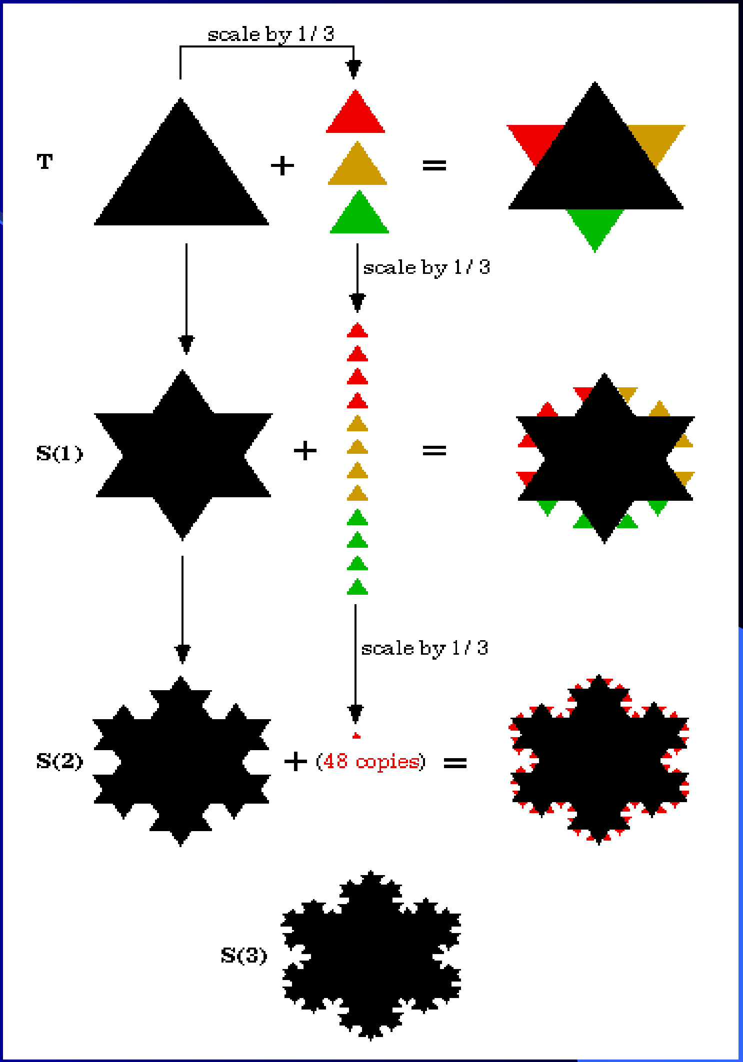

Constructing fractals by iterative reduction and translation

- The Koch curve can be constructed mathematically by an iterative process applied to any arbitrary object *X*.
- Define four transformations
- $w_0(X)$: scale 1/3, rotate 0, translate (+0,+0)
- $w_1(X)$: scale 1/3, rotate +60°, translate (+1/3,+0)
- $w_2(X)$: scale 1/3, rotate –60°, translate (+1/2,+$\sqrt{3}/6$)
- $w_3(X)$: scale 1/3, rotate 0, translate (+2/3,+0)

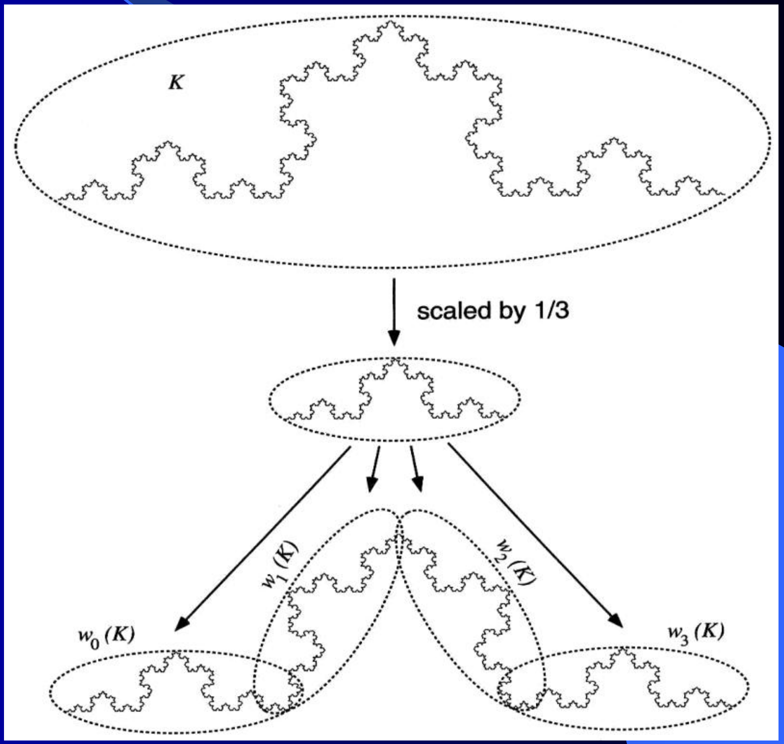

- Define the transformation
  - $W(X) = w_0(X) \cup w_1(X) \cup w_2(X) \cup w_3(X)$.

Defining the Koch curve

- We have an iterative function
  - $X_{n+1} = W(X_n)$
- The Koch curve is the invariant set, *K*, satisfying
  - $W(K) = K$
- i.e., the solution *K* of this equation is the Koch curve.

- So, it doesn't matter what the initial object is! Clearly what we have achieved a simple coding method that encodes a complex Koch curve into some transformation parameters.
- *APPLICATIONS: Image coding.*

Self-similarity revisited

Self-similarity in the Koch curve

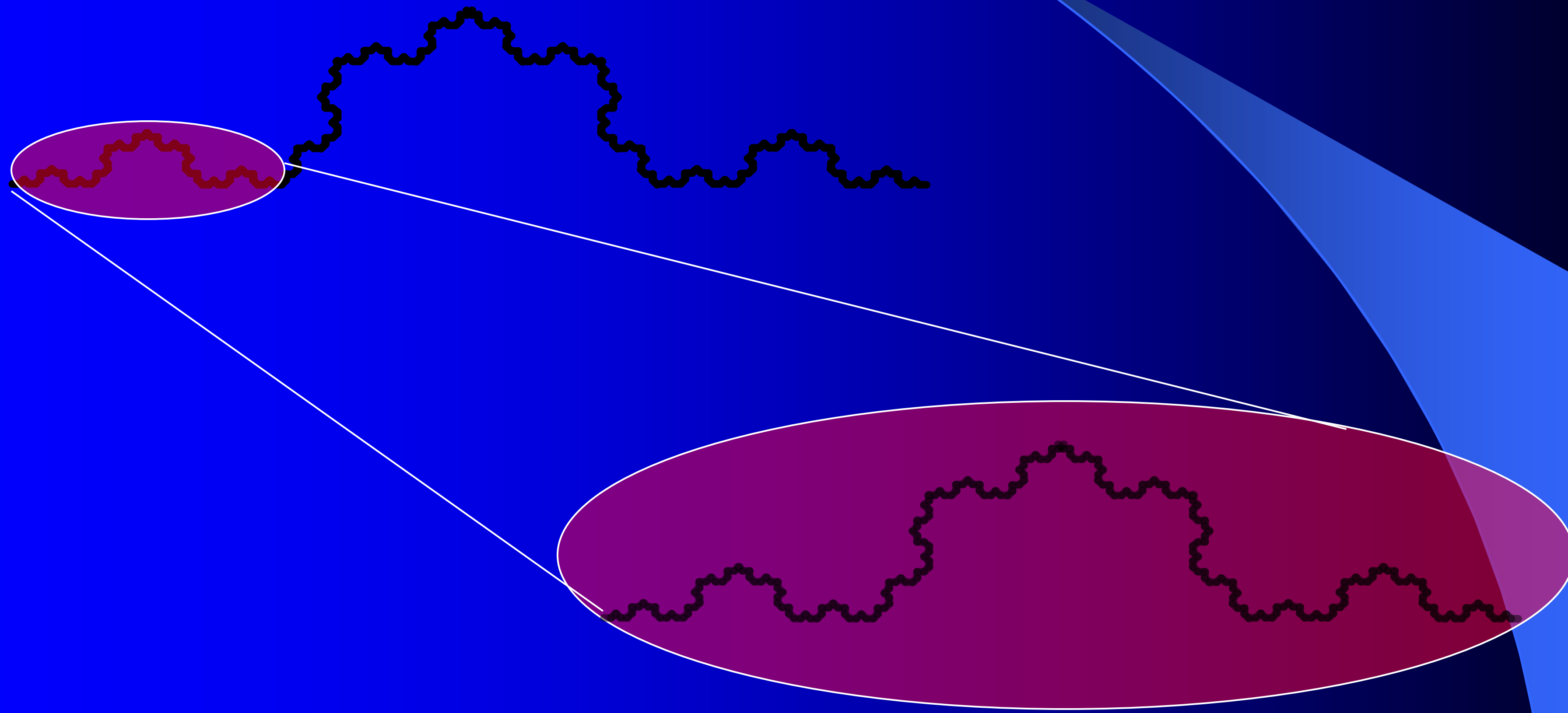

Sierpinski Gasket re-defined

- We may define another W(X) for the Sierpinski Gasket.
- Define three transformations
- $w_0(X)$: scale 1/3, translate (+0,+0)
- $w_1(X)$: scale 1/3, translate (+1/2,+0)
- $w_2(X)$: scale 1/3, translate (+1/4,+$\sqrt{3}/4$)
- Define W(X) as
- $W(X) = w_0(X) \cup w_1(X) \cup w_2(X)$.
- The Sierpinski Gasket is the solution o $W(X)=X$.
- In practice it is the object that remains after many iterations under W(X).

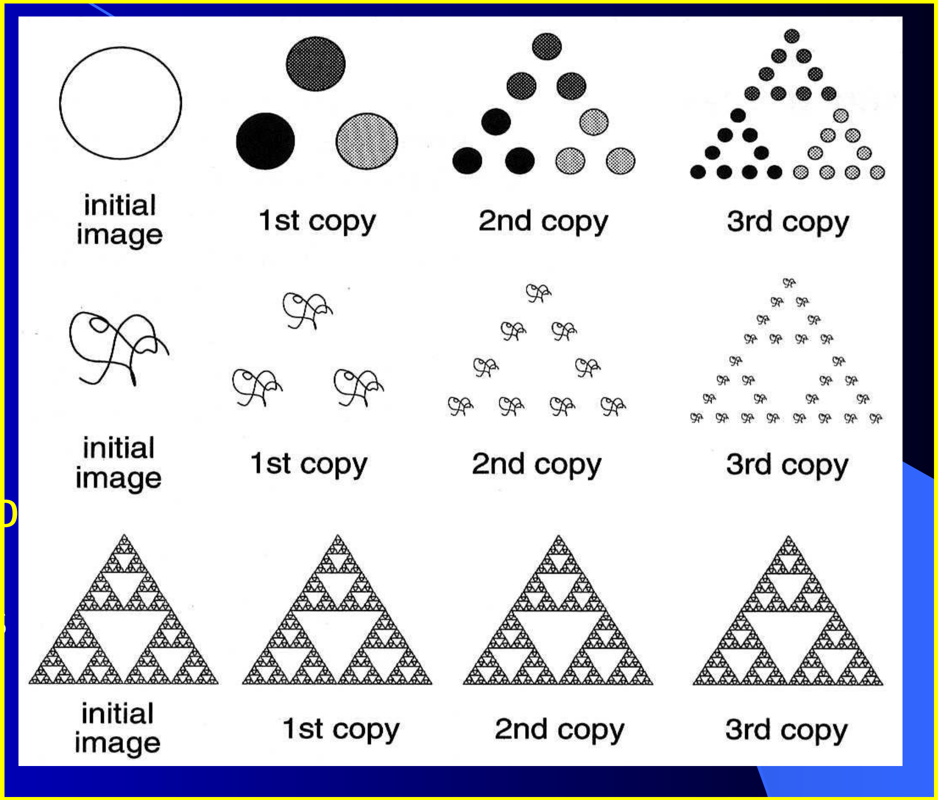

The problem of measuring fractals

- Benoit Mandelbrot, "How long is the coast of Britain?" *Science* 155 (1967), 636-638.
- *Border of Spain and Portugal:*
  - *A Spanish encyclopedia says 616 miles.*
  - *A Portugese encyclopedia says 758 miles.*
- *Coast of Britain:*
  - *Various sources claim it between 4500 and 5000 miles!*

Problem of measuring fractal objects

Euclid dimension

- In Euclid geometry, dimensions of objects are defined by integer numbers.
- 0 - A point
- 1 - A curve or line
- 2 - Triangles, circles or surfaces
- 3 - Spheres, cubes and other solids

- For a square we have N^2 self-similar pieces for the magnification factor of N

dimension=log(number of self-similar pieces) /log(magnification factor)

=log(N^2)/logN=2

For a cube we have N^3 self-similar pieces

dimension=log(number of self-similar pieces) /log(magnification factor)

=log(N^3)/logN=3

Sierpinski triangle consists of three self-similar pieces with magnification factor 2 each

dimension=log3/log2=1.58

Dimension of a two dimensional sqaure

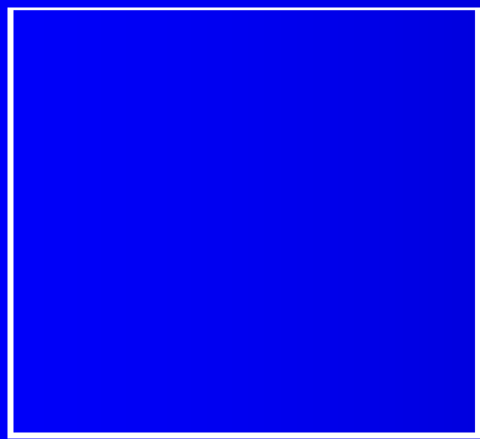

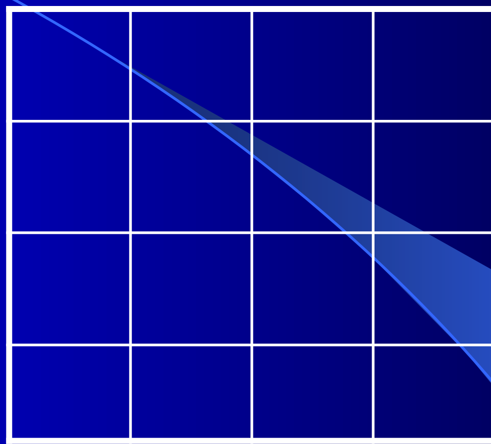

Fractal dimension

- Fractal dimension can be non-integers
- Intuitively, we can represent the fractal dimension as a measure of how much space the fractal occupies.

- Given a curve, we can transform it into 'n' parts (n actually represents the number of segments), and the whole being 's' times the length of each of the parts. The fractal dimension is then :

$$d = \log n / \log s$$

Scaling/dimension of the von Koch curve

- Scale by 3 – need four self-similar pieces
- D=log4/log3=1.26

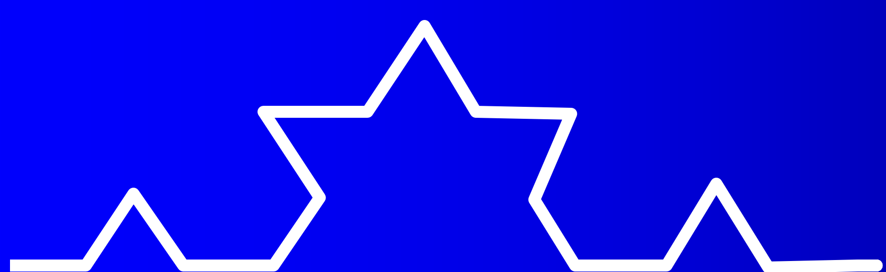

Length of the coastline of Britain

$$D = \frac{\ln(L_1)/\ln(L_2)}{\ln(S_1)/\ln(S_2)}$$

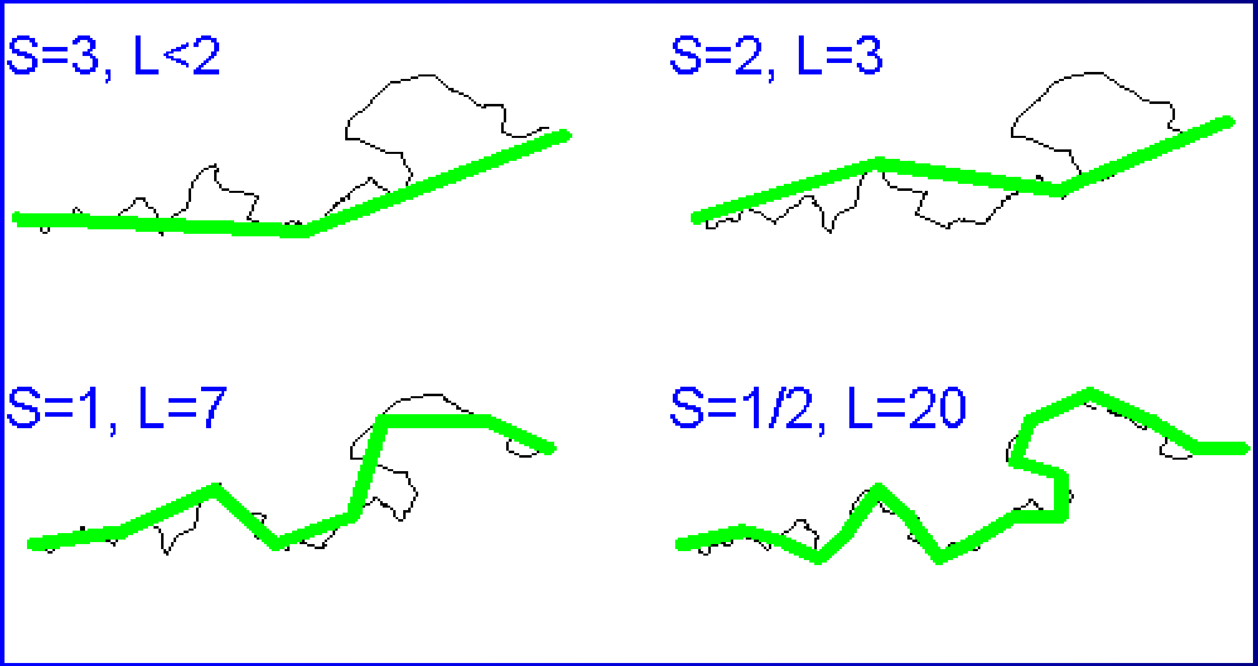

Real world fractals

A cloud, a mountain, a flower, a tree or a coastline…

The coastline of Britain

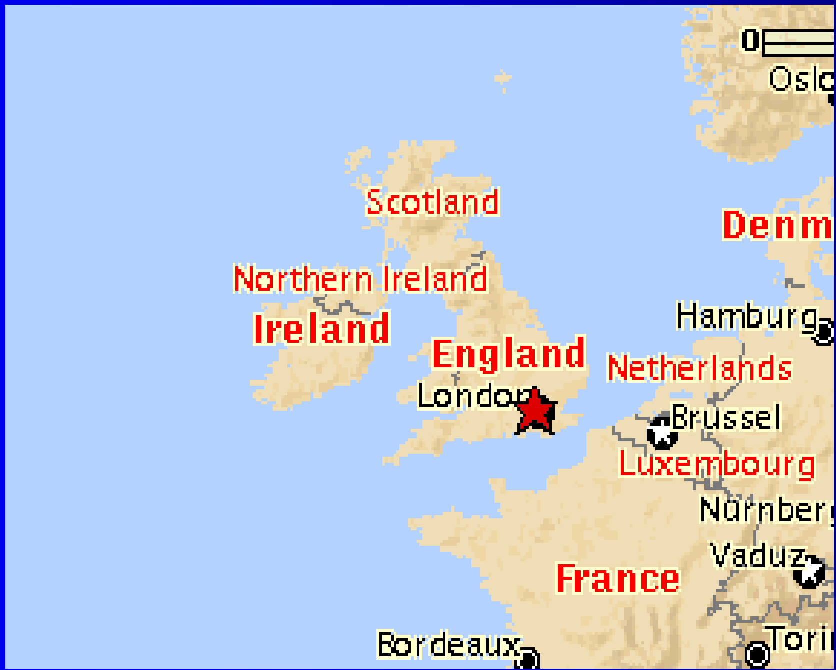

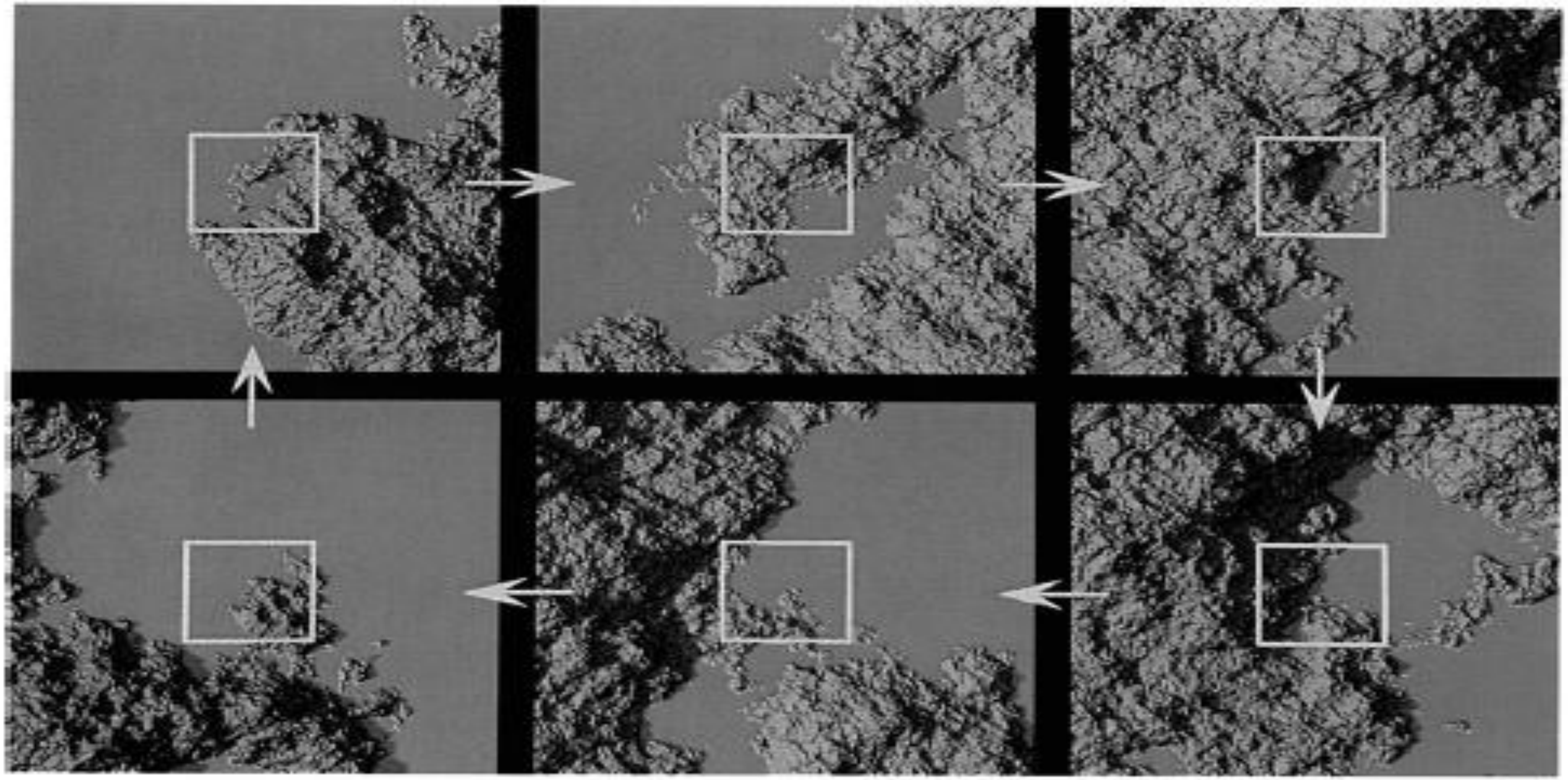

Fractal Coastline (6 magnifications)

Practical measurements

- There is no formula for coastlines, or defined construction process.
- The shape is the result of millions of years of tectonic activities and never stopping erosions, sedimentations, etc.
- In practice we measure on a geographical map.
- Measurement procedure:
  - Take a compass, set at a distance *s* (in true units).
  - Walk the compass along the coastline.
  - Count the number of steps *N*.
  - Note the scale of the map. For example, if the map is 1:1,000,000, then a compass step of 1cm corresponds to 10km. So, *s*=10km.
  - The coast length ≈ *sN.*

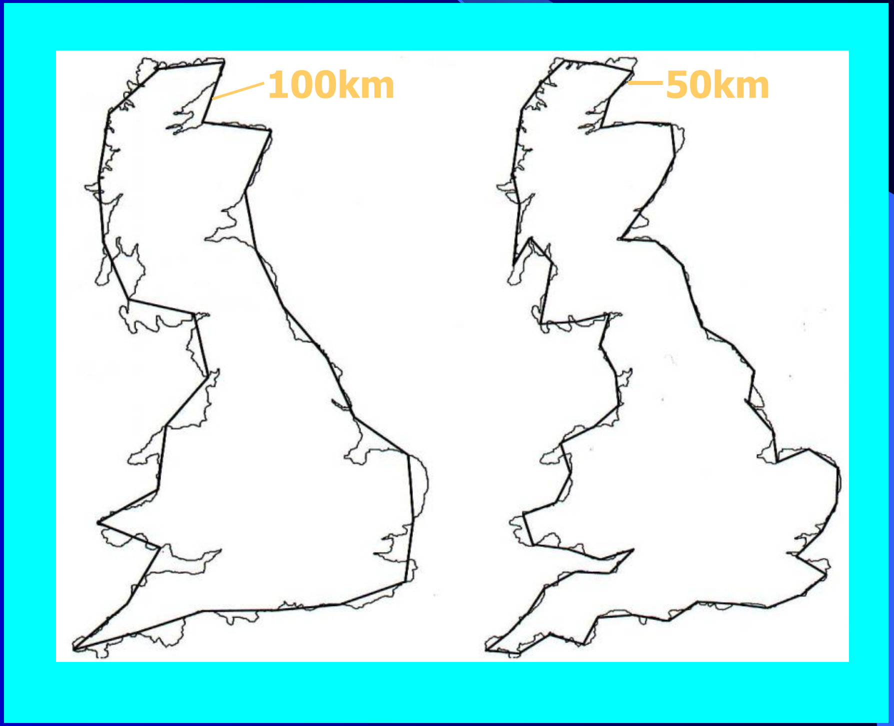

The Hong Kong coast

- Apply the procedure with different s.
- Results:
  - **The measured length increases with decreasing *s*.**

Compass step *s*	Length *u*
2km	43.262km
1km	52.702km
0.5km	60.598km
0.1km	69.162km
0.02km	87.98km

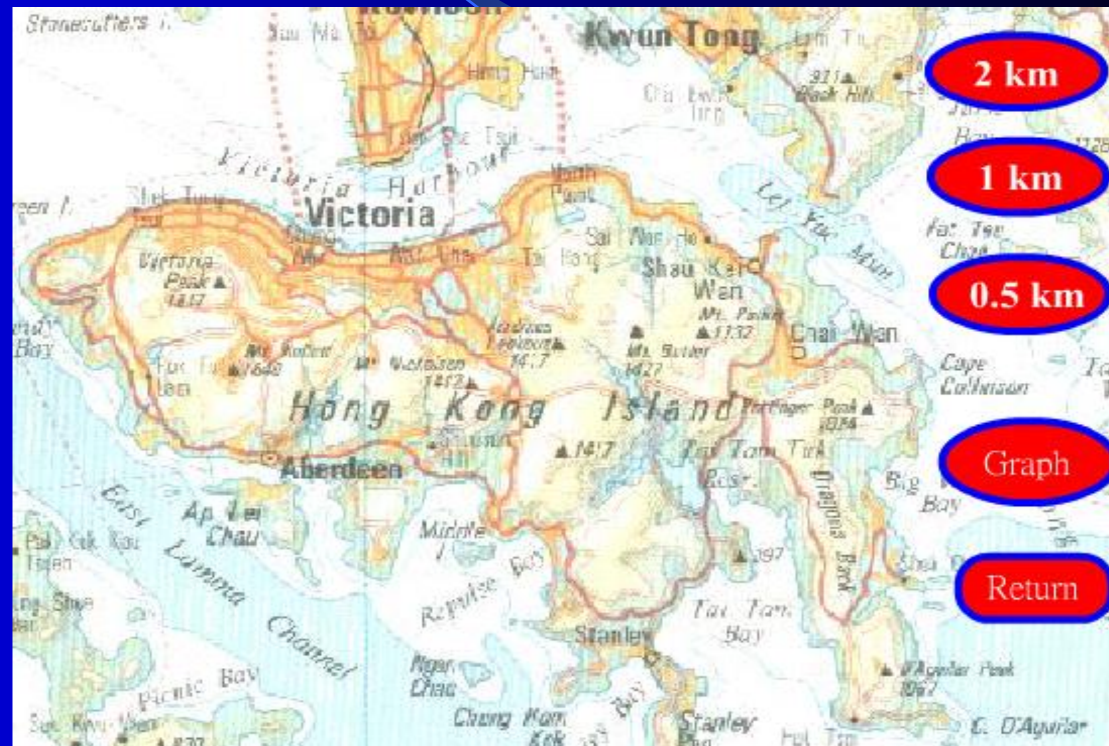

Power law of measurement

- If we plot log(u) versus log($1/s$), we can see that
  - $\log(u) = d \log(1/s) + k$

  which is equivalent to
  - $u = c\,(1/s)^d$
- The slope is d.
- For the Hong Kong coast,
  $d \approx 0.14$.
- For a circle, d=0.
- **We expect the length *u* continues to increase as we decrease *s*.**

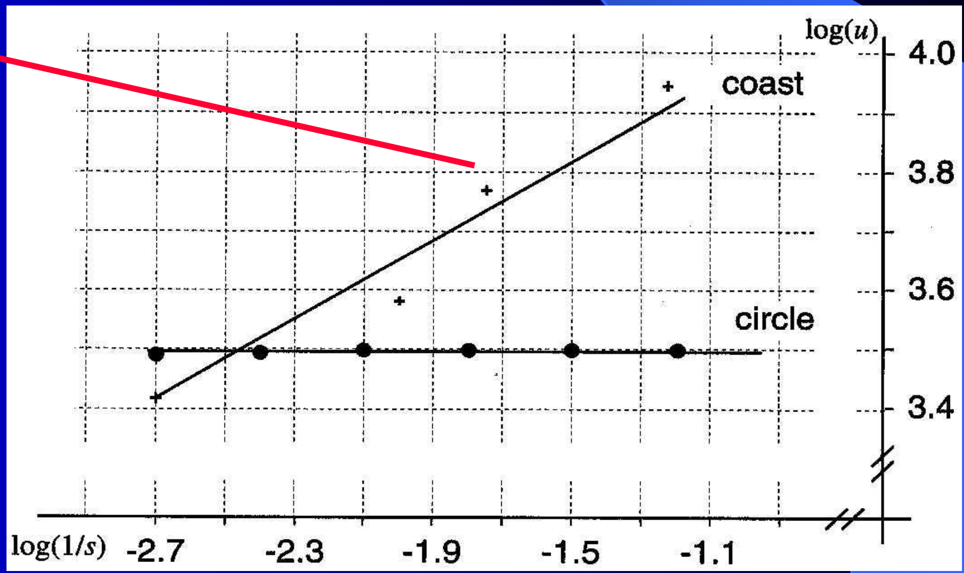

Length of the Koch curve

Earlier on, we found the length of the Koch curve to be infinity.
Can we measure it in a similar way as we did for the British coast?

If s=1, u=1.
If s=1/3, u=4.
If s=1/9, u=16, etc.

So, $u \to \infty$ as $s \to 0$.

Clearly, we have

$$\log u = d \log(1/s) + k$$

Here, d = 0.2619

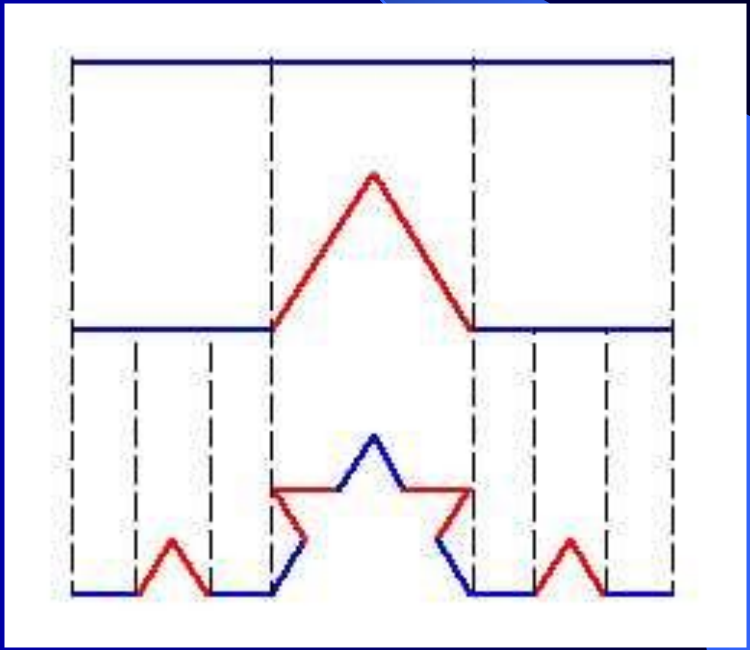

So, how long is it? —An ill-posed question!

- We may say that the coastline and the Koch curve (and all fractals) *have practically no length!*
- It depends on the size of the measuring instrument.
- What is meaningful is the value of *d, which measures the level of convolution of the curve.* So, the Hong Kong coast can be less convoluted than the Koch curve.

- Many biological structures are organized in a fractal way to fit an infinite length within finite area or volume.
  - Blood capillaries
  - Kidney vessels
  - --> SPACE-FILLING FRACTALS

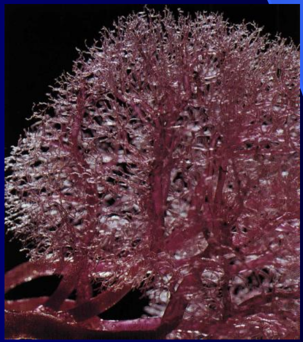

Dimension

- The question of “how long” can be ill-posed, as we have seen.
- Similarly, measurement of areas and volumes could be meaningless.
- What seems to be relevant is the *d* in the power law.
- This *d* is related to the concept of DIMENSION.

  – Self-similarity dimension
  – Compass dimension
  – Box-counting dimension

FRACTAL DIMENSION

Self-similarity

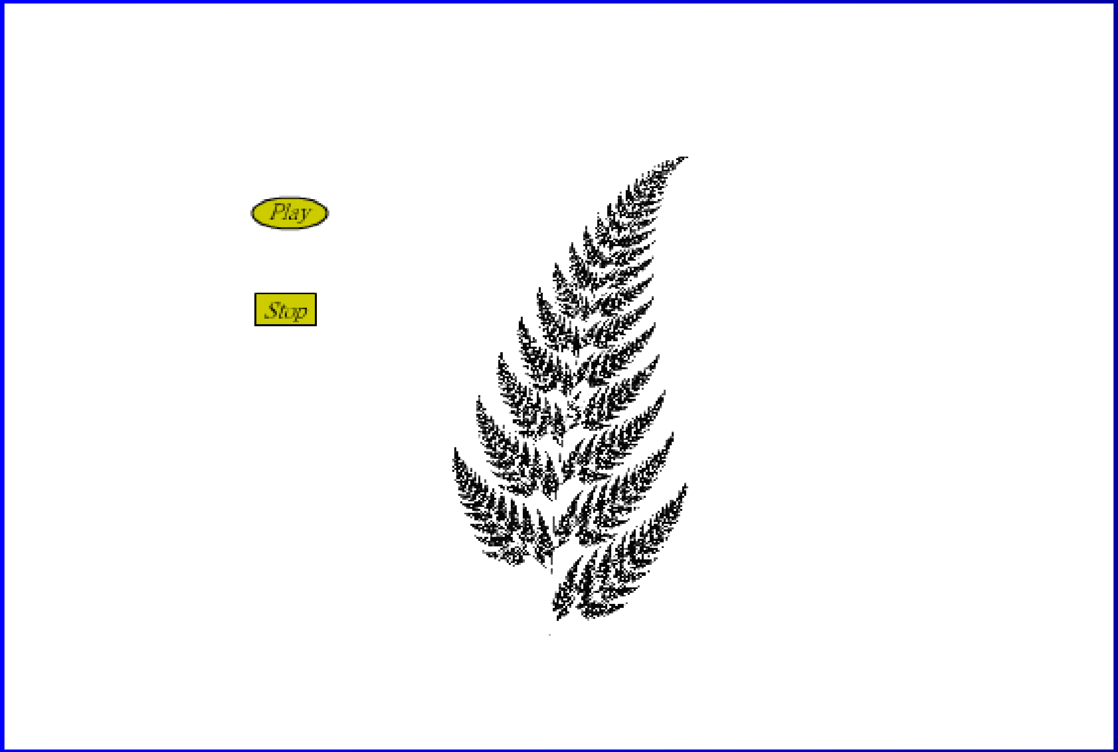

Self-similarity dimension

- **Fractals are self-similar. Assume that a fractal object is *n* copies of itself scaled down by a factor of *s*.**
- **So, we can define a power law as**

$$\boxed{– \; n = (1/s)^D}$$

- **<u>Examples:</u>**
- The Koch curve copies itself 4 times with scaling factor of 3. (n=4, s=3, and <u>D = 1.2619</u>)
- A line copies itself N times with scaling factor N, where N can be any integer. (n=s=N and <u>D=1</u>)
- A square copies itself N^2 times with scaling factor N, where N can be any integer. (n= N^2, s=N and <u>D=2</u>)
- ***D* = self-similarity dimension**

More examples

- Sierpinski Gasket:
  - s = 2 (scaling)
  - n = 3 (copy number)
  - Hence, $D = \log(n)/\log(1/s)$ = **1.585**

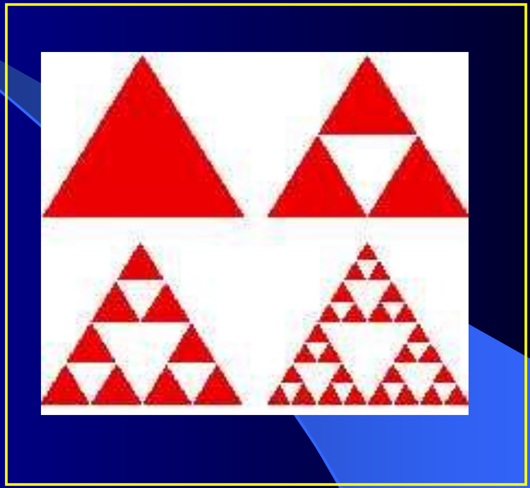

- Cantor set:
  - s = 3 (scaling)
  - n = 2 (copy number)
  - Hence, $D = \log(n)/\log(1/s)$ = **0.6309**

Relation between *D* and *d*

- **Two power laws:**
  - Number of self copies $n = (1/s)^D$ or $\log(n) = D \log(1/s)$
  - Total length $u = (1/s)^d$ or $\log(u) = d \log(1/s)$
- When measuring u, we simply use
  - $u = n \times s$ *or* $\log(u) = \log(n) + \log(s)$
- Thus, we have $d \log(1/s) = D \log(1/s) + \log(s)$
  - **i.e., $D = 1 + d$**
  - **The HK coast has a fractal dimension of 1+0.14=1.14**
  - **We may define 1+d as the COMPASS dimension.**

Compass dimension

- Start with a length (or area, etc) measurement.
- Find d in the power law $u = (1/s)^d$.
- Then, the dimension found by adding 1 to d is the ***compass dimension*** — another way to find fractal dimension.

- Just a different way of computation
  - For mathematical fractals like the Cantor set and Koch curve, the self-similarity dimension and the compass dimension are identical.
  - For natural fractals like coastlines, no self-similarity dimension can be found. So, compass dimension becomes useful.

Are organisms fractal?

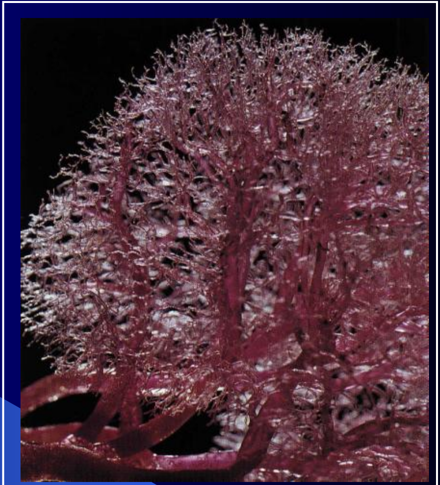

child lung

- M. Sernetz *et al.* (1985 paper in J. Theoretical Biology)
- Contrary to common belief, metabolic rate is not proportional to body weight. Instead, it fits in a power law relationship.

- $m = cw^{\alpha}$

Metabolic rate
Slope $\alpha \approx 0.75$

Body weight

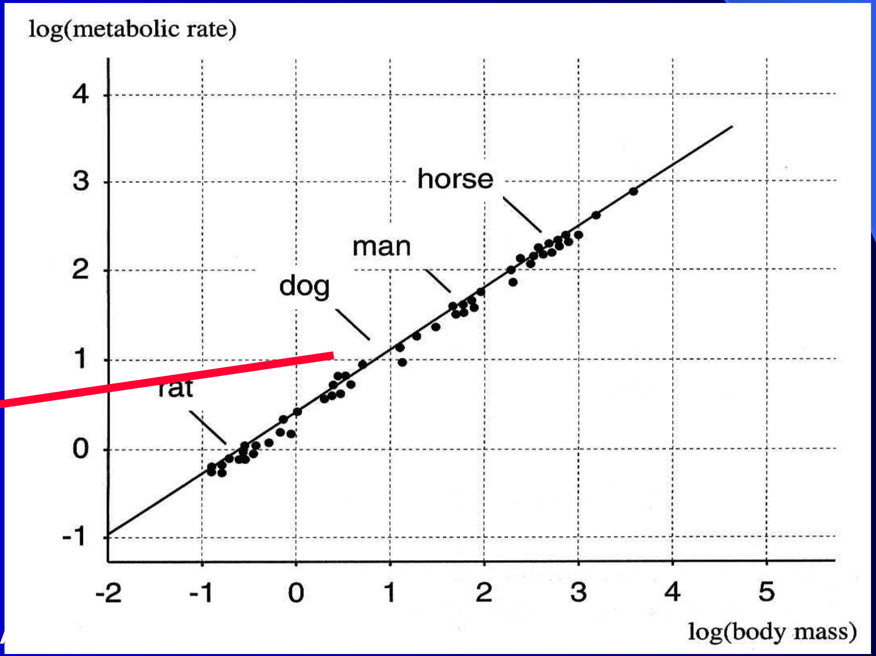

Dimension of organisms

- We can deduce the fractal dimension from $\alpha \approx 0.75$.
- Suppose r is the scaling factor (like *s*). Since weight is r^3, the power law can be modified to $m = cr^{3\alpha}$.
- Thus, $D = 3\alpha \approx 2.25$.
- **The body is not a solid volume, it is rather a fractal (highly convoluted surface) of dimension 2.25!**
  - **Would the dimension change when an organ malfunctions?**
  - **Is the dimension different for different animals?**

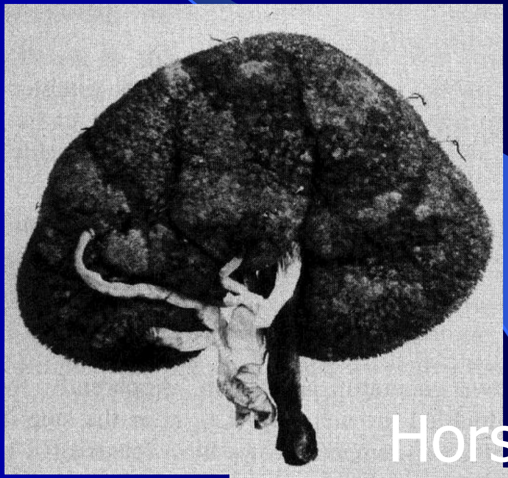

Horse kidney

Fractal Geometry of the Heart and Circulatory Structures

- **the main areas where fractal geometry can be seen in the circulatory system are:**
- Arteries and veins - Their cells and organization display the properties of fractals, such as the power-law distribution in the diameter distribution of arteries and veins.
- Organization of heart muscle groups - Show properties of self-similarity, fine structure, etc. Branching of certain muscles inside the heart
- - resemble the bifurcations seen in fractals such as the Feigenbaum plot
- His-Purkinje network - The branches and bifurcation of this electrical system are essential to human biology and resilience.
- The tendons that connect the tricuspid valve to the papillary muscles. - These again show bifurcation along with other fractal properties.
- The aortic valve leaflets - These are layered providing a huge surface area, while keeping a small volume

How does the fractal structure help?

-The fractal structure of the veins, arteries, and heart muscles help protect the circulatory system from the strong, violent pumping of the human heart.

-The fractal structure, which is usually unnecessary, can come into play when the His-Purkinje network is damaged. This helps the heart be resilient and resistant to damage.

- The fractal geometry of the heart could possibly save us everyday.

Cantor square

- Fractal dimension: d = log 4 / log 3 = 1.26

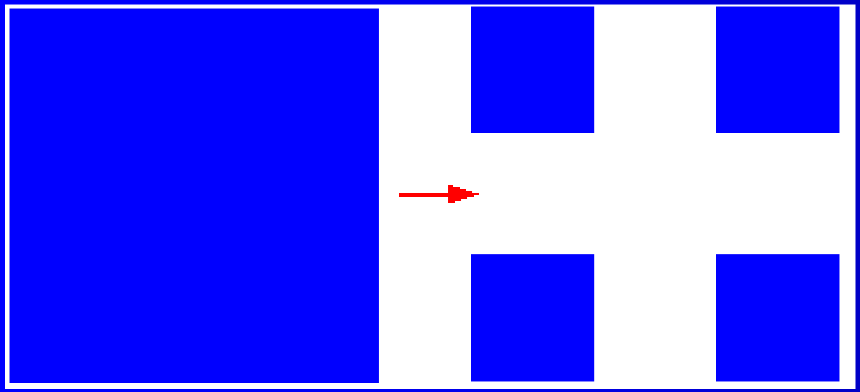

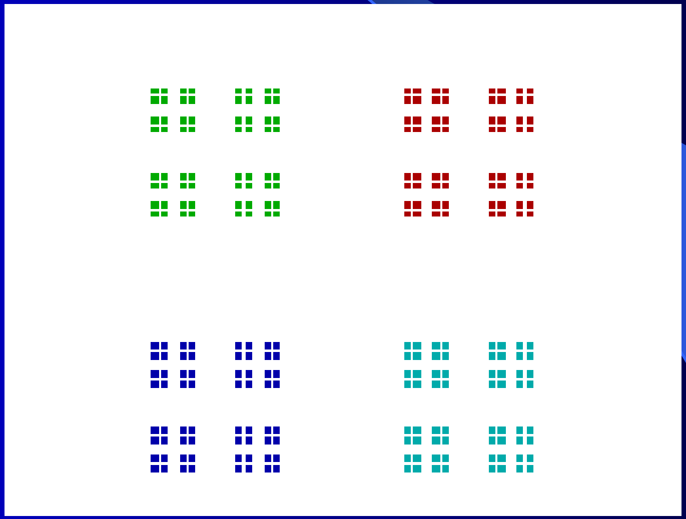

Sierpiński Fractals

- Named for Polish mathematician Waclaw Sierpinski

- Involve basic geometric polygons

Sierpinski Chaos Game

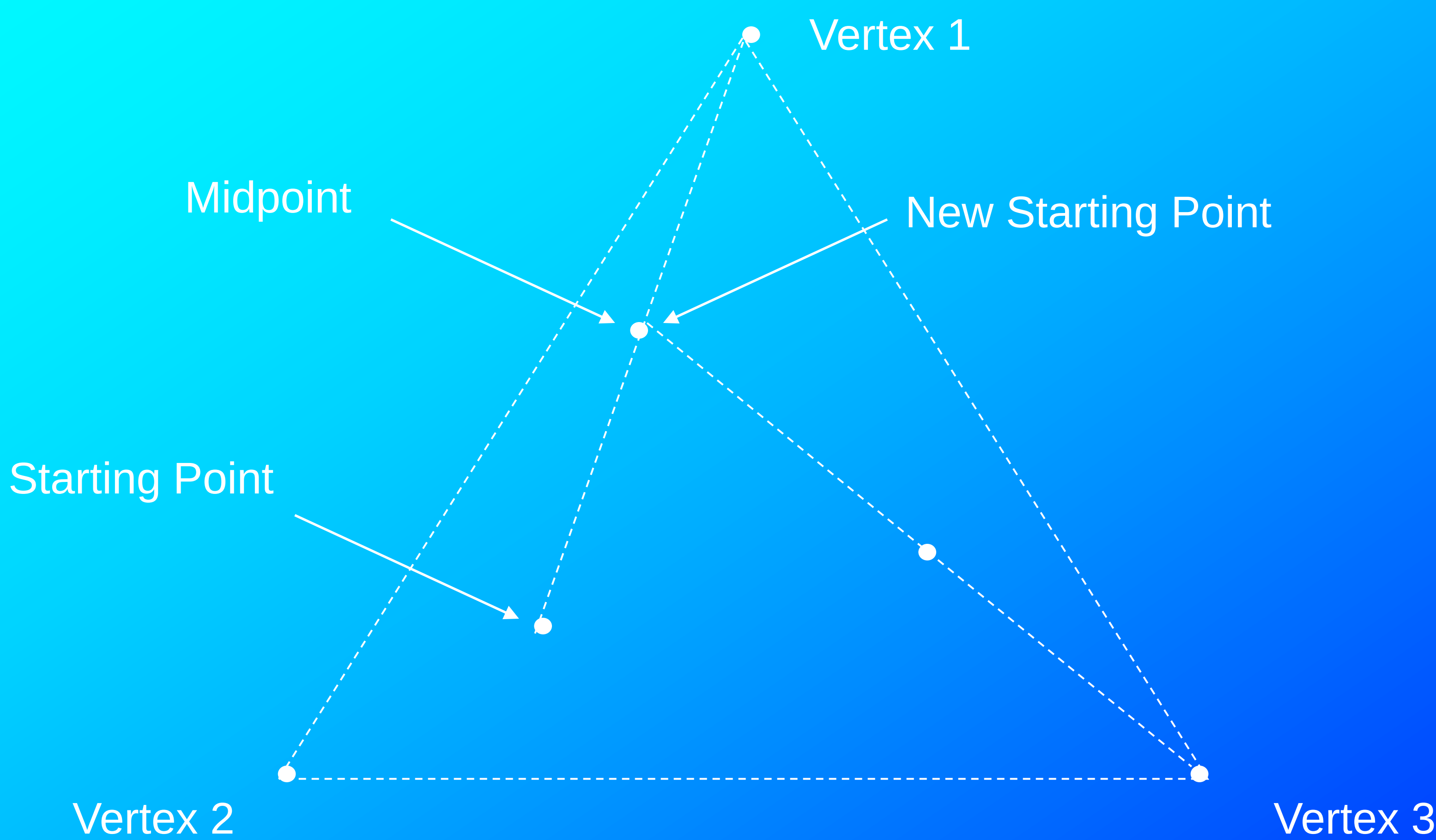

Sierpinski Chaos Game

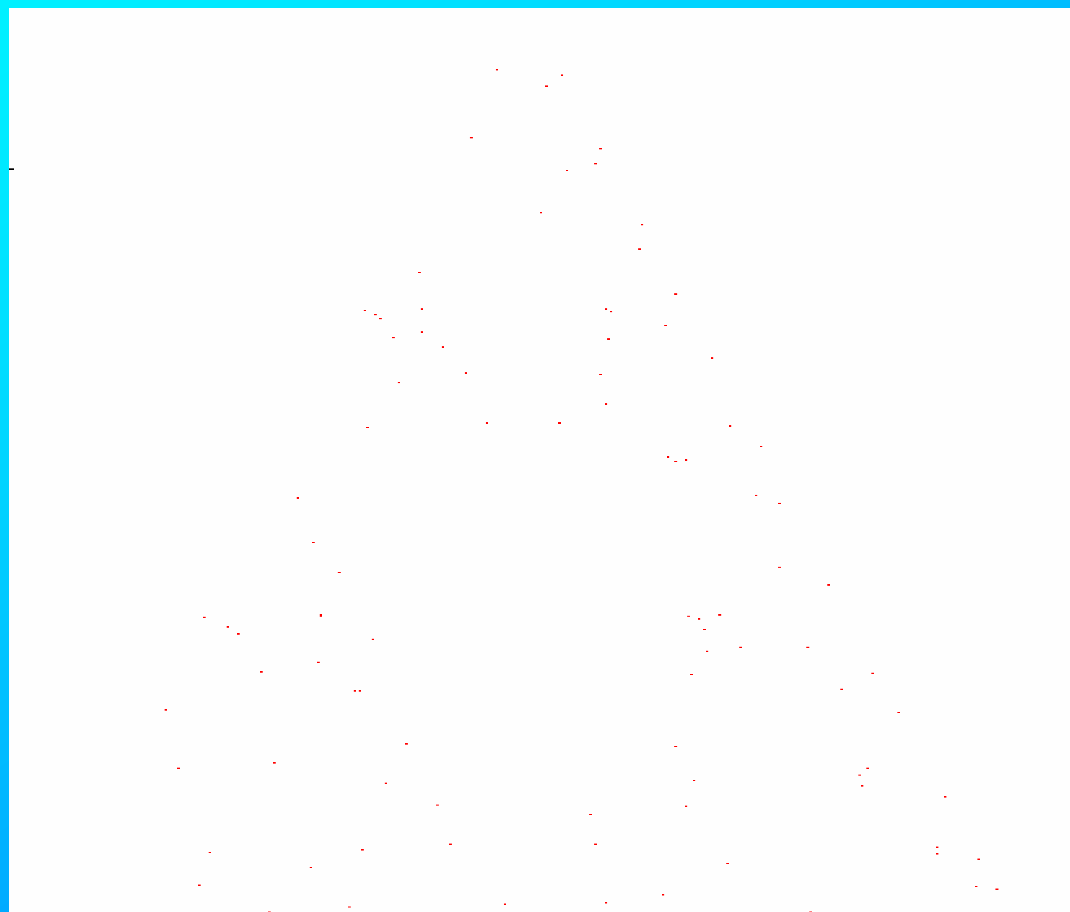

100 pts

Sierpinski Chaos Game

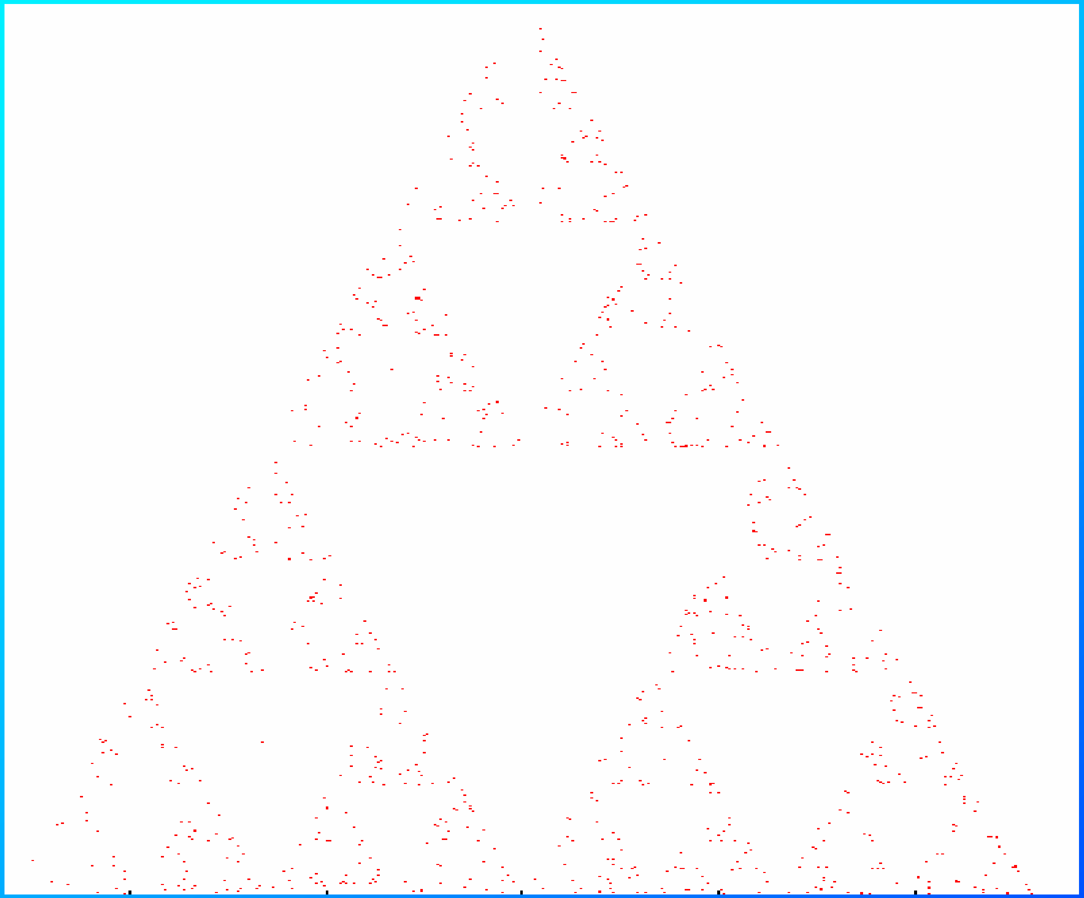

1000 pts

Sierpinski Chaos Game

Fractal dimension = 1.8175…

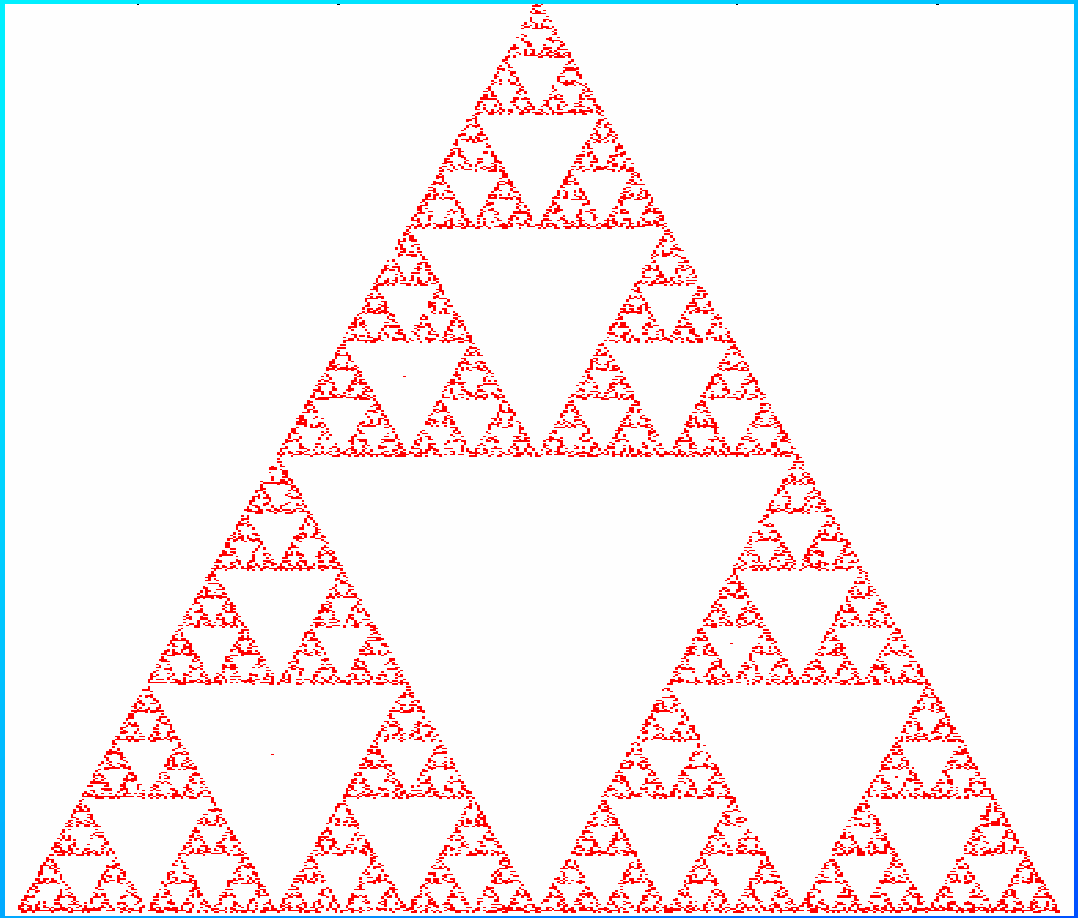

- 20000 pts

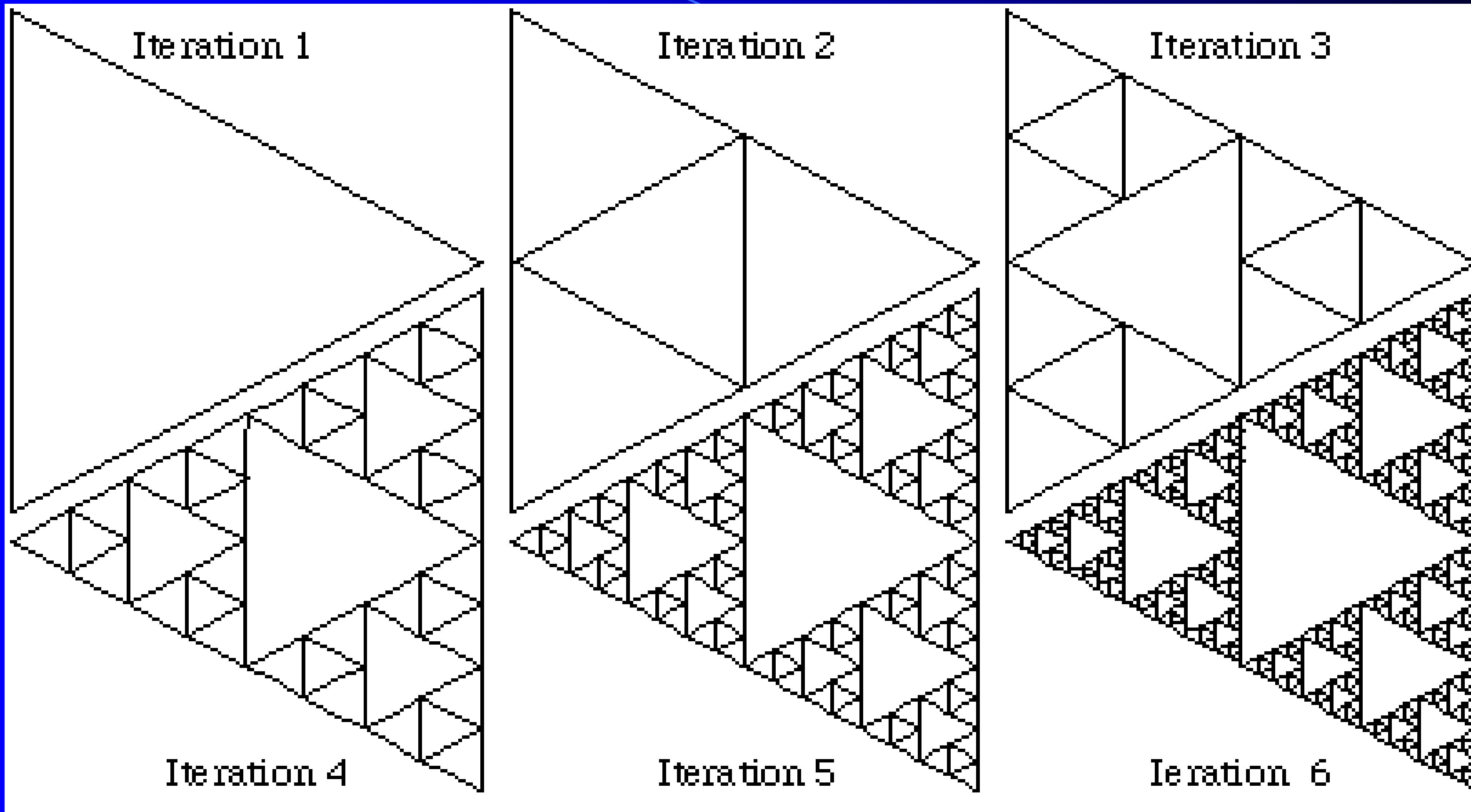
Iteration 1
Iteration 2
Iteration 3
Iteration 4
Iteration 5
Ieration 6

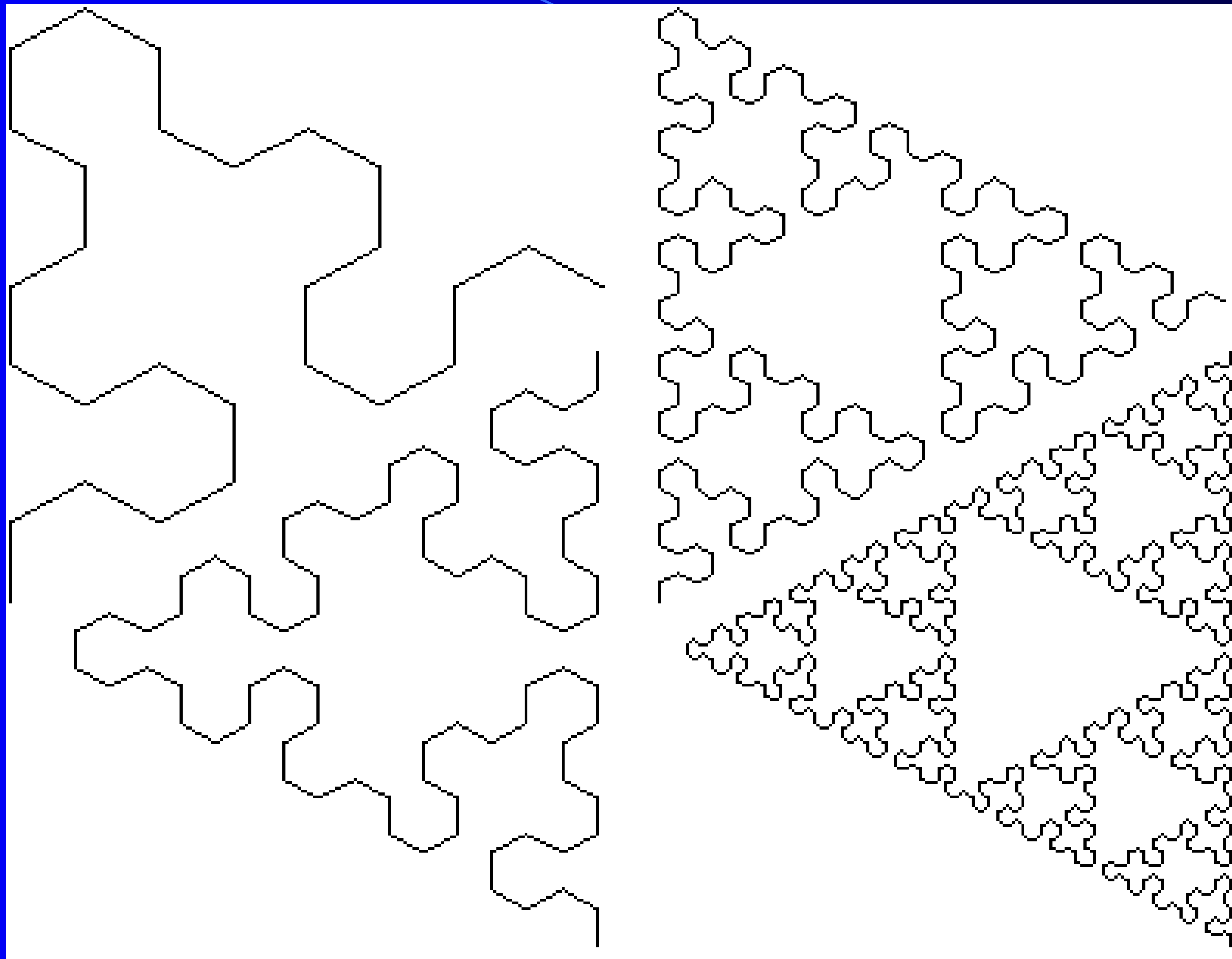

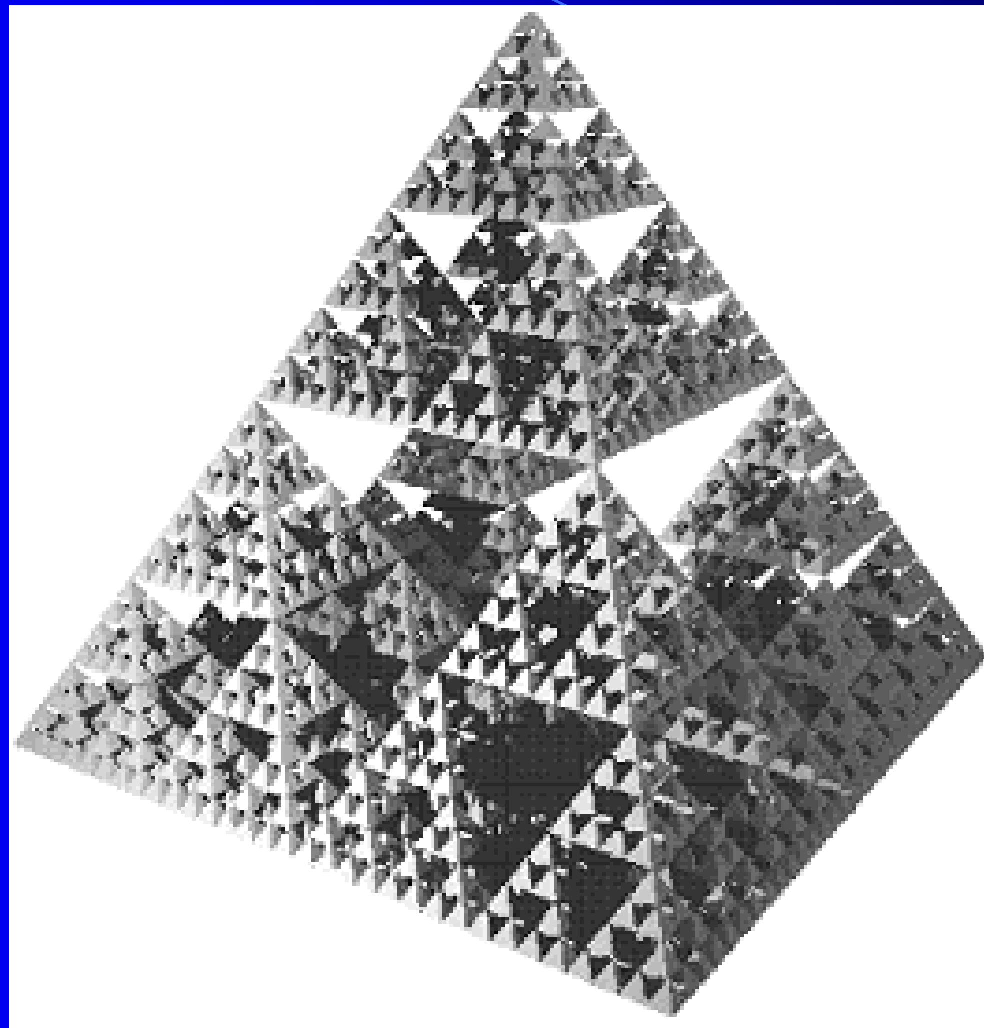

Menger's sponge

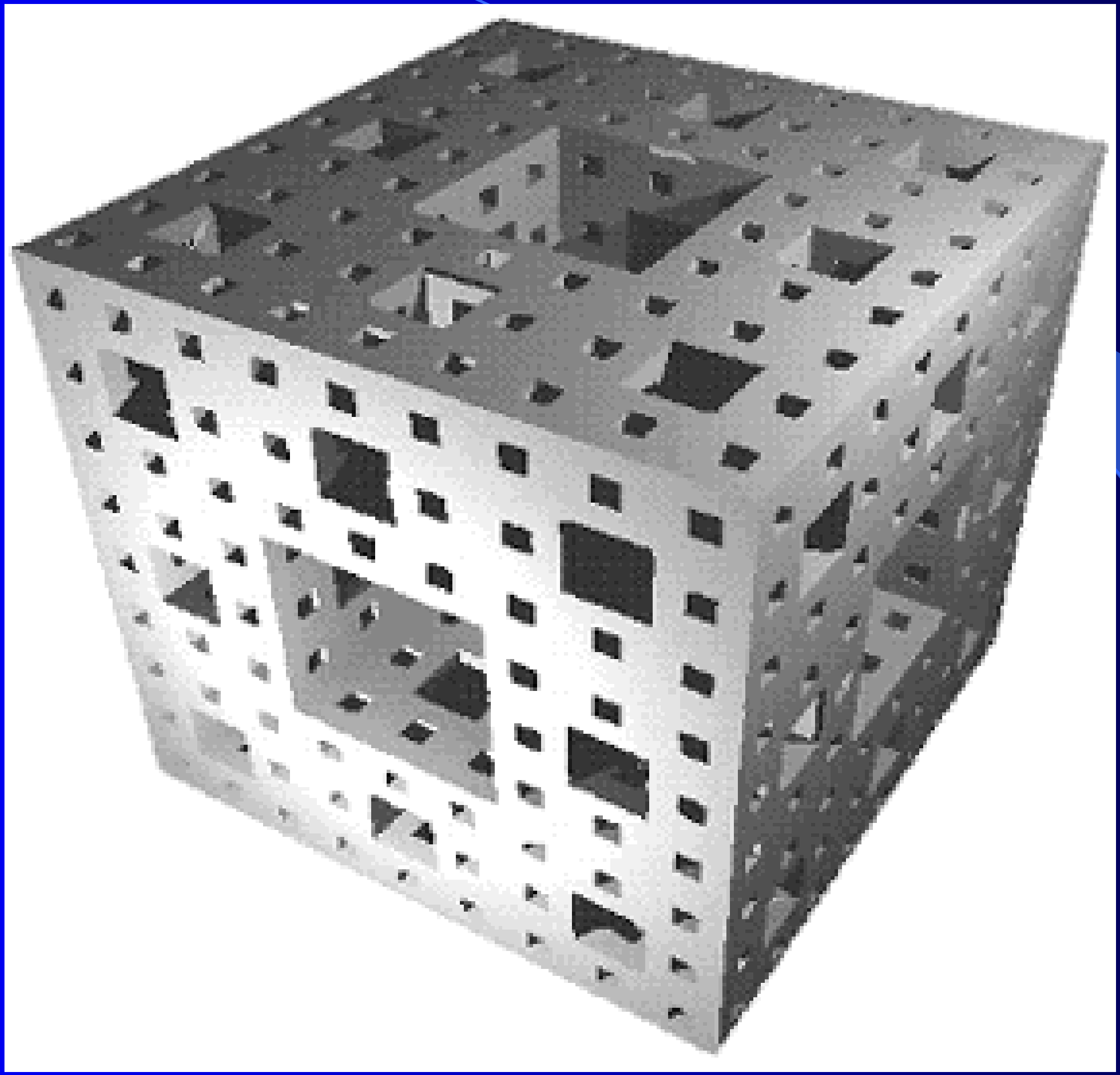

IFS (Iterated Function Systems)

$$\begin{bmatrix} x \\ y \end{bmatrix} \rightarrow \begin{bmatrix} r\cos(\theta) & -s\sin(\varphi) \\ r\sin(\theta) & s\cos(\varphi) \end{bmatrix} \begin{bmatrix} x \\ y \end{bmatrix} + \begin{bmatrix} e \\ f \end{bmatrix}$$

Here, (x,y) is a point on the image,

(r,s) tells you how to scale and reflect the image at the various points,

(theta,phi) tells you how to rotate,

(e,f) tells you how to translate the image.

Various Fractal Images are produced by differences in these values,

or by several different groups of values.

IFS (continued)

Remember that matrix from the previous slide? Lets rewrite it as a system of two equations :

x` = rcos(theta)x – ssin(phi)y + e
y` = rsin(theta)x + scos(phi)y + f

(x,y) being the pair we are transforming, and (x`,y`) being the point in the plane where the old (x,y) will be transformed to.

EVERY Transformation follow this pattern. So for file transmission, all we need to include would be the constants from above : r,s,theta,phi,e,f, x,y
This greatly simplifies the Task parsing.

On return you would only need to include the (x,y)->(x`,y`)

Julia set

- Defined as boundary between bounded and unbounded sequences in complex plane for the nonlinear maps $z^n + c$ ($z, c \in \mathbf{C}$, n usually 2).
- Sets are either totally connected or disconnected (latter called *dust*).
- Manifest themselves in such contexts as familiar *Newton-Raphson* algorithm for complex case — e.g. $z^3 - 1 = 0$:

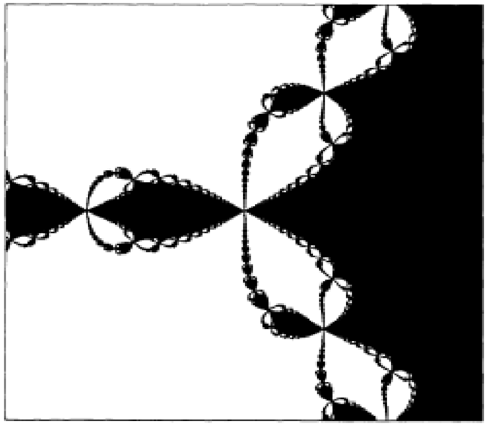

Basin of attraction for $z = 1$ solution.

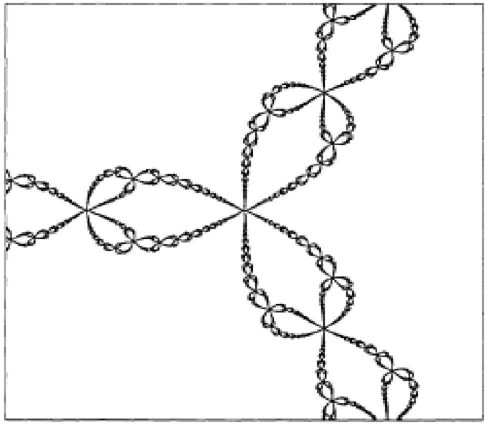

Basin boundaries.

The Mandelbrot Set

- The Mandelbrot set is a connected set of points in the complex plane
- Calculate: $Z_1 = Z_0^2 + Z_0$, $Z_2 = Z_1^2 + Z_0$, $Z_3 = Z_2^2 + Z_0$
- If the sequence Z_0, Z_1, Z_2, Z_3, ... remains within a distance of 2 of the origin forever, then the point Z_0 is said to be in the Mandelbrot set.
- If the sequence diverges from the origin, then the point is not in the set

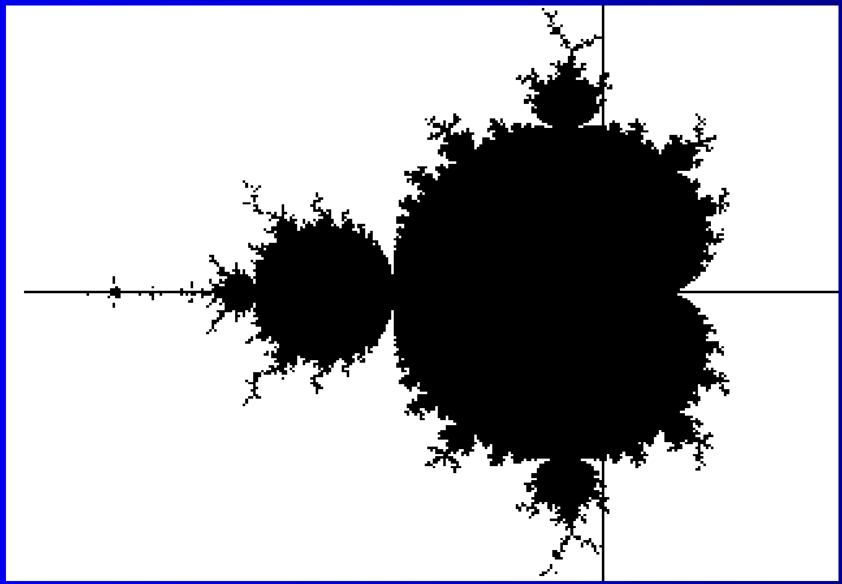

- Most popular and complex object of contemporary mathematics.
- Constructed via simple recipe $\{c \in \mathbf{C} : c^2 + c \not\to \infty\}$, called *prisoner set*.
- Zoom views of set:

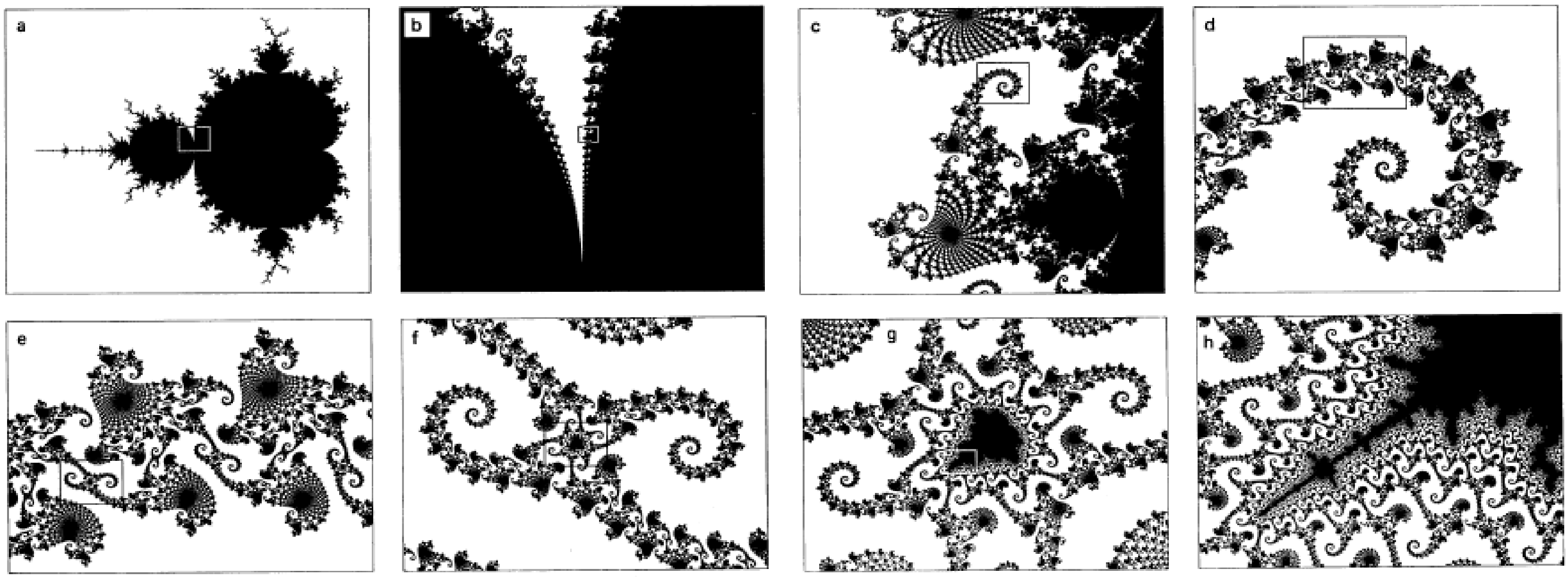

Colored Mandelbrot Set

- The colors are added to the points that are not inside the set. Then we just zoom in on it

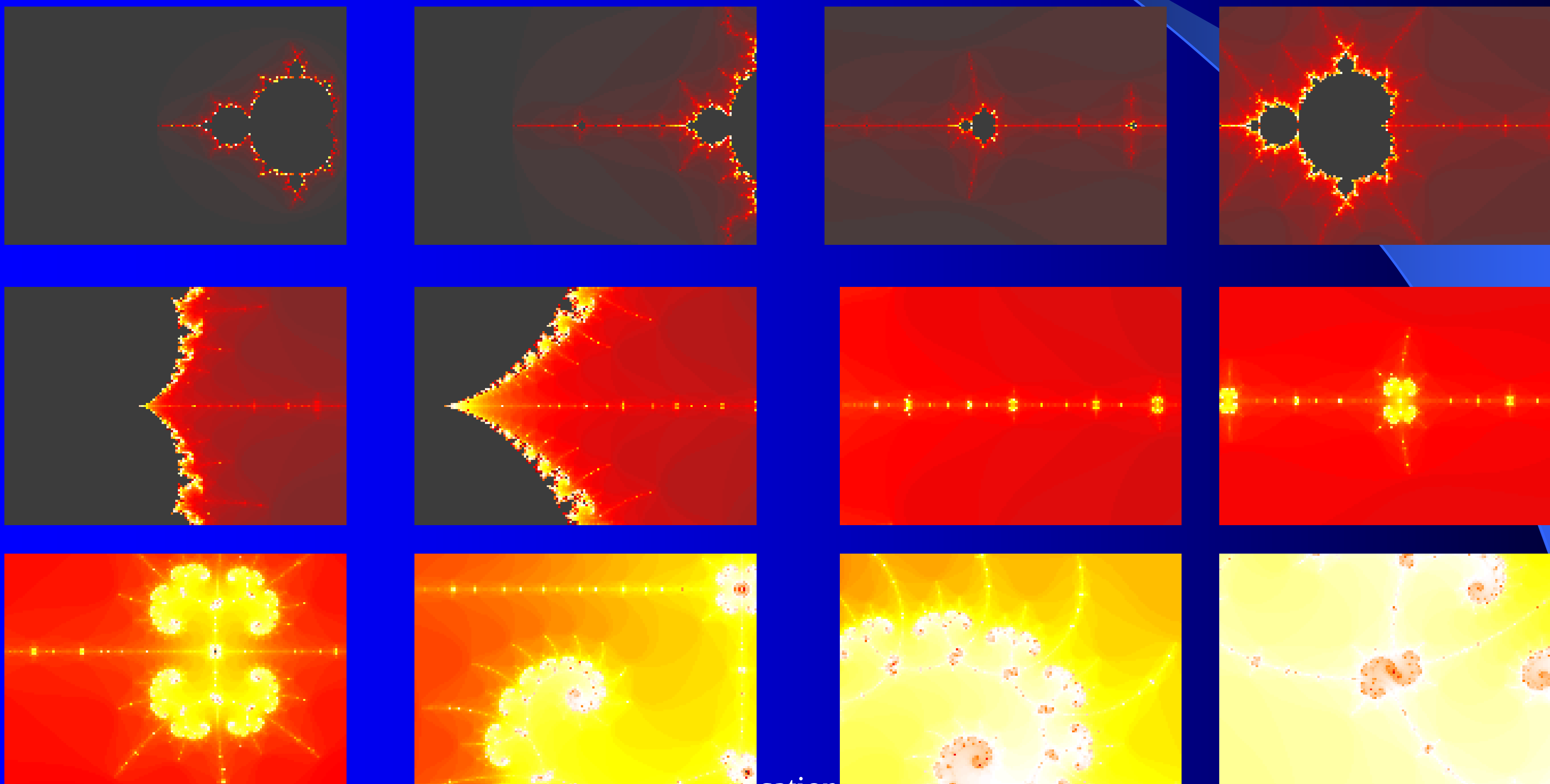

$$z_{n+1} = z_n^{\;2} + c$$

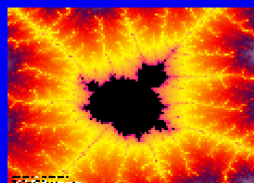   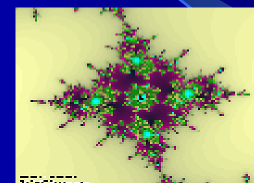 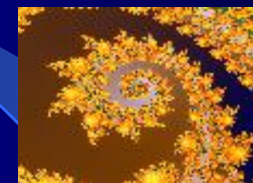

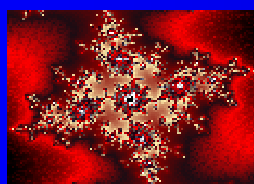 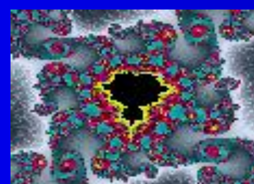 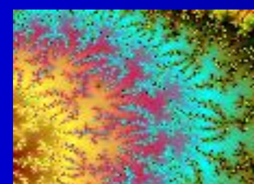 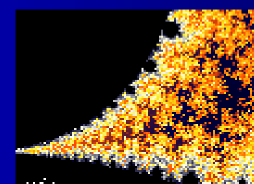 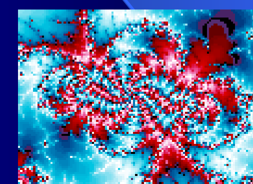

 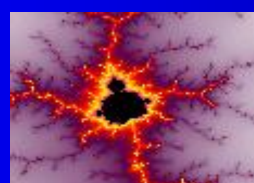 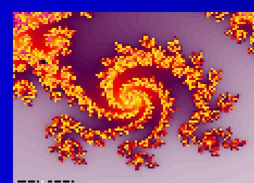 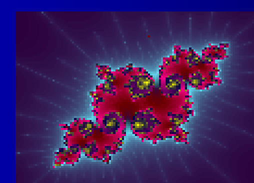 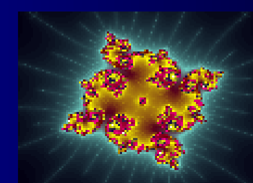

Fractals in biology

Plate 3: Broccoli Romanesco.

Plate 5: Broccoli Romanesco, detail.

Space-filling curve (SFC) definition

Curves that pass through every point of an *n*-dimensional region with positive area (for *n*=2) or volume (for *n*=3), such as the unit square Ω in R^2 or the unit cube in R^3, are called space-filling curves.

Two main characteristics:

- continuous
- surjective

It can be shown that if *f* generates a space-filling curve, then it can not be bijective.

Contents

1. Basic notions
2. Types of space-filling curves
   1. The Hilbert space-filling curve
   2. The Peano space-filling curve
   3. The Sierpinski space-filling curve
   4. The Lebesgue space-filling curve
3. Application of space-filling curves

The Hilbert curve: geometric generation

- If *I* can be mapped continuously on Ω, then after partitioning *I* into four congruent subintervals and Ω into four congruent subsquares, each subinterval can be mapped continuously onto one of the subsquares. This partitioning can be carried out ad infinitum.
- The subsquares must be arranged such that adjacent subintervals are mapped onto adjacent subsquares.
- Inclusion relationship: if an interval corresponds to a square, then its subintervals must correspond to the subsquares of that square.
- This process defines a mapping $\boxed{f_h(I)}$, called the Hilbert space-filling curve.

The Hilbert curve: geometric generation

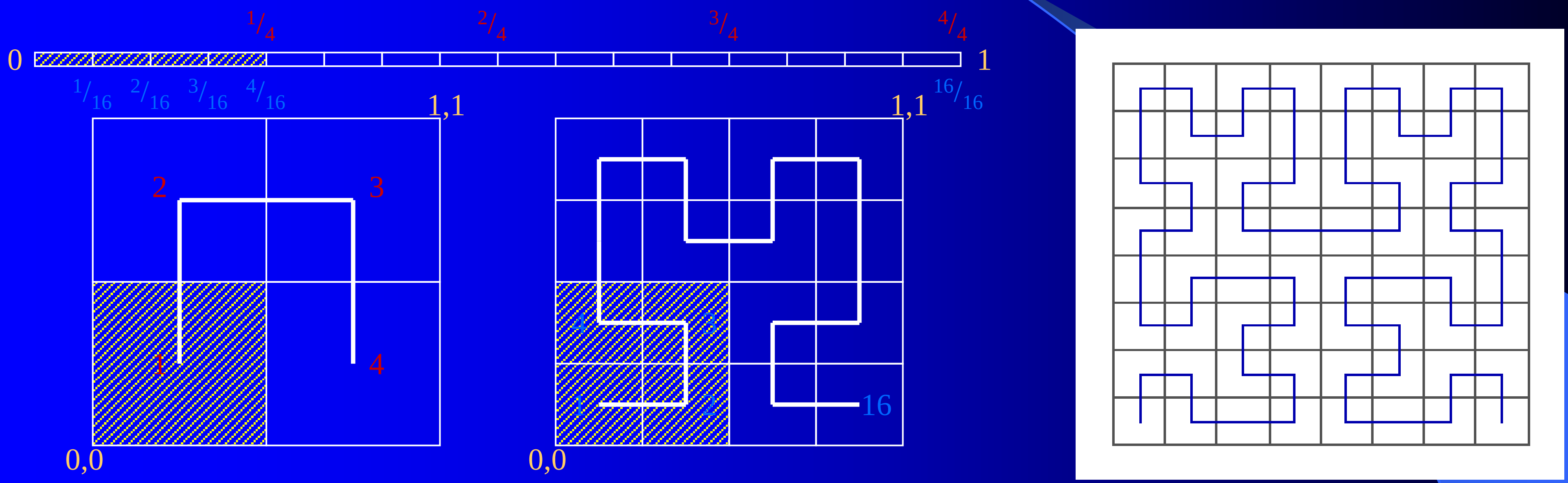

1st iteration

2nd iteration

3rd iteration

The Hilbert curve: geometric generation

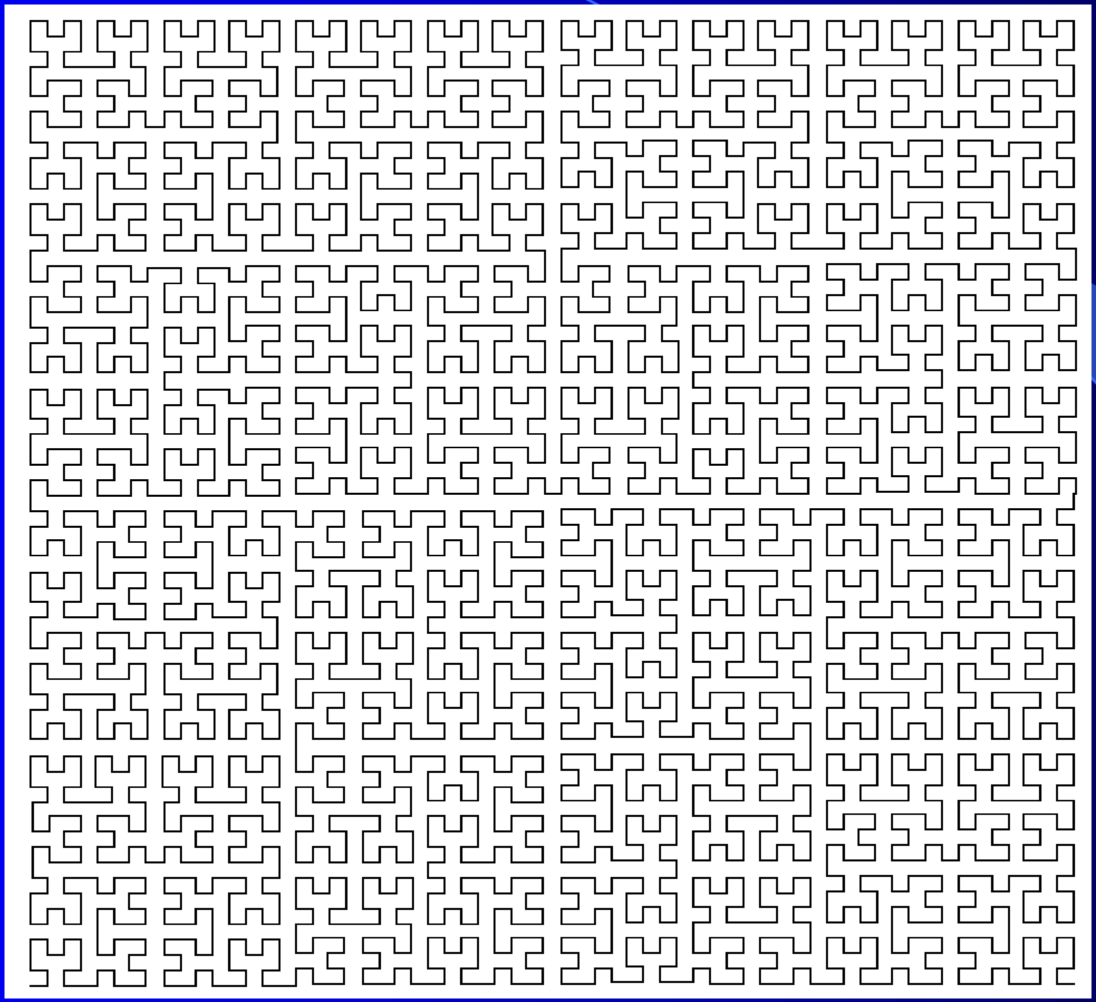

6th iteration

The Hilbert curve: geometric generation

The mapping $f_h : I \longrightarrow \Omega$ is surjective: with every sequence of nested closed squares corresponds a sequence of nested closed intervals that define a unique $t_0 \in I$.

The mapping $f_h : I \xrightarrow{onto} \Omega$ is continuous: in the *n*-th iteration *I* is partitioned in 2^{2n} subintervals, thus

$$t_1, t_2 \in I \ni |t_1 - t_2| < 1/2^{2n} \ then \ \| f_h(t_1) - f_h(t_2) \| \leq \sqrt{5}/2^n$$

The mapping $f_h : I \xrightarrow{onto} \Omega$ is nowhere differentiable.

The Hilbert curve: a complex representation [Sagan]

- Establish a formula to calculate the exact coordinates of an image point if

$$t = k / 2^{2n}, \;\; n = 0,1,2,3,\ldots, \;\; k = 0,1,2,3,\ldots 2^{2n}$$

- Use complex representation $z \in Z$, and affine transformations to wich Ω will be subjected recursively.
- Give an orientation to each subsquare such that the exit point of a subsquare coincides with the entry point of the next subsquare.

The Hilbert curve: a complex representation

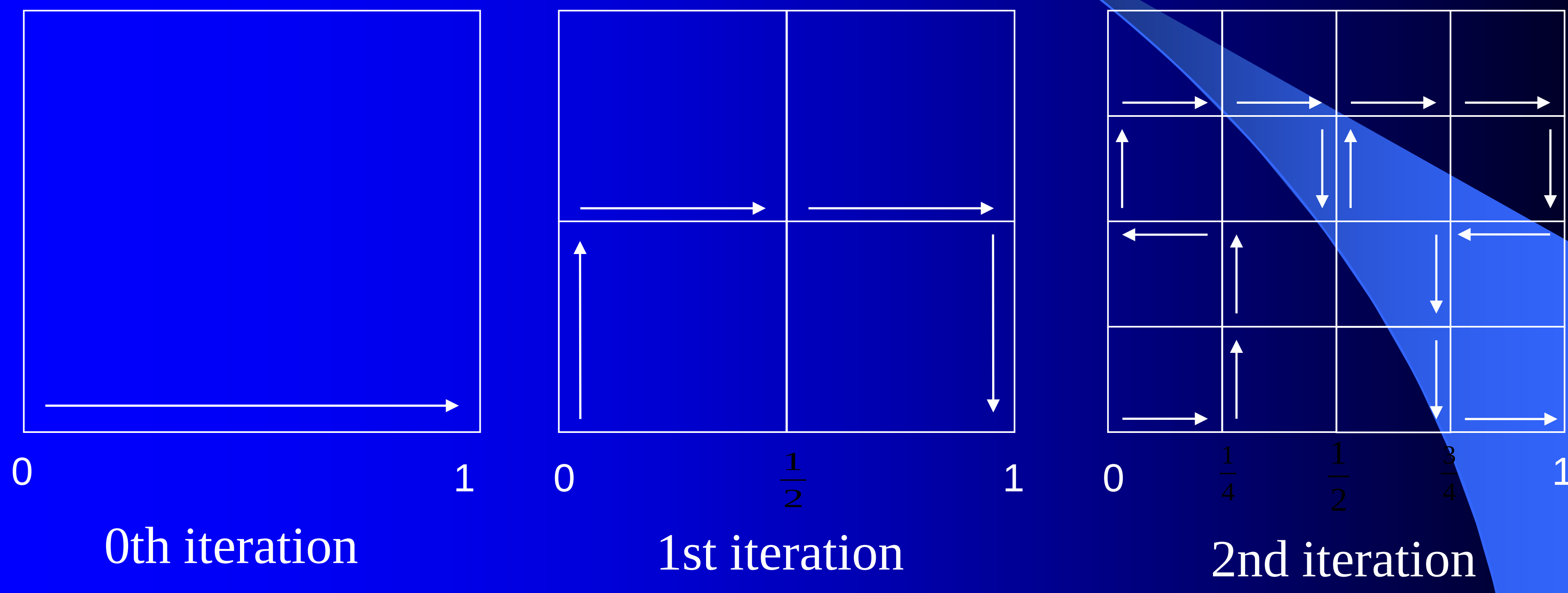

The Hilbert curve: a complex representation

The four basic transformations (2 dimensional case):

$$\boldsymbol{h}_0 z = \frac{1}{2}\bar{z}i$$

$$\boldsymbol{h}_1 z = \frac{1}{2}z + \frac{i}{2}$$

$$\boldsymbol{h}_2 z = \frac{1}{2}z + \frac{1}{2} + \frac{i}{2}$$

$$\boldsymbol{h}_3 z = -\frac{1}{2}\bar{z}i + 1 + \frac{i}{2}$$

$$: \boldsymbol{h}_0 \begin{pmatrix} x_1 \\ x_2 \end{pmatrix} = \frac{1}{2}\begin{bmatrix} 0 & 1 \\ 1 & 0 \end{bmatrix}\begin{pmatrix} x_1 \\ x_2 \end{pmatrix} + \frac{1}{2}\begin{pmatrix} 0 \\ 0 \end{pmatrix} = \frac{1}{2}H_0\begin{pmatrix} x_1 \\ x_2 \end{pmatrix} + \frac{1}{2}h_0$$

$$: \boldsymbol{h}_1 \begin{pmatrix} x_1 \\ x_2 \end{pmatrix} = \frac{1}{2}\begin{bmatrix} 1 & 0 \\ 0 & 1 \end{bmatrix}\begin{pmatrix} x_1 \\ x_2 \end{pmatrix} + \frac{1}{2}\begin{pmatrix} 0 \\ 1 \end{pmatrix} = \frac{1}{2}H_1\begin{pmatrix} x_1 \\ x_2 \end{pmatrix} + \frac{1}{2}h_1$$

$$: \boldsymbol{h}_2 \begin{pmatrix} x_1 \\ x_2 \end{pmatrix} = \frac{1}{2}\begin{bmatrix} 1 & 0 \\ 0 & 1 \end{bmatrix}\begin{pmatrix} x_1 \\ x_2 \end{pmatrix} + \frac{1}{2}\begin{pmatrix} 1 \\ 1 \end{pmatrix} = \frac{1}{2}H_2\begin{pmatrix} x_1 \\ x_2 \end{pmatrix} + \frac{1}{2}h_2$$

$$: \boldsymbol{h}_3 \begin{pmatrix} x_1 \\ x_2 \end{pmatrix} = \frac{1}{2}\begin{bmatrix} 0 & -1 \\ -1 & 0 \end{bmatrix}\begin{pmatrix} x_1 \\ x_2 \end{pmatrix} + \frac{1}{2}\begin{pmatrix} 2 \\ 1 \end{pmatrix} = \frac{1}{2}H_3\begin{pmatrix} x_1 \\ x_2 \end{pmatrix} + \frac{1}{2}h_3$$

The Hilbert curve: a complex representation

- Represent $t \in I$ as $t = 0_4 q_1 q_2 q_3 \ldots,\ with\ \ q_j = 0, 1, 2\ or\ 3$
- $f_h(t) \in \boldsymbol{h}_{q_1} \Omega$, $f_h(t) \in \boldsymbol{h}_{q_1} \boldsymbol{h}_{q_2} \Omega$ ad infinitum:

$$f_h(t) = \lim_{n \to \infty} \boldsymbol{h}_{q_1} \boldsymbol{h}_{q_2} \boldsymbol{h}_{q_3} \ldots \boldsymbol{h}_{q_n} \Omega$$

- For finite quaternaries (edges of subintervals in *n*th iteration):

$$f_h(0_4 q_1 q_2 q_3 \ldots q_n) = \boldsymbol{h}_{q_1} \boldsymbol{h}_{q_2} \boldsymbol{h}_{q_3} \ldots \boldsymbol{h}_{q_n} \underbrace{\boldsymbol{h}_0 \boldsymbol{h}_0 \boldsymbol{h}_0 \ldots \Omega}_{\begin{pmatrix} 0 \\ 0 \end{pmatrix}}$$

$$f_h(0_4 q_1 q_2 q_3 \ldots q_n) = \boldsymbol{h}_{q_1} \boldsymbol{h}_{q_2} \boldsymbol{h}_{q_3} \ldots \boldsymbol{h}_{q_n} \begin{pmatrix} 0 \\ 0 \end{pmatrix}$$

The Hilbert curve: a complex representation

- continued...

$$\boldsymbol{h}_{q_1}\boldsymbol{h}_{q_2}\boldsymbol{h}_{q_3}\ldots\boldsymbol{h}_{q_n}\begin{pmatrix}0\\0\end{pmatrix}=\ldots=\sum_{j=1}^{n}\left(\frac{1}{2^j}\right)H_{q_0}H_{q_1}H_{q_2}H_{q_3}\ldots H_{q_{j-1}}h_{q_j}$$

$$\overset{f_h\ is\ cont.}{\Longrightarrow}\quad f_h(0_4q_1q_2q_3\ldots)=\sum_{j=1}^{\infty}\left(\frac{1}{2^j}\right)H_{q_0}H_{q_1}H_{q_2}H_{q_3}\ldots H_{q_{j-1}}h_{q_j}$$

- Taking into account some properties of H_{q_j}:

$$f_h(0_4q_1q_2q_3\ldots)=\sum_{j=1}^{\infty}\left(\frac{1}{2^j}\right)H_0^{e_{0j}}H_3^{e_{3j}}h_{q_j}\ ,$$

$with\ \ e_{kj}=number\ of\ k\acute{}s\ preceding\ q_j\ (\mathrm{mod}\ 2),\ k=0\ or\ 3$

The Hilbert curve: a complex representation

- Further simplifications of the formula are possible...
- An example:

$$f_h(0_4 203) = \boldsymbol{h}_2 \boldsymbol{h}_0 \boldsymbol{h}_3 \begin{pmatrix} 0 \\ 0 \end{pmatrix} = \begin{pmatrix} 5/8 \\ 3/4 \end{pmatrix}$$

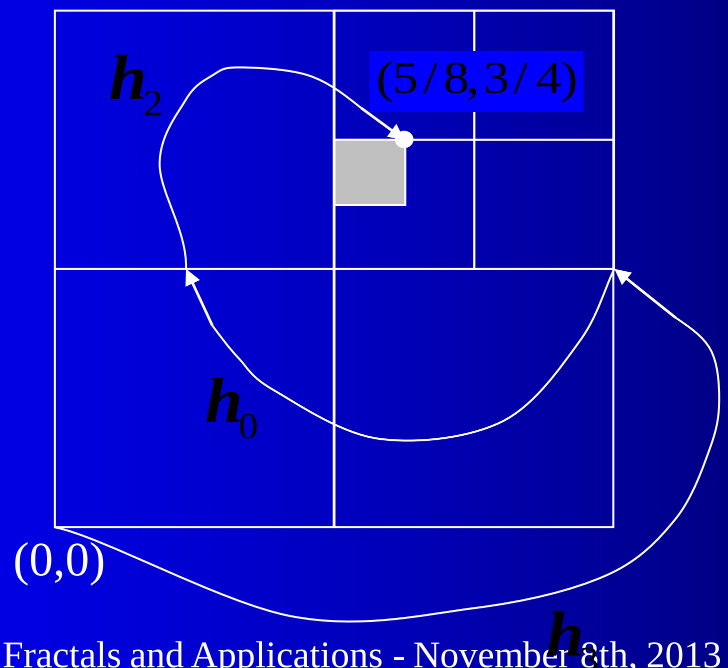

Approximating polygons for the Hilbert curve

The polygonal line that runs through the points

$$f_h(0),\ f_h(1/2^{2n}),\ f_h(2/2^{2n}),\ f_h(3/2^{2n}),\ldots,\ f_h((2^{2n}-1)/2^{2n}),\ f_h(1),$$

is called the *n*th approximating polygon or a discrete space filling curve.

Parametrization:

$$p_n : I \to \Omega : p_n(t) = 2^{2n}\left(t - \frac{k}{2^{2n}}\right) f_h\left(\frac{k+1}{2^{2n}}\right) - 2^{2n}\left(t - \frac{k+1}{2^{2n}}\right) f_h\left(\frac{k}{2^{2n}}\right),$$

$$for\ k/2^{2n} \le t \le (k+1)/2^{2n},\ k = 0,1,2,3,\ldots 2^{2n}-1$$

$\{p_n\}$ converges uniformly to the Hilbert curve

The Hilbert curve: representation through grammars

- Make use of four distinct templates to generate the discrete Hilbert curve: *H,A,B* and *C.*
- These templates will be translated to a first iteration of the curve according to a fixed scheme.

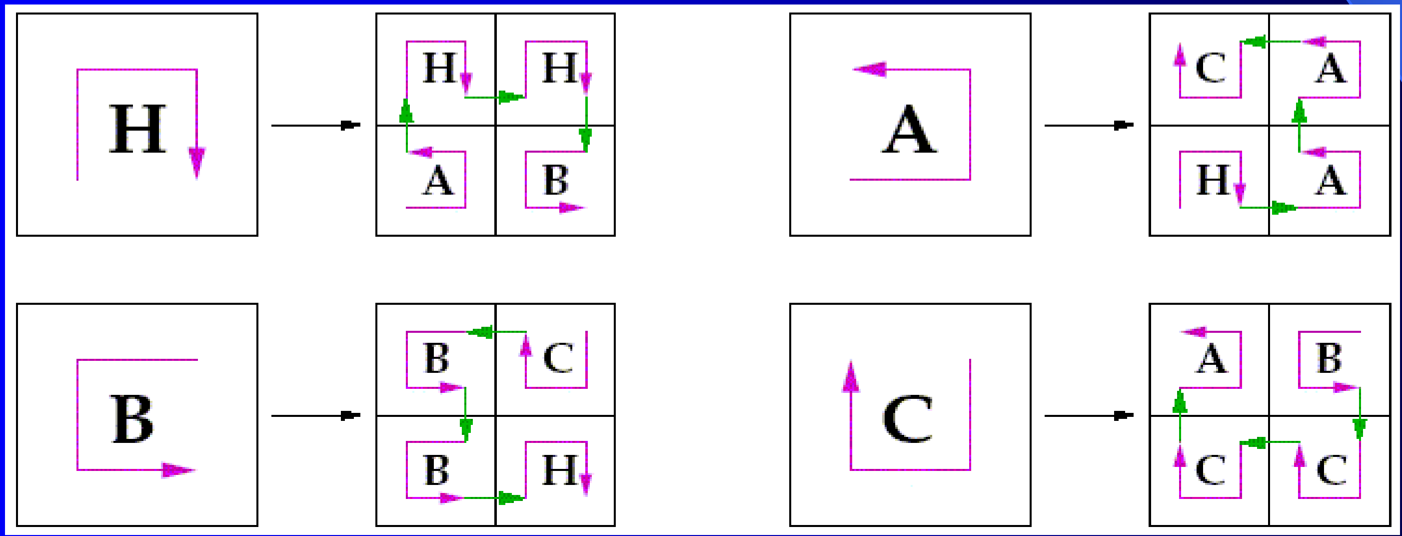

The Hilbert curve: representation through grammars

$$
\begin{array}{lll}
H & \longleftarrow & A \uparrow H \rightarrow H \downarrow B \\
A & \longleftarrow & H \rightarrow A \uparrow A \leftarrow C \\
B & \longleftarrow & C \leftarrow B \downarrow B \rightarrow H \\
C & \longleftarrow & B \downarrow C \leftarrow C \uparrow A
\end{array}
$$

- The resulting rules and transitions can be used to implement the recursive construction of the discrete Hilbert curve.

$$
\begin{array}{lll}
H & \longleftarrow & A \uparrow H \rightarrow H \downarrow B \\
 & \longleftarrow & H \rightarrow A \uparrow A \leftarrow C \uparrow A \uparrow H \rightarrow H \downarrow B \rightarrow A \uparrow H \rightarrow H \downarrow B \downarrow C \leftarrow B \downarrow B \rightarrow H
\end{array}
$$

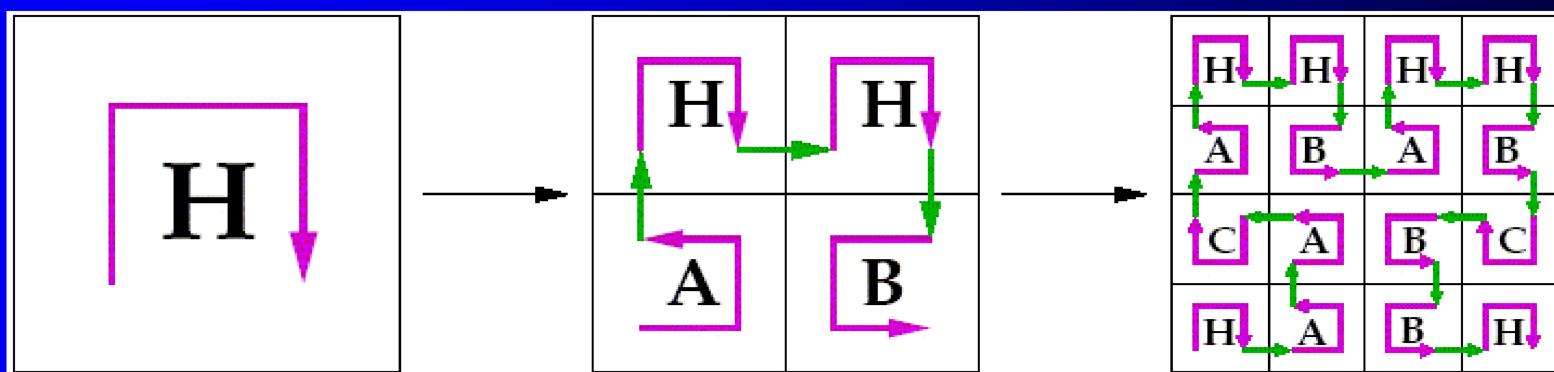

Contents

The Peano curve: definition

- $f_p : I \to \Omega$ with

$$f_p(0_3 t_1 t_2 t_3 t_4 \ldots) = \begin{pmatrix} 0_3 t_1 (k^{t_2} t_3)(k^{t_2+t_4} t_5)\ldots \\ 0_3 (k^{t_1} t_2)(k^{t_1+t_3} t_4)\ldots \end{pmatrix}$$

$$\text{with } \; kt_j = 2 - t_j \;\; (t_j = 0,1,2) \; \text{ and } \; k^{\nu} \text{ is the } \nu\text{th it. of } k$$

is surjective and continuous on *I*, and represents a SFC.

- More interesting: geometric generation according to Hilbert

The Peano curve: a complex representation

- Define orientation of the sub-squares:

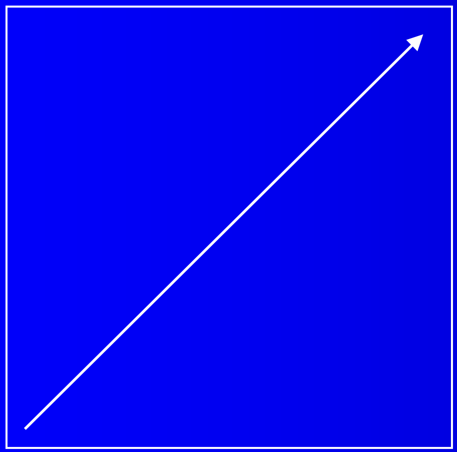

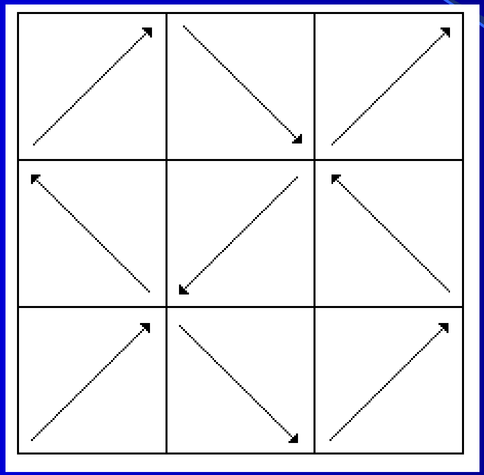

- Define similarity transforms: $$\boldsymbol{p}_0 z = \frac{1}{3} z,\ \boldsymbol{p}_1 z = -\frac{1}{3}\bar{z} + \frac{1}{3} + \frac{i}{3}, \ldots$$

with $$\boldsymbol{p}_j \begin{pmatrix} x_1 \\ x_2 \end{pmatrix} = \frac{1}{3} P_j \begin{pmatrix} x_1 \\ x_2 \end{pmatrix} + \frac{1}{3} p_j, \quad j = 0, 1, \ldots 8$$

The Peano curve: a complex representation

- Use ternary representation of : $t \in I$

$$0_3 t_1 t_2 \ldots t_{2n-2} t_{2n} \ldots = 0_9 (3t_1 + t_2)(3t_3 + t_4)\ldots(3t_{2n-1} + t_{2n})\ldots$$

$$f_p(t) = \lim_{n \to \infty} \boldsymbol{p}_{3t_1+t_2} \boldsymbol{p}_{3t_3+t_4} \cdots \boldsymbol{p}_{3t_{2n-1}+t_{2n}} \Omega$$

- Continue as with Hilbert´s curve...

→ we get the same result as in Peano´s definition

Approximating polygons for the Peano curve

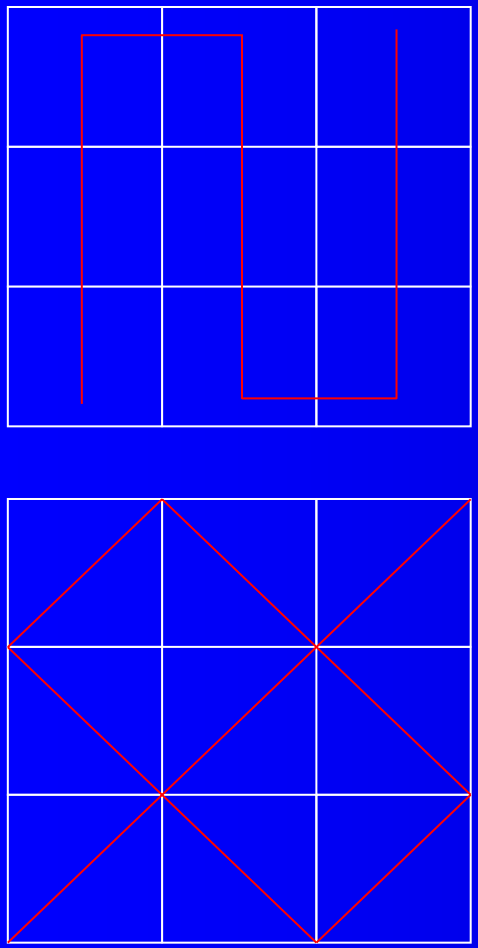

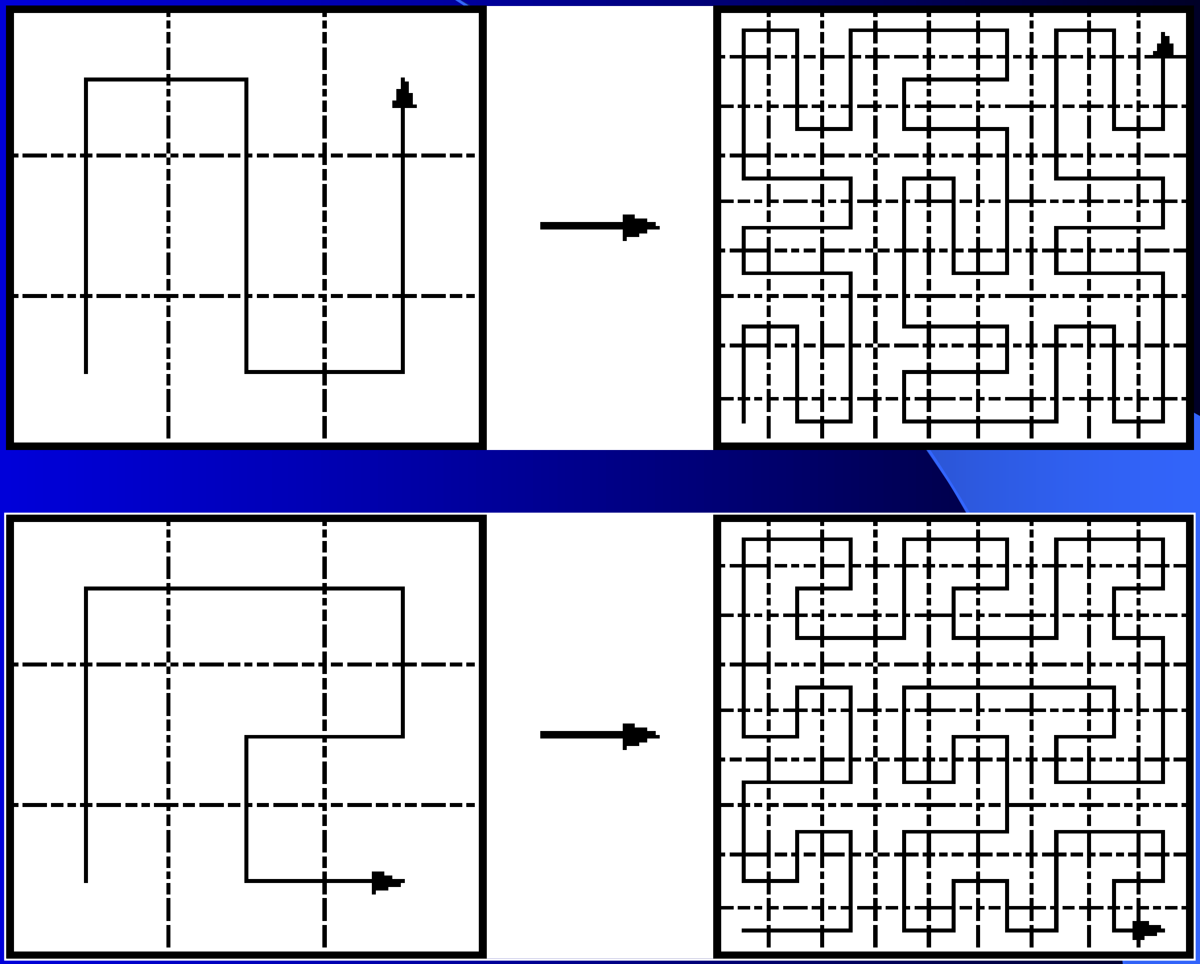

The Peano curve: representation through grammars

$$
\begin{array}{lll}
P & \longleftarrow & P \uparrow Q \uparrow P \rightarrow S \downarrow R \downarrow S \rightarrow P \uparrow Q \uparrow P \\
Q & \longleftarrow & Q \uparrow P \uparrow Q \leftarrow R \downarrow S \downarrow R \leftarrow Q \uparrow P \uparrow Q \\
R & \longleftarrow & R \downarrow S \downarrow R \leftarrow Q \uparrow P \uparrow Q \leftarrow R \downarrow S \downarrow R \\
S & \longleftarrow & S \downarrow R \downarrow S \rightarrow P \uparrow Q \uparrow P \rightarrow S \downarrow R \downarrow S
\end{array}
$$

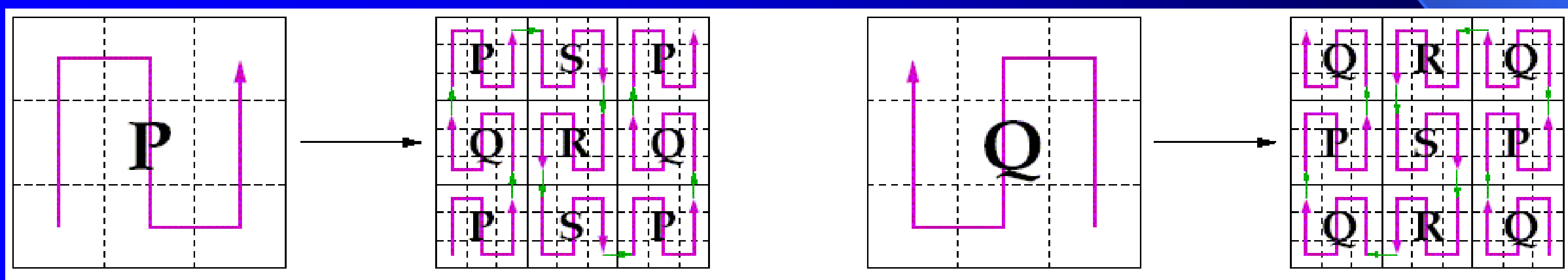

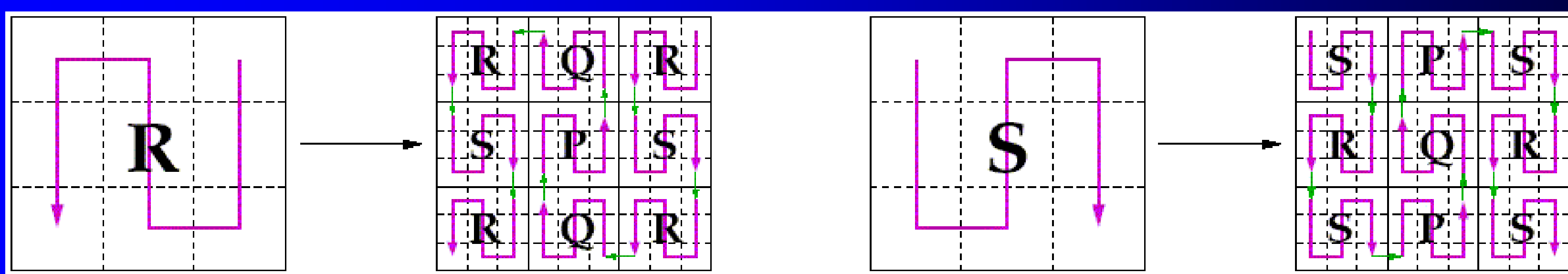

Contents

The Sierpinski curve: generation

- Partition *I* into 2^n congruent subintervals and τ into 2^n congruent subtriangles.

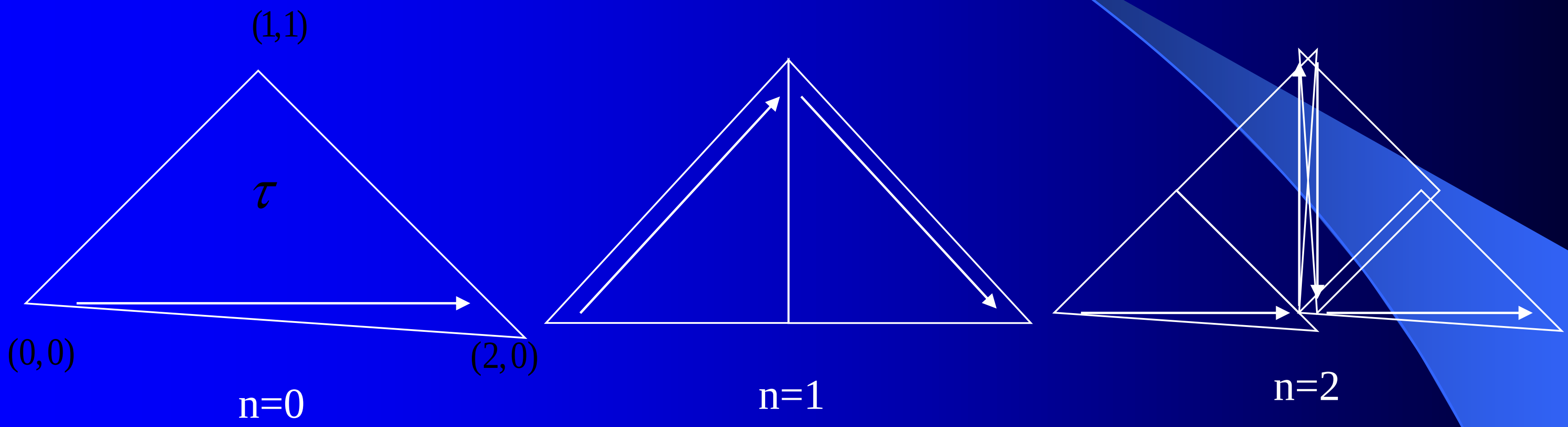

- In deriving an algabraic representation it is easier to divide *I* into 2^{2n} subintervals, thus using quaternaries:

$$f_s(0_4 q_1 q_2 q_3 \ldots) = \sum_{j=1}^{\infty} \frac{1}{2^j} S_{q_0} S_{q_1} S_{q_2} \ldots S_{q_{j-1}} s_{q_j}$$

The Sierpinski curve: generation

with similarity transforms:

$$\boldsymbol{S}_0 z = z/2$$

$$\boldsymbol{S}_1 z = zi/2+1$$

$$\boldsymbol{S}_2 z = -zi/2+1+i$$

$$\boldsymbol{S}_3 z = z/2+1$$

$$: \boldsymbol{S}_0\begin{pmatrix}x_1\\x_2\end{pmatrix} = \frac{1}{2}\begin{pmatrix}1 & 0\\0 & 1\end{pmatrix}\begin{pmatrix}x_1\\x_2\end{pmatrix} + \frac{1}{2}\begin{pmatrix}0\\0\end{pmatrix} = \frac{1}{2}S_0\begin{pmatrix}x_1\\x_2\end{pmatrix} + \frac{1}{2}s_0$$

$$: \boldsymbol{S}_1\begin{pmatrix}x_1\\x_2\end{pmatrix} = \frac{1}{2}\begin{pmatrix}0 & -1\\1 & 0\end{pmatrix}\begin{pmatrix}x_1\\x_2\end{pmatrix} + \frac{1}{2}\begin{pmatrix}2\\0\end{pmatrix} = \frac{1}{2}S_1\begin{pmatrix}x_1\\x_2\end{pmatrix} + \frac{1}{2}s_1$$

$$: \boldsymbol{S}_2\begin{pmatrix}x_1\\x_2\end{pmatrix} = \frac{1}{2}\begin{pmatrix}0 & 1\\-1 & 0\end{pmatrix}\begin{pmatrix}x_1\\x_2\end{pmatrix} + \frac{1}{2}\begin{pmatrix}2\\2\end{pmatrix} = \frac{1}{2}S_2\begin{pmatrix}x_1\\x_2\end{pmatrix} + \frac{1}{2}s_2$$

$$: \boldsymbol{S}_3\begin{pmatrix}x_1\\x_2\end{pmatrix} = \frac{1}{2}\begin{pmatrix}1 & 0\\0 & 1\end{pmatrix}\begin{pmatrix}x_1\\x_2\end{pmatrix} + \frac{1}{2}\begin{pmatrix}2\\0\end{pmatrix} = \frac{1}{2}S_3\begin{pmatrix}x_1\\x_2\end{pmatrix} + \frac{1}{2}s_3$$

The Sierpinski curve: generation

- Taking into account some properties of S_{q_j} :

$$f_s(0_4 q_1 q_2 q_3 \ldots) = \sum_{j=1}^{\infty} \frac{1}{2^j} (-1)^{\eta_j} S^{\delta_j} s_{q_j}$$

$$\begin{aligned} &\textit{with } \ \eta_j = \textit{number of } \ 2\acute{}s \ \textit{preceding } \ q_j \ (\mathrm{mod}\, 2) \\ &\textit{and } \ \delta_j = \textit{number of } \ 1\acute{}s \ \textit{and } \ 2\acute{}s \ \textit{preceding } \ q_j \ (\mathrm{mod}\, 4) \end{aligned}$$

The Sierpinski curve: approximating polygons

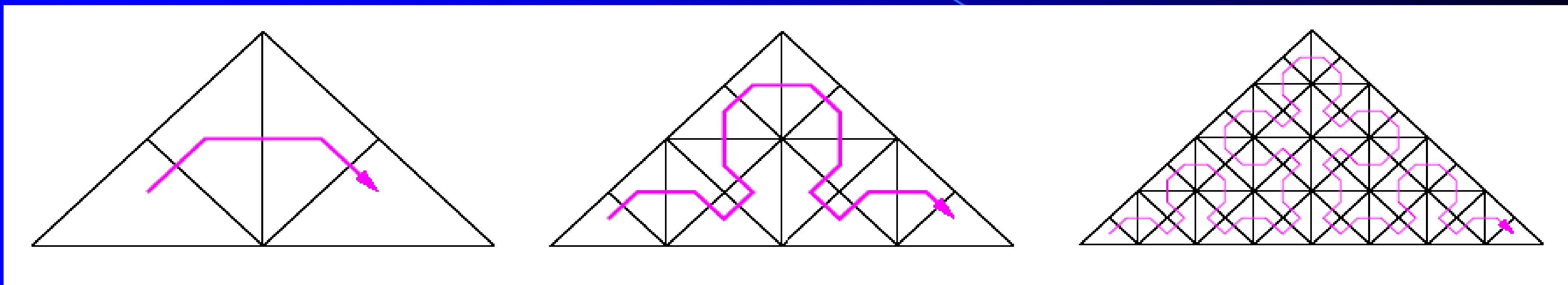

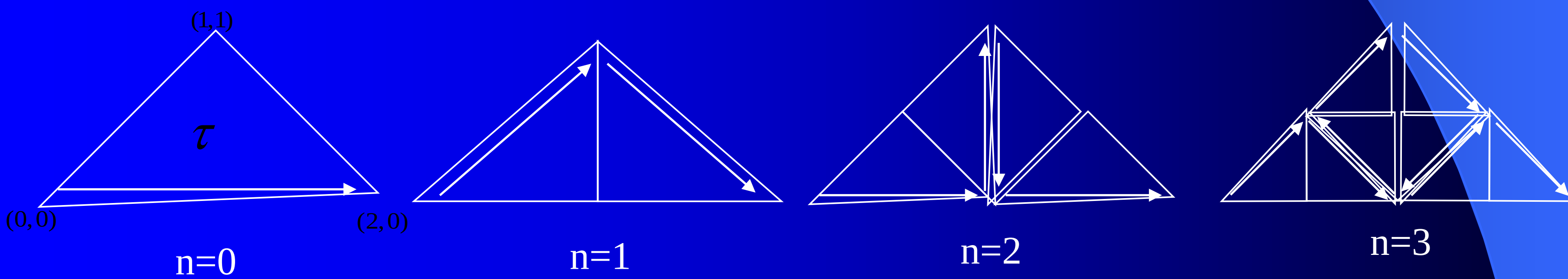

The Sierpinski curve: generation

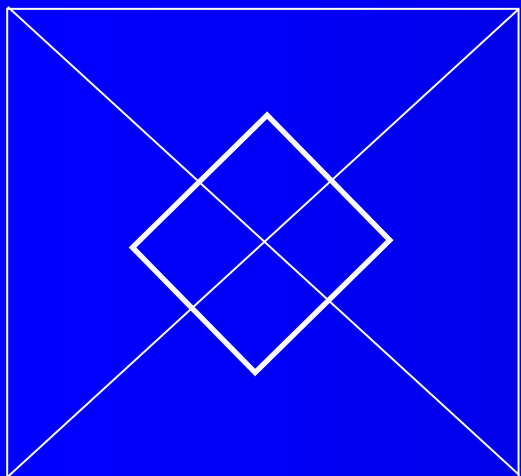

Originaly defined as a map f_s from *I* onto $[-1,1]^2$, but it can be considered as a map from *I* onto a right isosceles triangle $\mathcal{T}$.

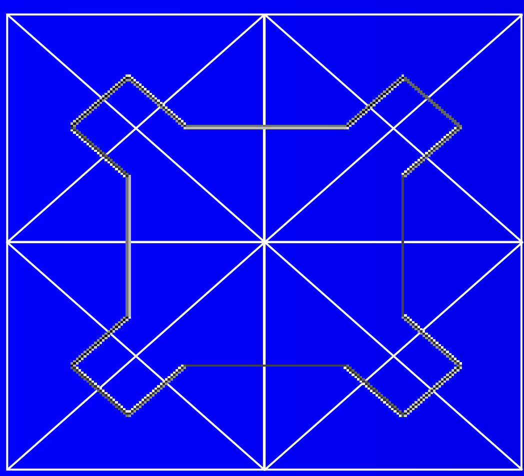

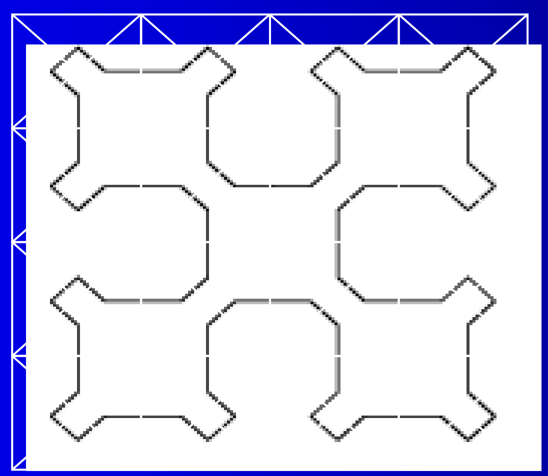

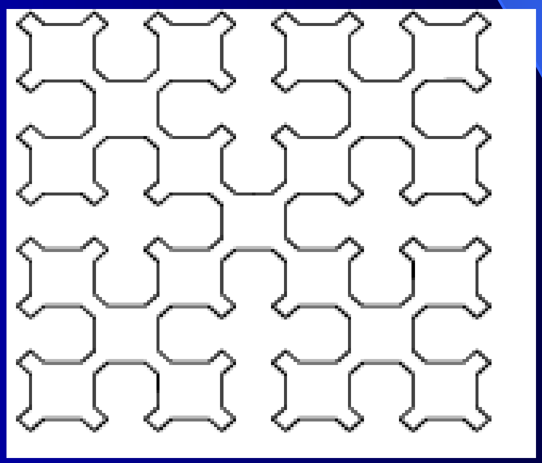

Contents

The Lebesgue curve: generation and approximating polygons

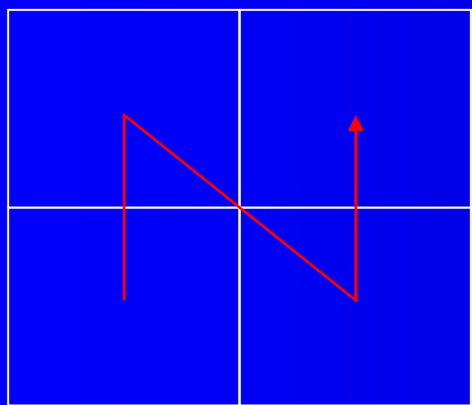

1st iteration

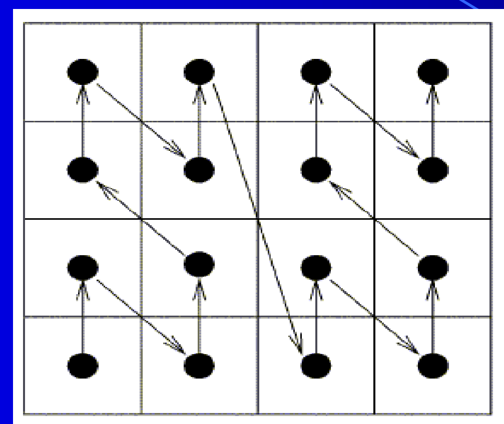

2nd iteration

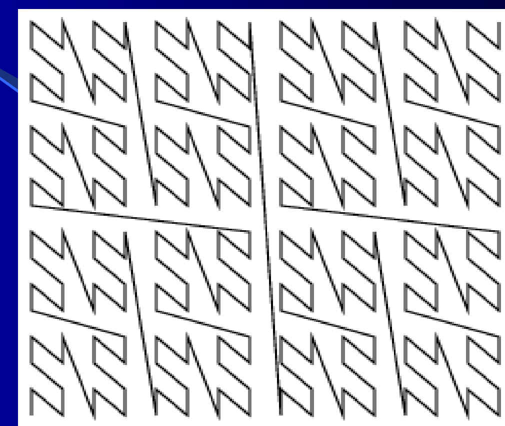

4th iteration

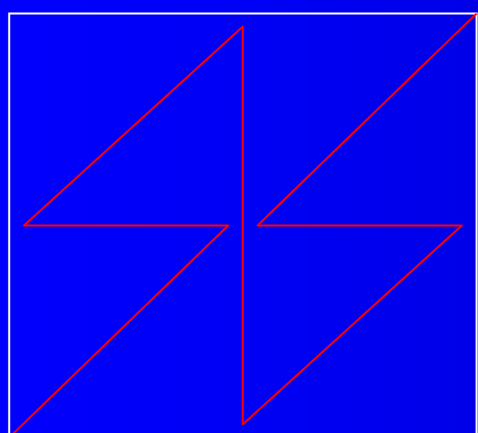

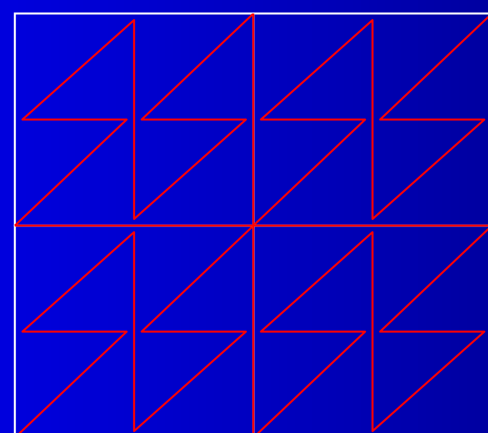

Essential properties for applications:

- Finite area – infinite perimeter !
- Self-similarity (same properties and shapes at different scales)

Physical relations for capacitors

Both electrodes have a surface A (in m^2) separated by distance d (in m). The applied voltage ΔU (in Volt) creates an electric field $E = \Delta U/d$ storing the electrical energy. Capacitance C in Farad (F) and stored energy J in Ws is:

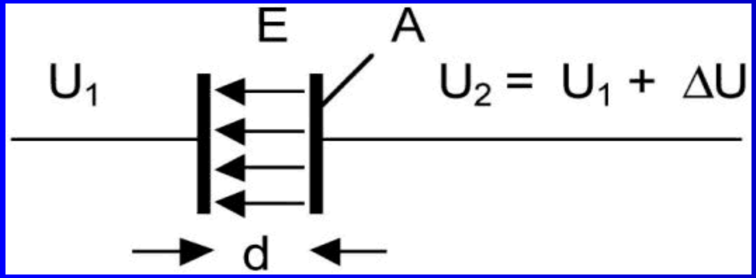

$$C = \varepsilon_0 \cdot \varepsilon_r \frac{A}{d} \qquad J = \tfrac{1}{2} C \cdot \Delta U^2$$

where ε_r (e.g. 1 for vacuum or 81 for water) is the relative dielectric constant which depends on the material placed between the two electrodes and $\varepsilon_0 = 8.85 \cdot 10^{-12}$ F/m is a fundamental constant.

Capacitance in Farad	1000	$1 \cdot 10^{-3}$	$1 \cdot 10^{-6}$	$1 \cdot 10^{-9}$	$1 \cdot 10^{-12}$
Example	 supercapacitor with 1500 F, max. 2.5 V (positive electrode left)	 electrolyte capacitor with 1000 mF, max. 25 V (positive electrode left)	 electrolyte capacitor with 10 mF, max. 35 V (bent wire is positive electrode)	 rolled capacitor with 51 nF, max. 63 V	 plate capacitors with 50 pF. Left: an element from an old vacuum-tube radio in the form of two plates rolled to a cylinder, max. 450 V. Right: modern ceramic element, max. 100 V)
Energy Stored	Watt hours (Wh)	several Ws (Ws)	milli-Ws = 10^{-3} Ws (mWs)	milli-Ws = 10^{-3} Ws (mWs)	micro-Ws = 10^{-6} Ws (mWs)
Applications	Novel applications in power electronics: e.g. in cars, for replacing batteries in consumer electronics	Power supply units	Low frequency technology: general electronics, e.g. audio amplifiers	Low frequency technology: general electronics, e.g. audio amplifiers	High frequency technology: e.g. radio, TV, PC

How to create capacitors with larger C?

- Create capacitors with very large areas A – technologies to create fractal-type surfaces
- Use designs taking advantage of lateral capacitance in integrated circuits

Electrochemically modified glassy carbon is a promising material to be used in electrochemical capacitors. Oxidation of the surface of a glassy carbon electrode results in a porous layer with very large capacitance and fairly low internal resistance when using an aqueous electrolyte.

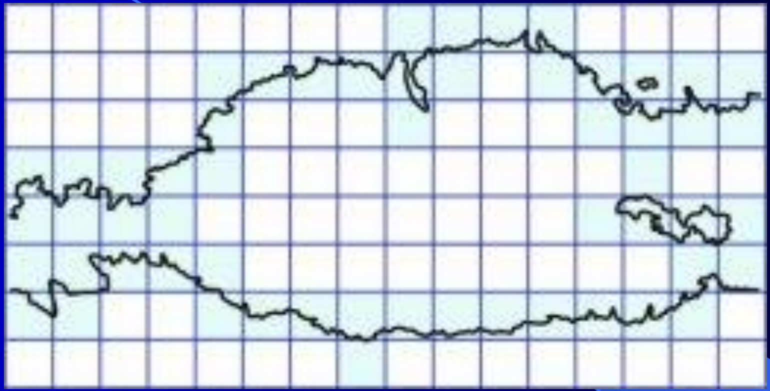

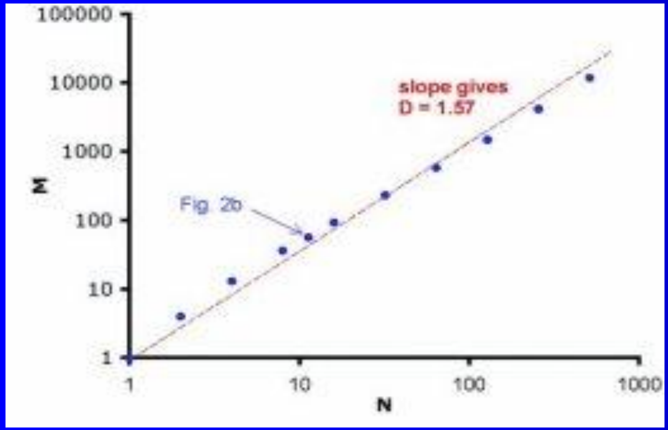

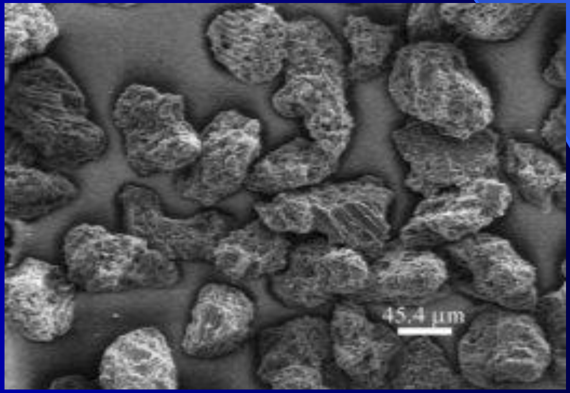

- Paul Scherrer Institute in Villigen, Switzerland - Rüdiger Kötz and his group have developed an electrode in collaboration with the Swiss company *Montena* (*Maxwell*).

- a) Micrograph of a cross section through a supercapacitor electrode.The white stripe is a part of the 30 µm thick metallic carrier-foil (total foil is 0.1 m wide, 2 m long). On both sides carbon particles provide a complex fractal surface responsible for the high capacity.The space taken by the green resin used to fix the delicate carbon structure before cutting and to provide a good contrast for imaging is normally filled with the electrolyte (an organic solvent containing salt ions).
  b) Borderline of the cross section through the electrode surface in (a) to be analyzed by the box-counting procedure, illustrated for a tiling with 128 squares:M = 56 squares (filled with light blue colour) are necessary to cover the borderline.Their side lengths are N = 11.3 (square root of 128) times smaller than the length scale of the whole picture.
  c) The box-counting procedure is repeated with a computer program for different N.The average fractal dimension of the borderline is the gradient of the straight line approximating the measured points in this Log(M) over Log(N) plot, giving D 1.6.This same dimension was measured in the lengthinterval covering nearly 3 decades between 0.6 mm (length of micrograph in Figs 2a, b) and about 1 µm (fine structure in Fig. 2d).
  d) Carbon particles as seen with an electron microscope show roughness also in the 1 µm scale. It is assumed that the above indicated fractal dimension D holds over the entire range of 8 decades between the macroscopic scale (i.e. the geometric size of the order of 0.1 m) and the microscopic scale (i.e. the micropores in the order of 1 nm = $1 \cdot 10^{-9}$ m).The electrode surface is therefore multiplied by $10^{8*0.6}$ or about 60’000 when compared to the normal two-dimensional surface of 0.2 m^2.

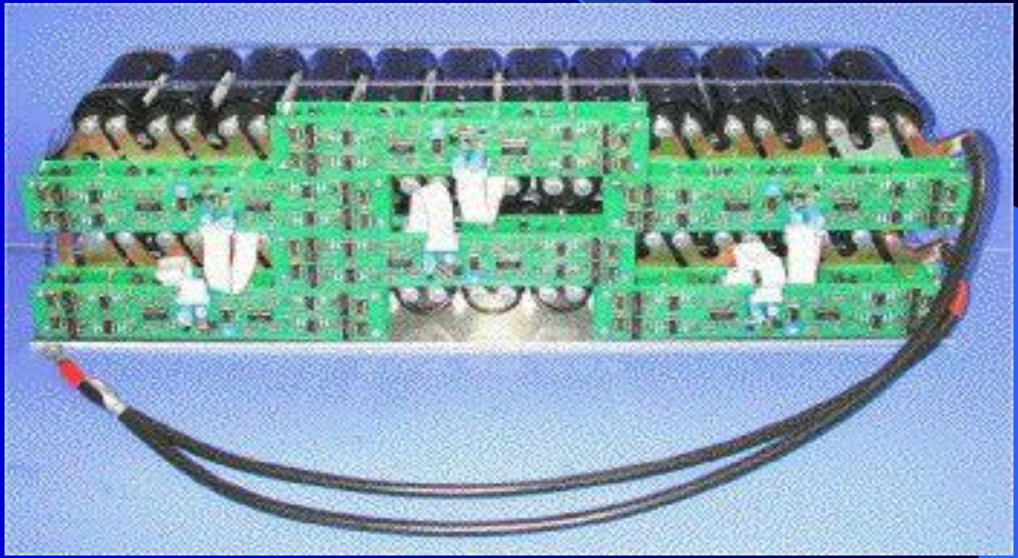

- *800 F boostcap by montena SA utilizing PSI electrode.*
- *Capacitor module with 2 x 24 capacitors resulting in 60 V , 60 F with an overall internal resistance of < 20 mOhm.*

- Supercapacitor module for HY-LIGHT.
  Capacitance: 29 F
  Power: 30 - 45 kW for 20 - 15 sec ; Weight: 53 kg
- HY-LIGHT accelerates to 100km/h in 12 seconds

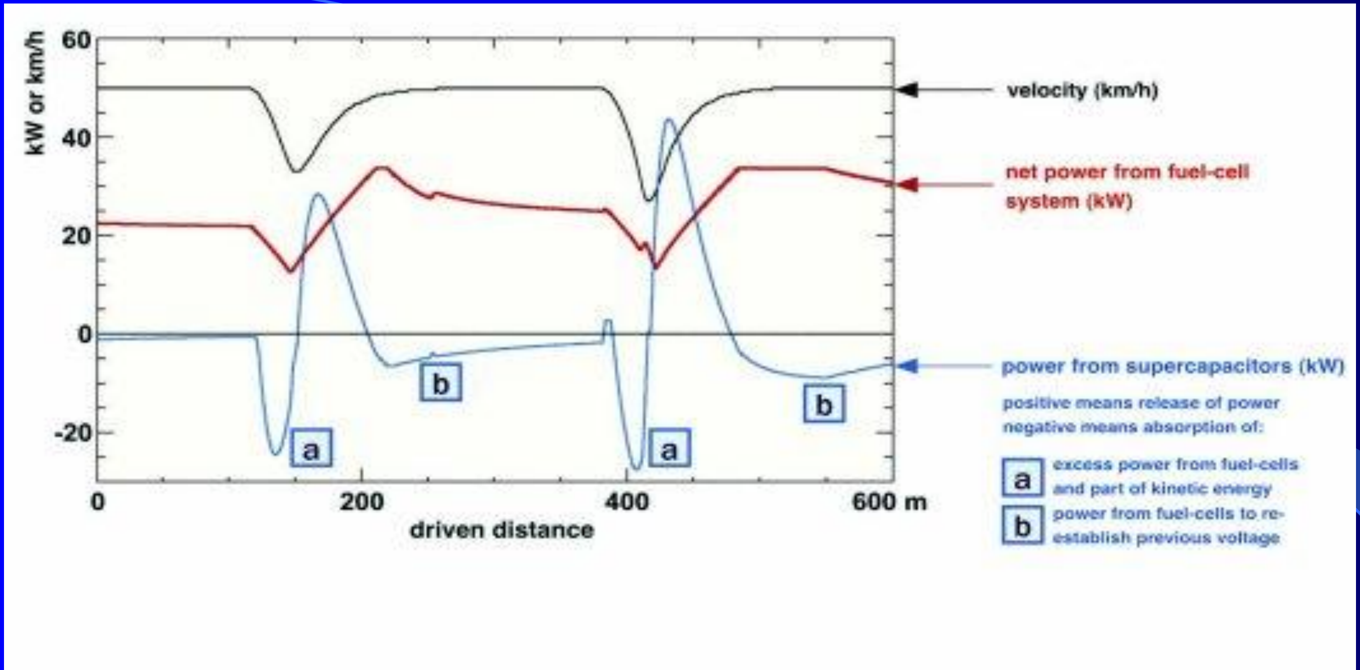
kW or km/h
60
40
20
0
-20
0
200
400
600 m
driven distance
velocity (km/h)
net power from fuel-cell system (kW)
power from supercapacitors (kW)
positive means release of power
negative means absorption of:
a excess power from fuel-cells and part of kinetic energy
b power from fuel-cells to re-establish previous voltage
a
b
a
b

Antenna properties

- Radiation pattern variation for a linear antenna with changing frequency – antennas are narrow-band devices!

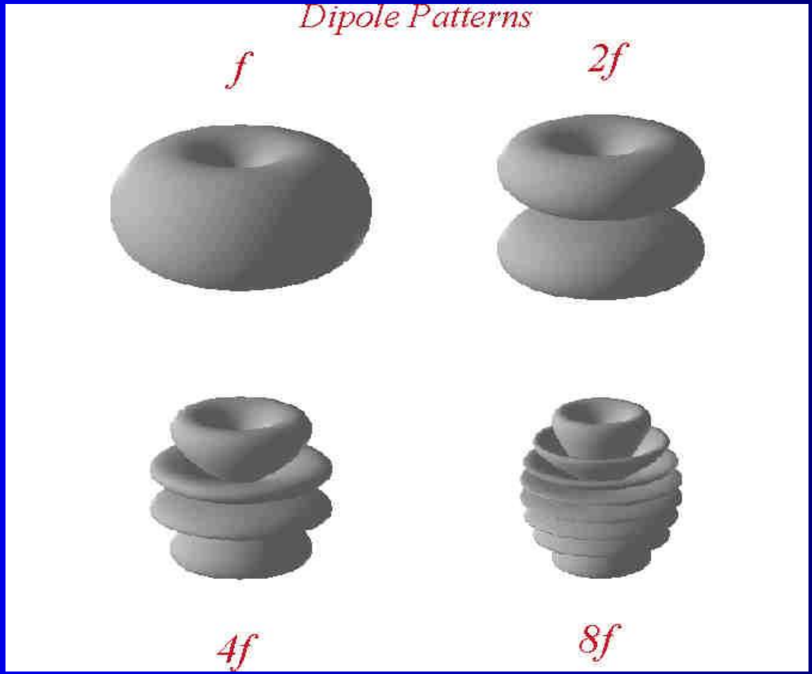

fractal antenna is an antenna that uses a self-similar design to maximize the length, or increase the perimeter (on inside sections or the outer structure), of material that can receive or transmit electromagnetic signals within a given total surface area. For this reason, fractal antennas are very compact, are multiband or wideband, and have useful applications in cellular telephone and microwave communications.

Fractal antenna response differs markedly from traditional antenna designs, in that it is capable of operating optimally at many different frequencies simultaneously. Normally standard antennae have to be "cut" for the frequency for which they are to be used—and thus the standard antennae only optimally work at that frequency. This makes the fractal antenna an excellent design for wideband applications.

- The first fractal antennas were arrays, and not recognized initially as having self similarity as their attribute. Log-periodic antennas are arrays, around since the 1950's (invented by Isbell and DuHamel), that are such fractal antennas. They are a common form used in TV antennas, and are arrow-head in shape. Antenna elements made from self similar shapes were first done by Nathan Cohen, a professor at Boston University, in 1988. Most allusions to fractal antennas make reference to these 'fractal element antennas'.

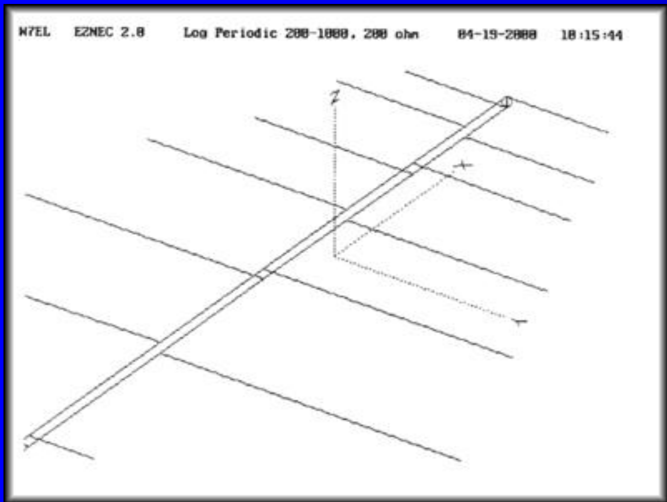
W7EL EZNEC 2.0 Log Periodic 200-1000, 200 ohm 04-19-2000 10:15:44
Z
X
Y

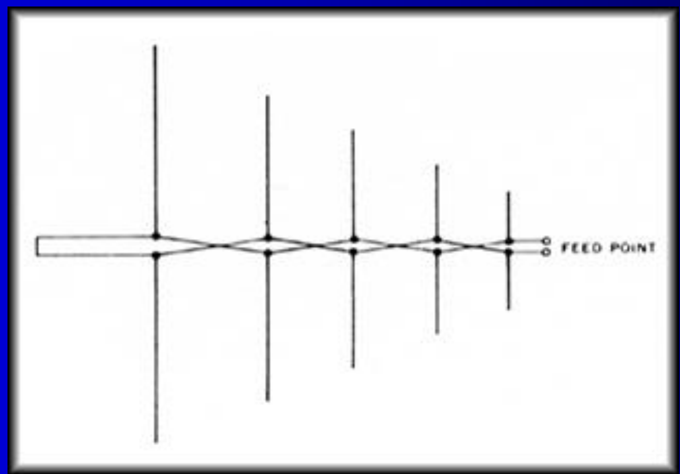
FEED POINT

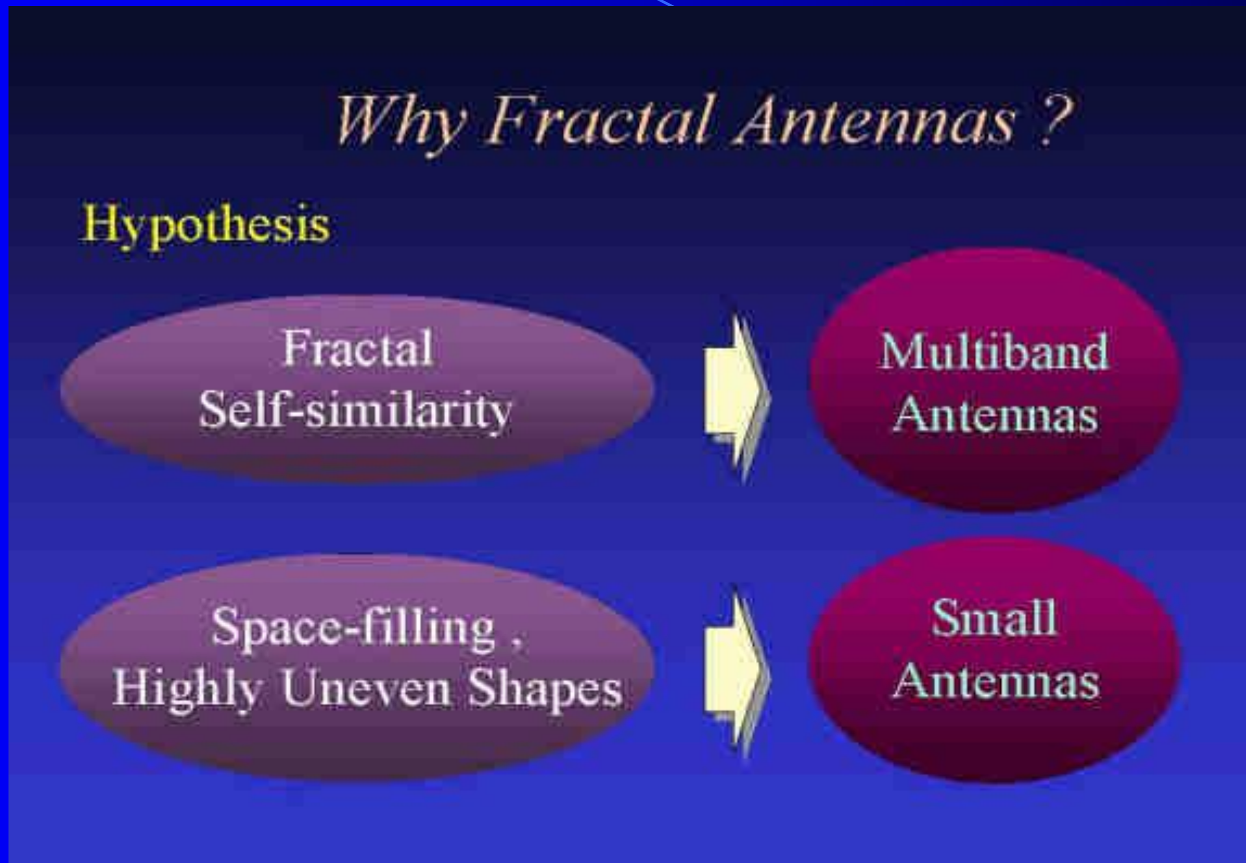
Why Fractal Antennas ?
Hypothesis
Fractal
Self-similarity
Multiband
Antennas
Space-filling ,
Highly Uneven Shapes
Small
Antennas

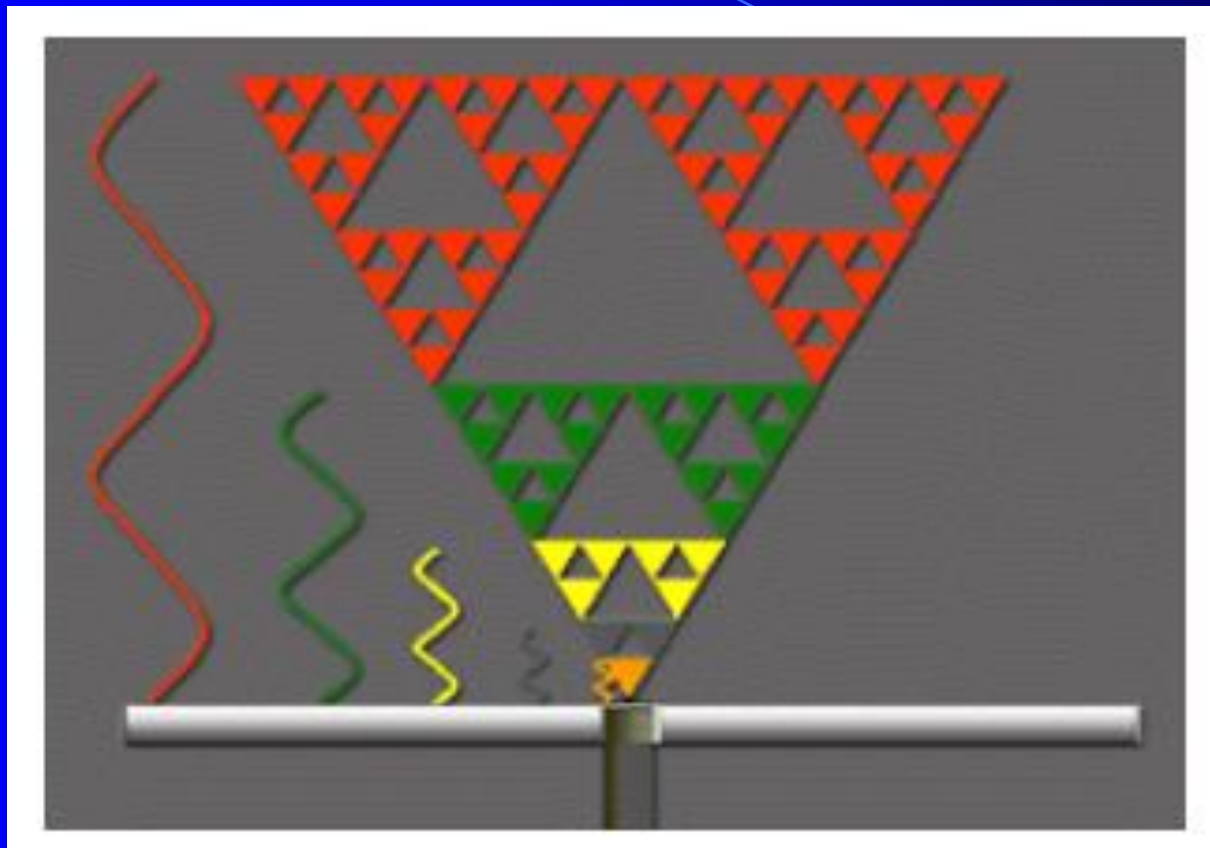

Which Fractals and Why?

Loops

Minimize Size

Increase Input Impedance

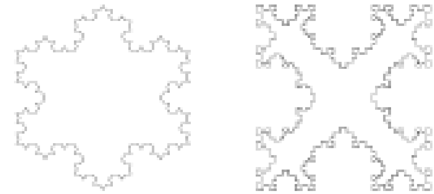

Dipoles

Minimize Heights

Increase Input Impedance

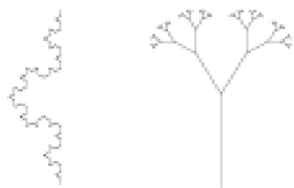

Dipoles

Multiband

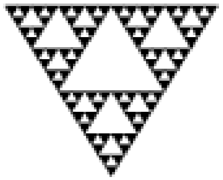

Small Fractal Loop Antennas

Main Benefit: Increased Input Impedance

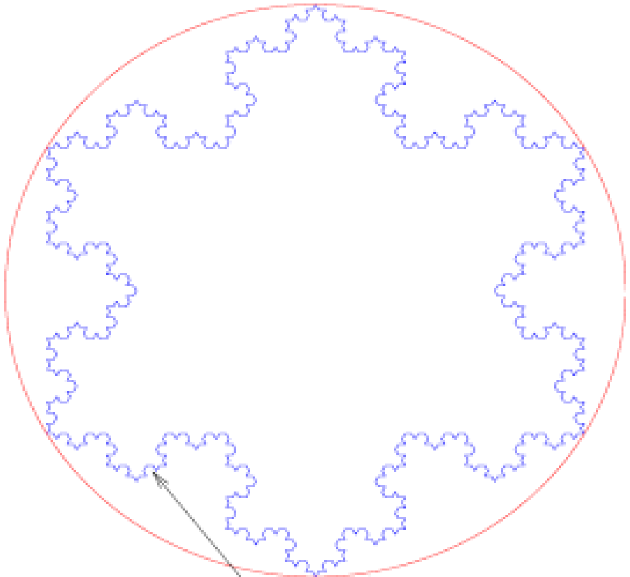

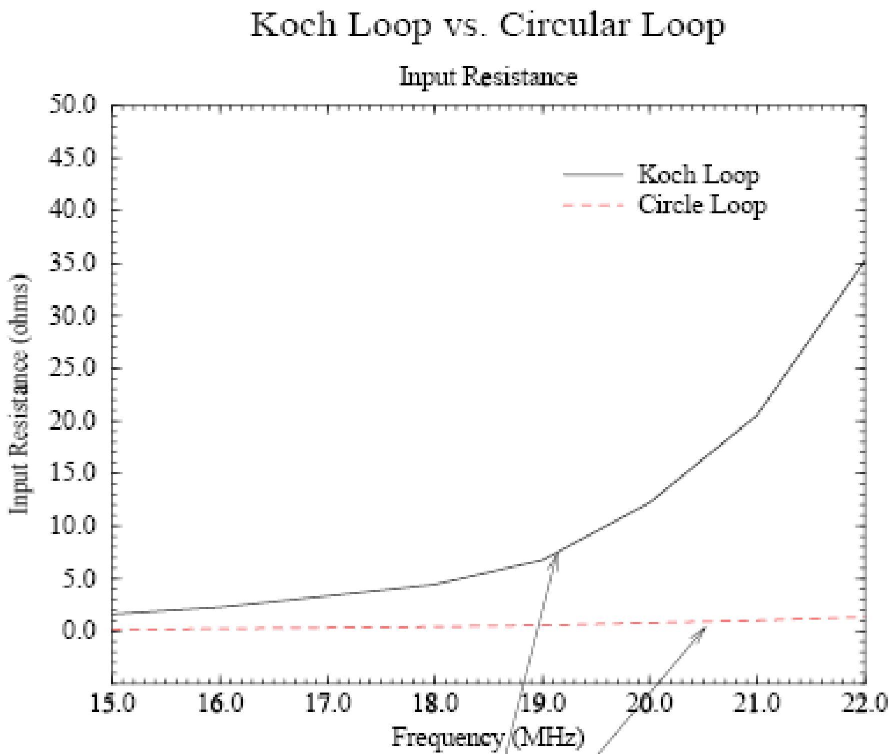

Both loops take up the same volume

But, the input impedance of the fractal loop is higher

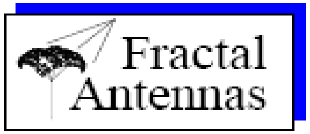

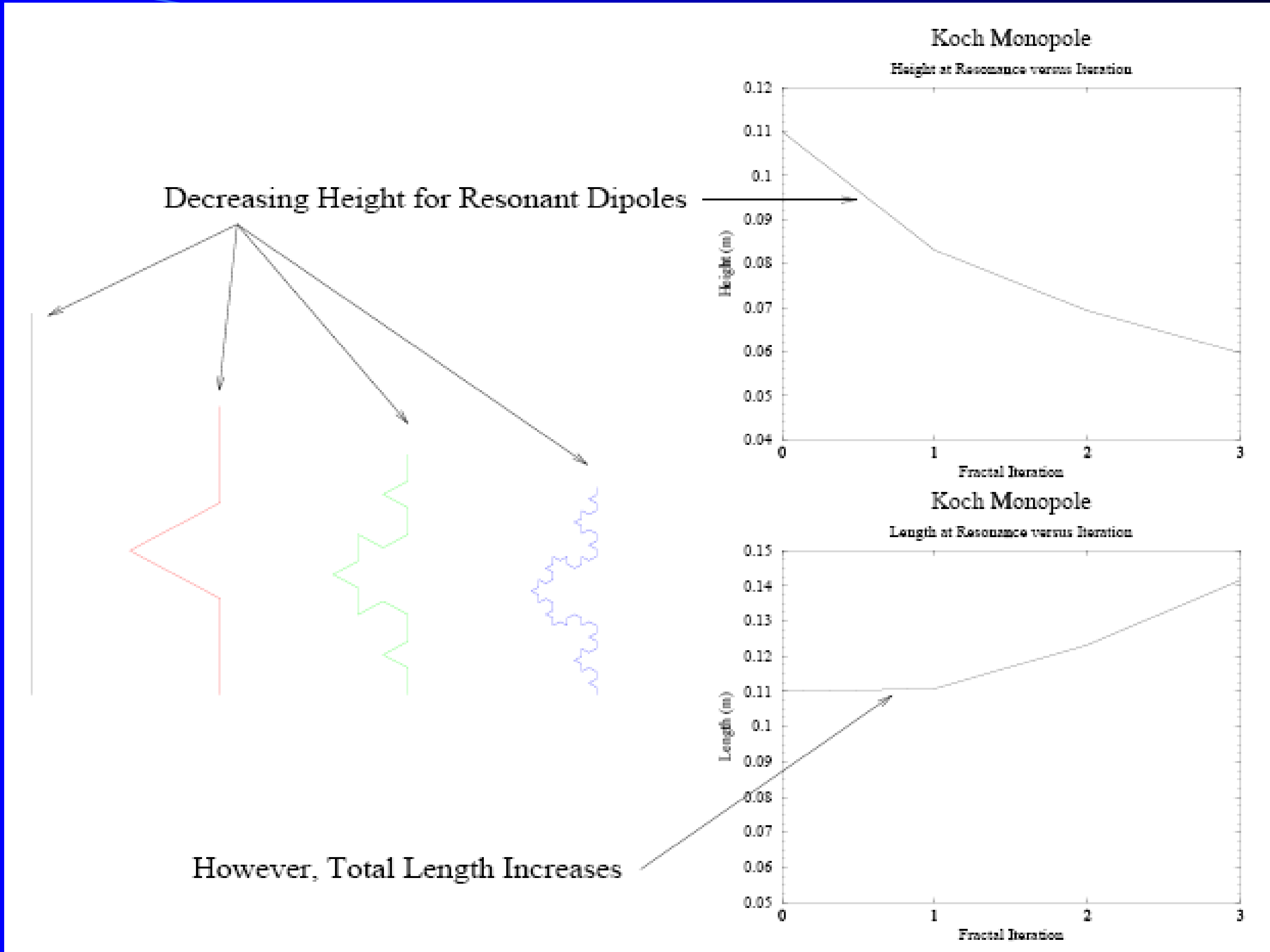
Decreasing Height for Resonant Dipoles
However, Total Length Increases
Koch Monopole
Height at Resonance versus Iteration
Height (m)
Fractal Iteration
Koch Monopole
Length at Resonance versus Iteration
Length (m)
Fractal Iteration

Main Benefit: Decreased Resonant Frequency

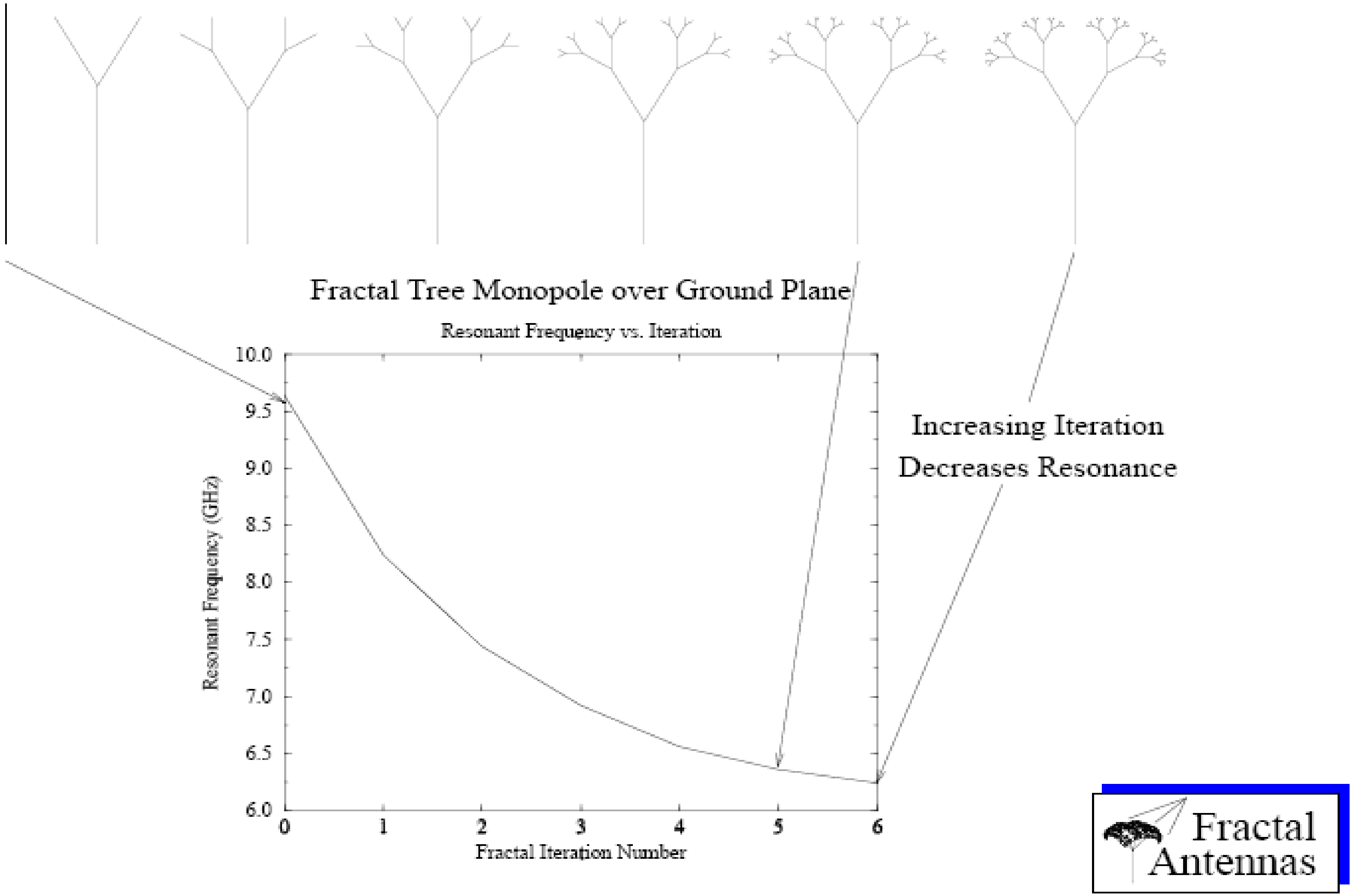

Main Benefit: Decreased Resonant Frequency

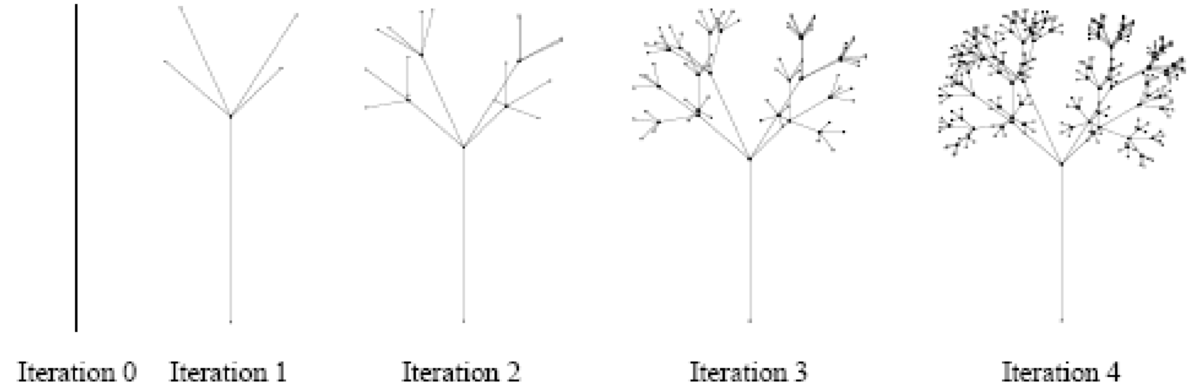

3D Fractal Tree

3D Fractal Tree

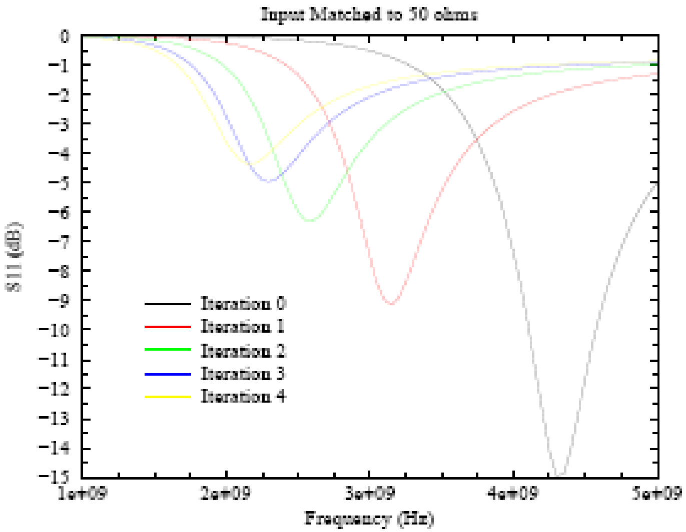

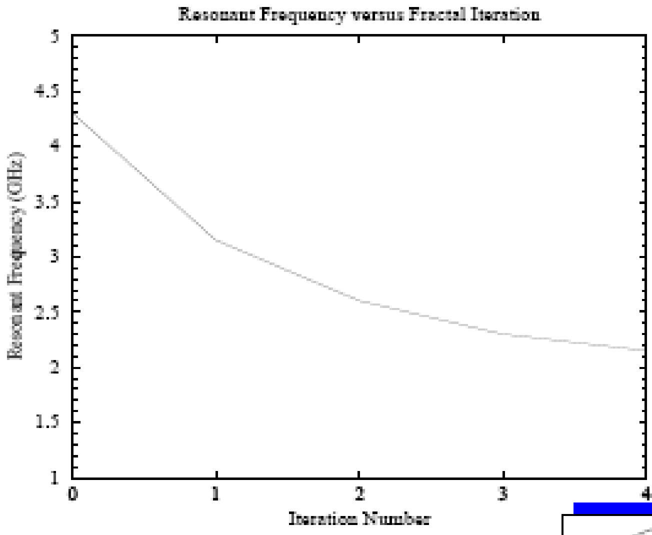

Fractal Antennas

Sierpinski Sieve Dipole Antennas

Main Benefit: Multiband

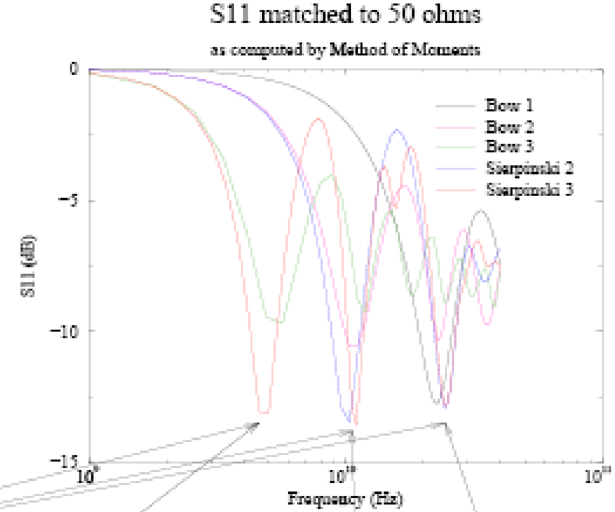

The 3 bands matched by 3 different bowtie dipoles
Are matched by 1 sierpinski dipole

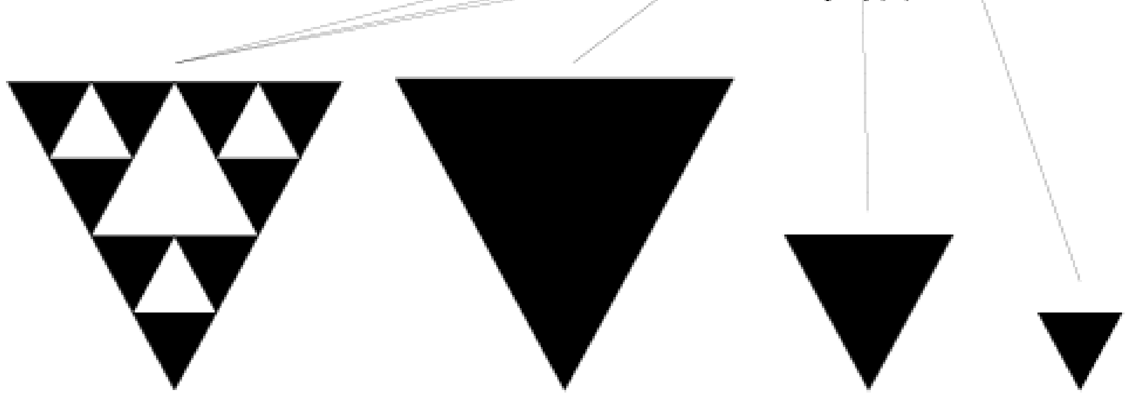

Fractal Antennas

Surface Currents Computed by Method of Moments

Surface Currents Clearly Show Multiband Behavior

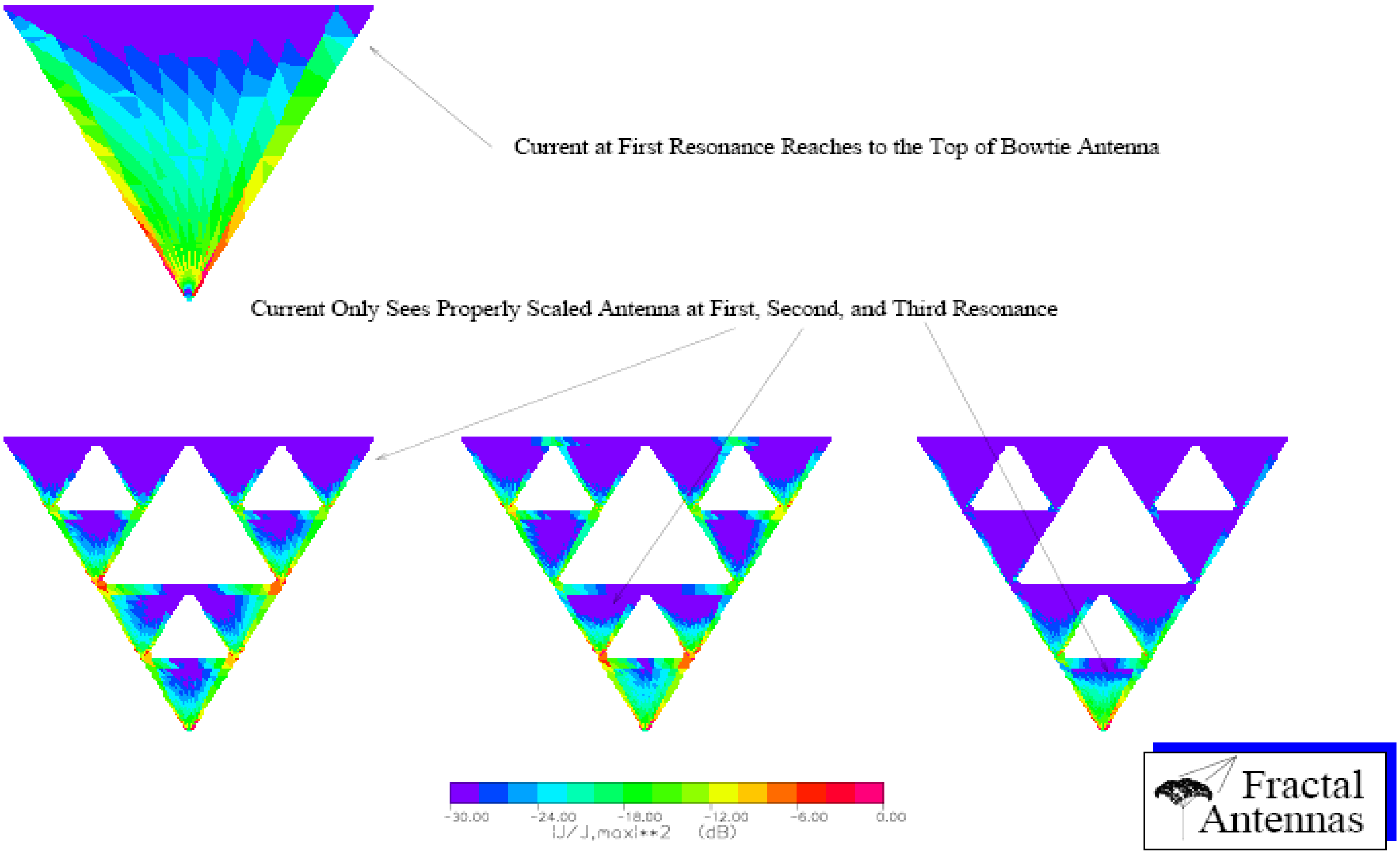

Fractal Square Loop Antennas

Main Benefit: Decreased Size

Decreased Antenna Width
Accompanies Increases in Iteration

For Second and Third Iteration

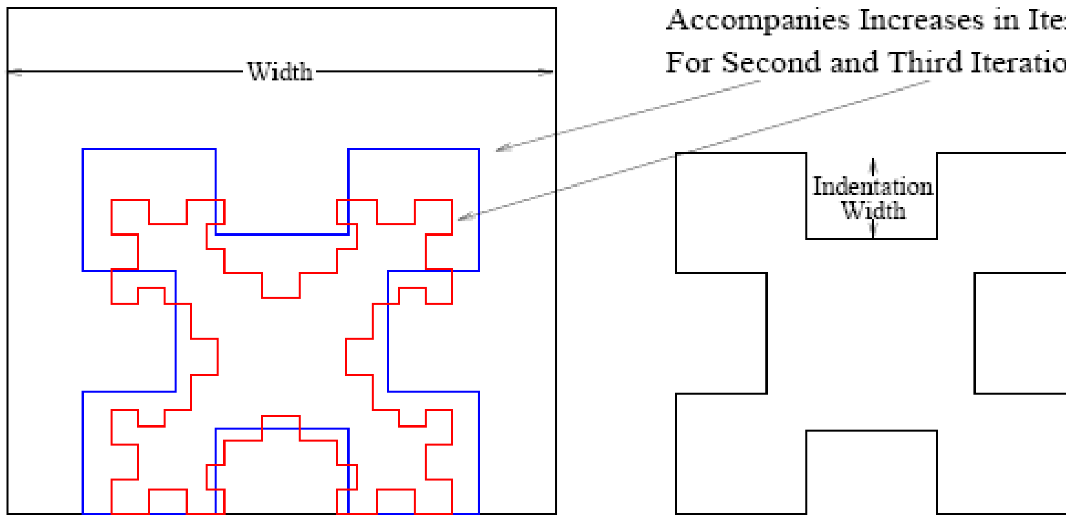

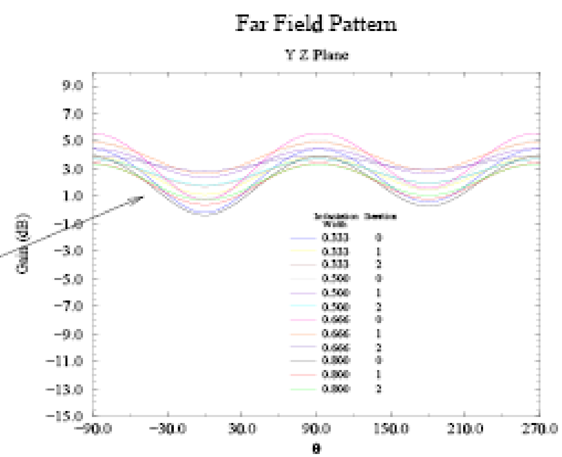

Far Field Pattern
Remains Similar
even with
Smaller Area

Fractal Antennas

Fractal Square Loop Antenna Design Curves

The Antenna can be Fabricated for a Given Iteration

$$Width = \frac{C}{e^{2*1.1}-1}$$

For a given indentation width, resonant loops can be designed using the above equation, where C is found empirically.

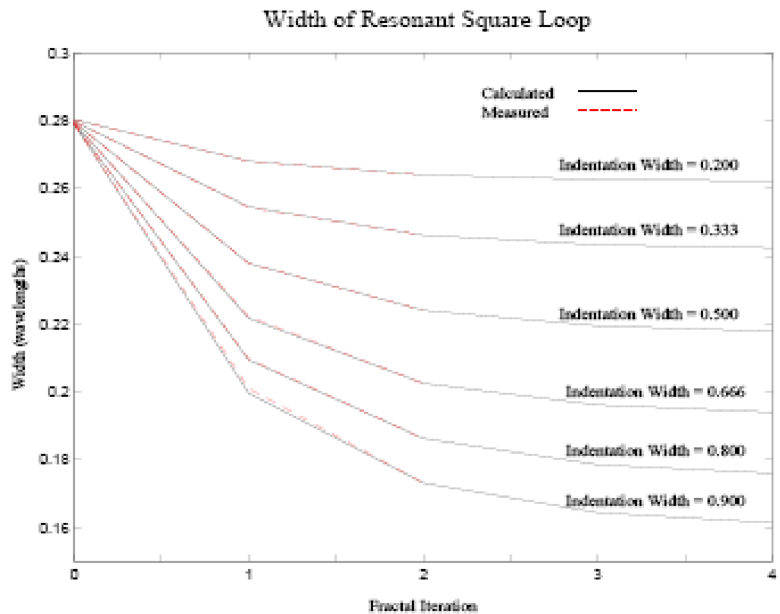

Fractal Antennas

Arrays with Fractal Elements

Main Benefit: Decreases Mutual Coupling between Elements

Separation Distance can be Maximized Using Fractal Elements

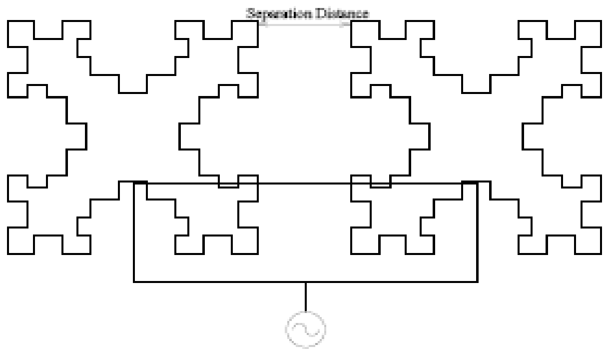

Thin Feeding Network for Fractal Array Elements

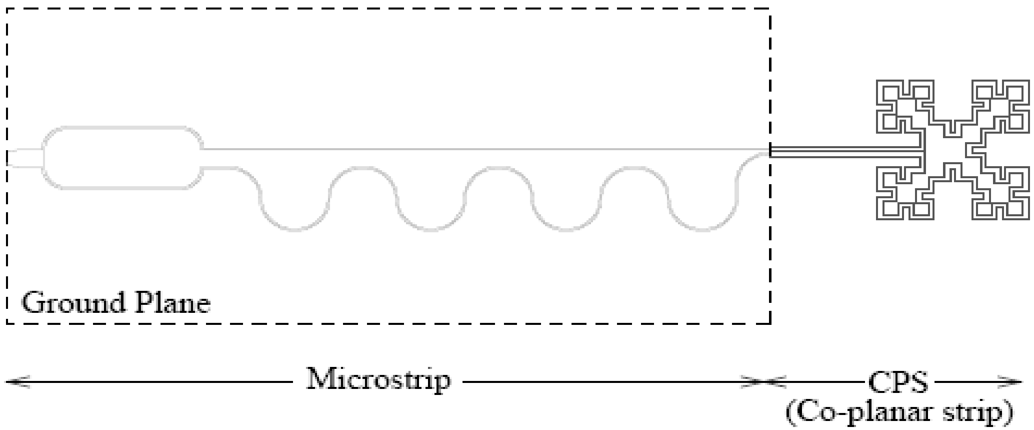

Fractal Antennas

John Gianvittorio - UCLA

Fabricated Fractal Array Antennas

Decreased inter-element coupling for fixed spacing

Increased packing ability with smaller fractal elements

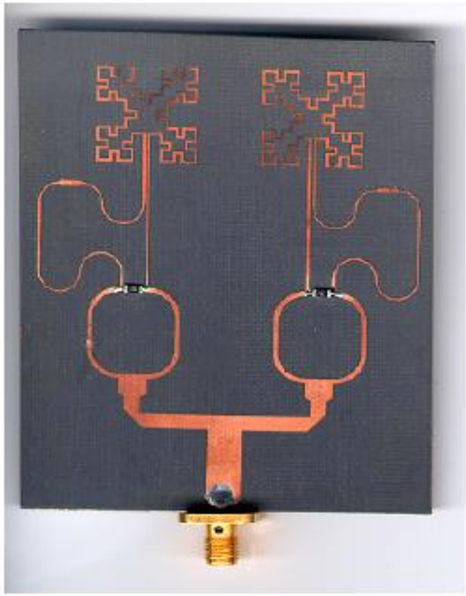

Fractal Array

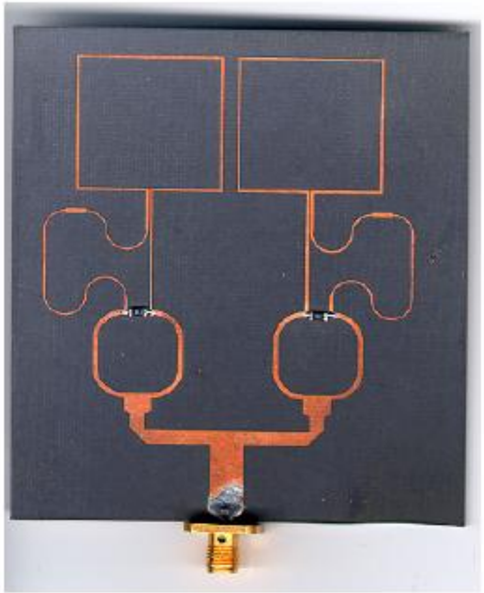

Standard Array

Fractal Antennas

Fractal antenna design

- **Sample fractal antenna elements:**

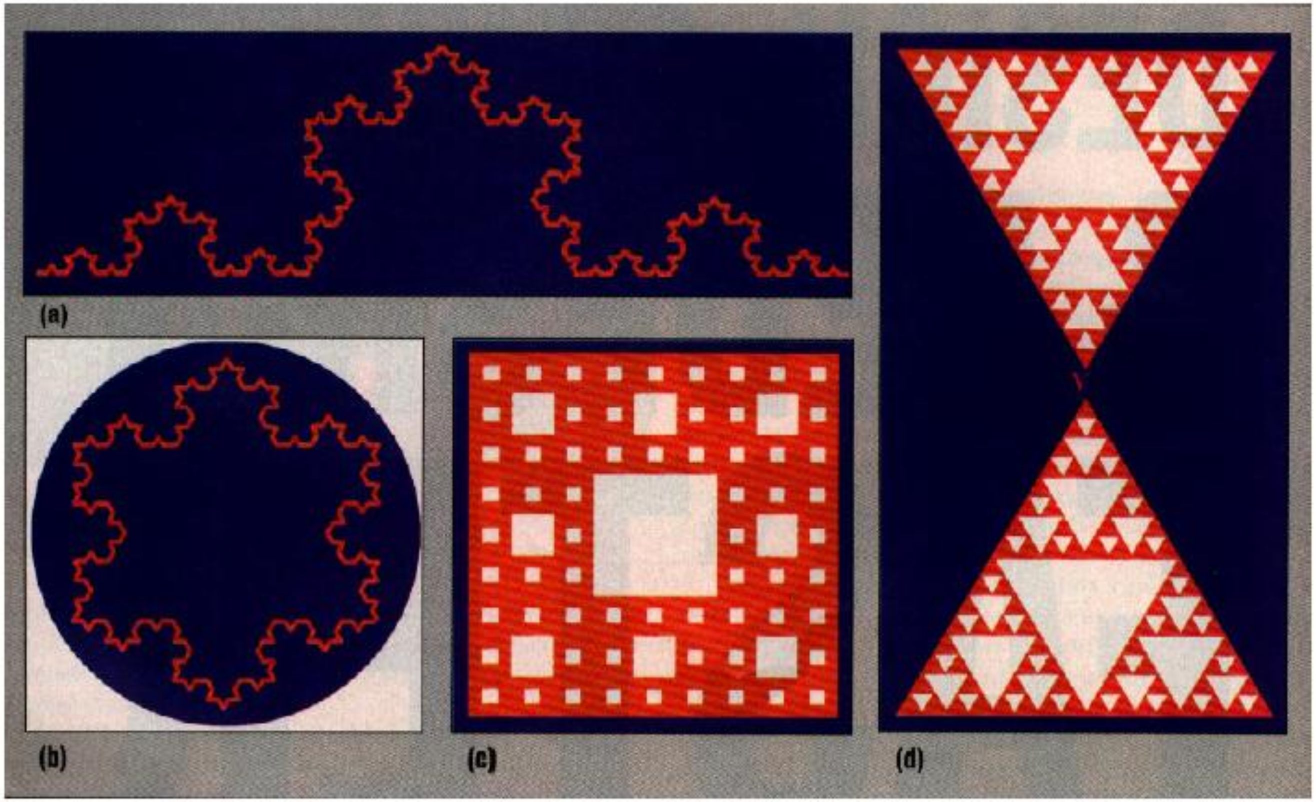

(a) Koch dipole (b) Koch loop (c) Cantor slot patch (d) Sierpinski dipole

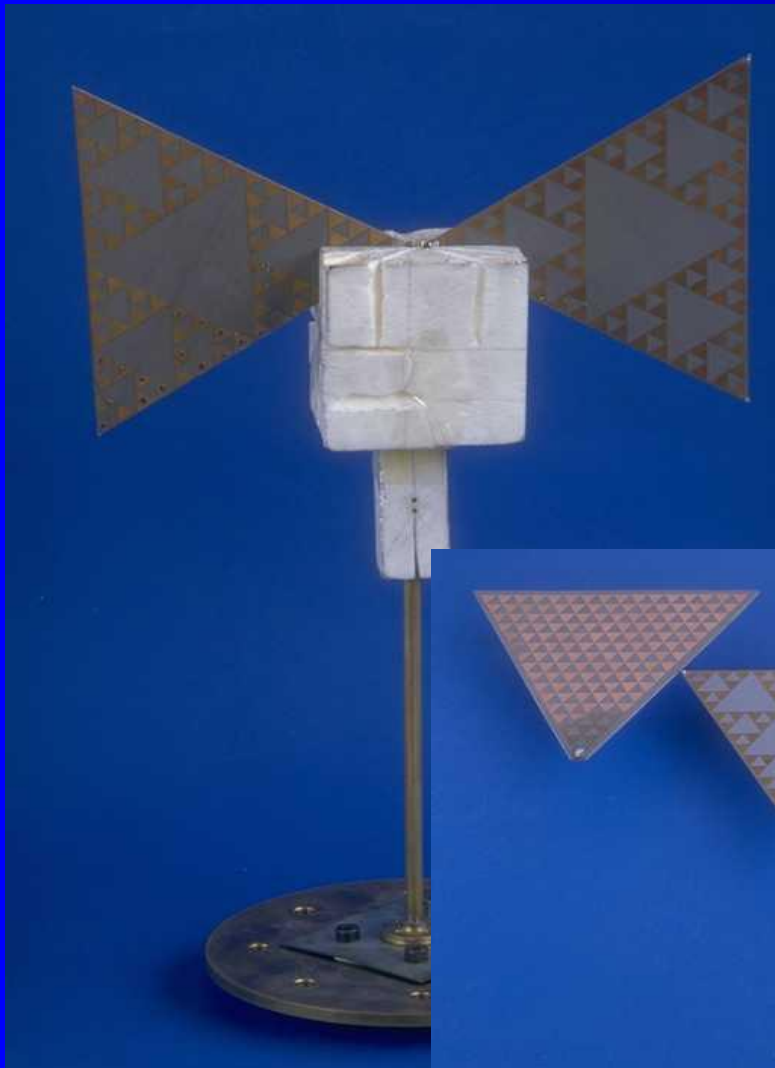
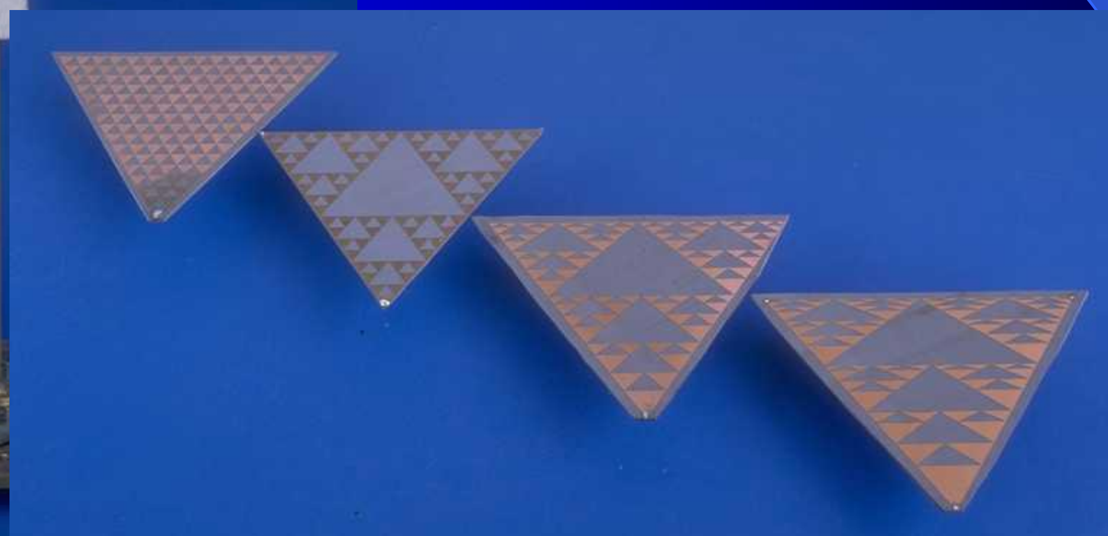

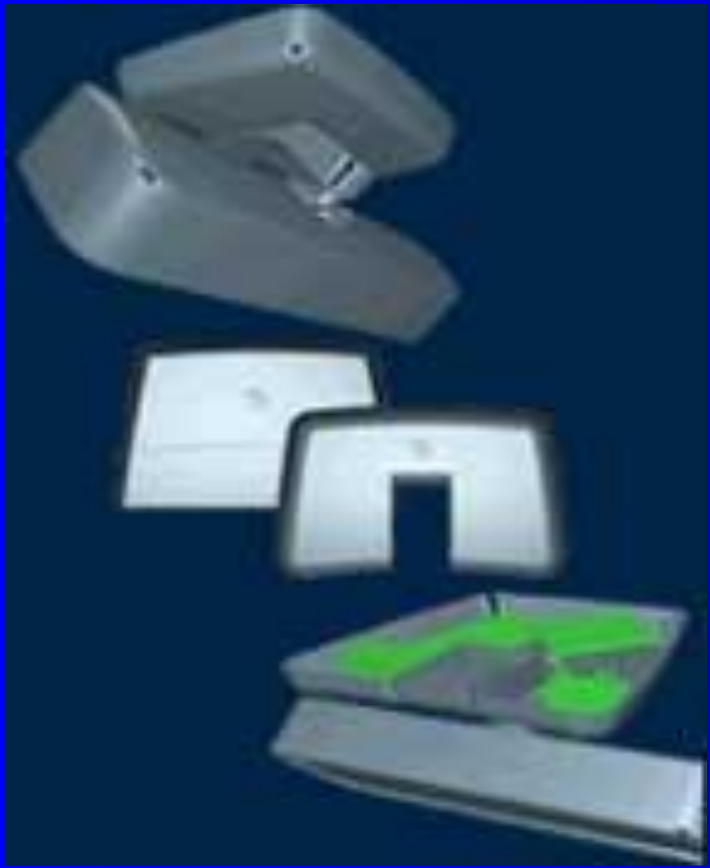

- Fractal antennas have superior multiband performance and are typically two-to-four times smaller than traditional aerials.
- Fractal antennas are the unique wideband enabler—one antenna replaces many.
- Multiband performance is at non-harmonic frequencies, and at higher frequencies the FEA is naturally broadband. Polarization and phasing of FEAs also are possible.

Fractal Antenna

- Practical shrinkage of 2-4 times are realizable for acceptable performance.
- Smaller, but even better performance

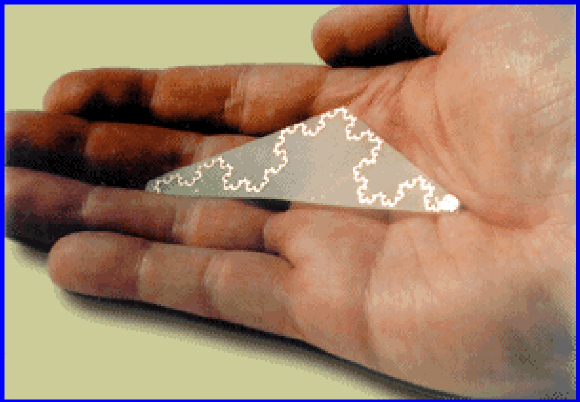

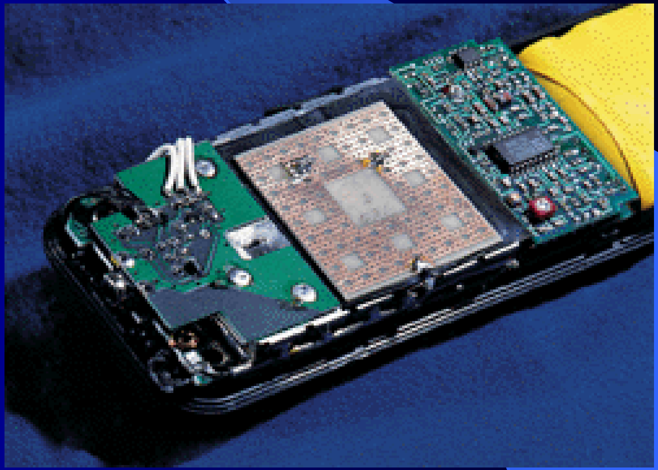

Visualization of antenna (the brown layer) integrated on a package substrate

AiP integrated on Bluetooth® adapter

Fractus® Julia-12 ISM 2.4 GHz VPol

P/N: FR03-02-N-0-002

The **JULIA-12 ISM 2.4 GHz panel antenna** is a cost effective solution with an excellent broad coverage in a tiny package. The antenna features an internal Fractal shaped element and is suitable for both indoor and outdoor aplications.

Frequency Range	2.4 - 2.5 GHz
Directivity/Gain	9.6 dBi / 8.8 dBi
Impedance	50 Ω
Polarisation	VPOL
F/B Ratio	> 18 dB
VSWR	< 1.5 : 1
Vertical Beamwith	65°
Horizontal Beamwith	70°
Connector (Pig Tail)	RP-TNC or RP-SMA
Radome	ABS
Dimensions	10 x 10 x 3 cm

Measured results from a standard

Patent Pending: WO0154225, WO0122528, PCT/EP01/10589, PCT/EP02/07837, US60/613394, US60/627653 and PCT/EP02/07836

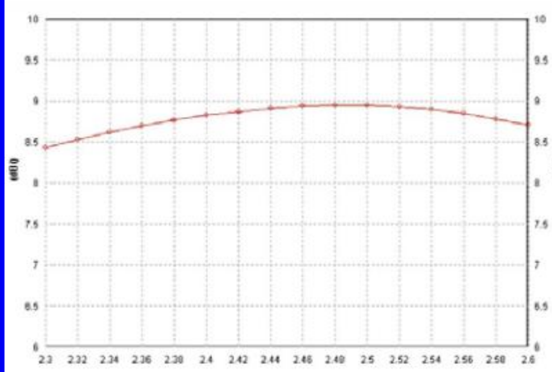

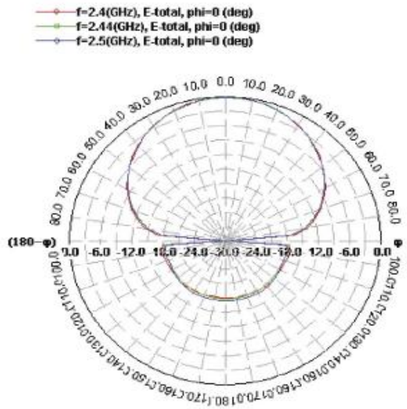

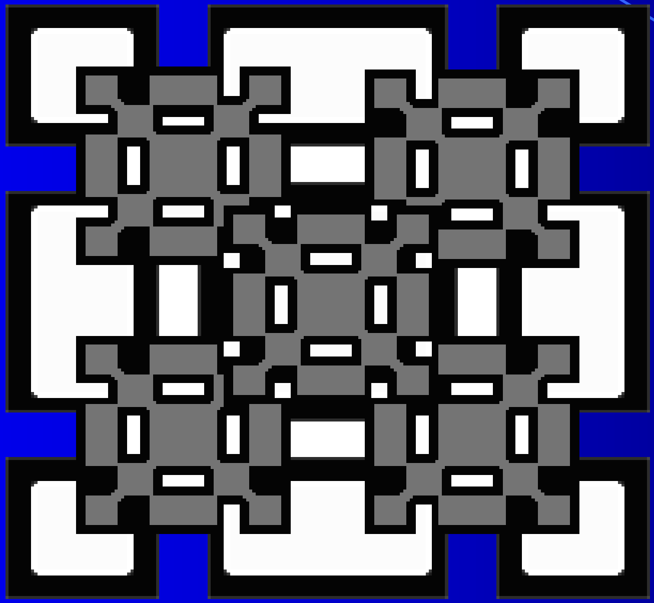

Fractus® Julia-10b ISM 2.4 GHz VPol — P/N: FR03-02-N-0-003

The **JULIA-10 ISM 2.4 GHz panel antenna** offers a superior gain to size ratio thanks to the Fractus' patented "Super Directive" patch design. JULIA-10 is the ideal choice to get extra range capacity in a tiny package.

Frequency Range	2.4 - 2.5 GHz
Directivity/Gain	16 dBi / 15 dBi
Impedance	50 Ω
Polarisation	VPOL
F/B Ratio	> 20 dB
VSWR	< 1.5 : 1
Vertical Beamwith	30°
Horizontal Beamwith	35°
Connector (Pig Tail)	RP-TNC or RP-SMA
Radome	ABS
Dimensions	21 x 21 x 3 cm

Measured results from a standard

Patent Pending: WO0154225, WO0122528, PCT/EP01/10589, PCT/EP02/07837, US60/613394, US60/627653 and PCT/EP02/07836

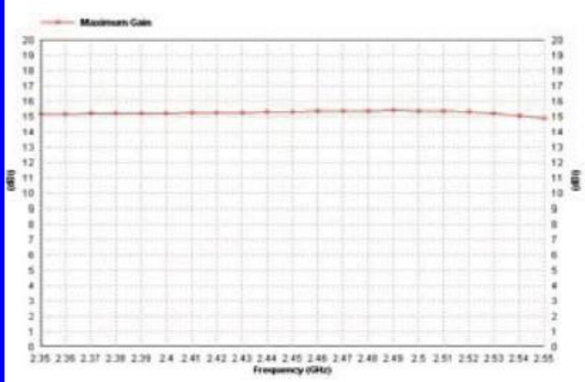

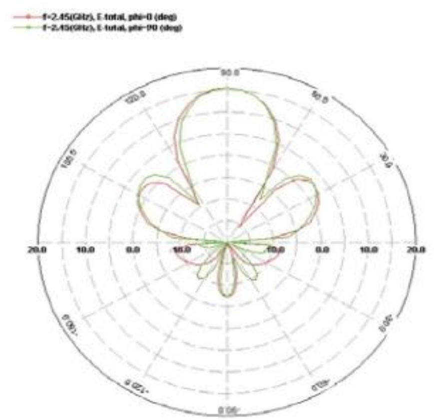

Fractal Geofind™ GPS Slim Chip Antenna — P/N: FR05-S1-E-0-103

The **Fractal Geofind** is an slim chip antenna engineered specifically for consumer electronic devices operating with GPS system where low-cost and robust performance is mandatory.

Taking advantage of the space-filling properties of fractals, this **small planar monopole** antenna is ideal for use low-cost consumer electronic devices to add personal location functionalities. The **Fractal Geofind GPS Slim Chip Antenna** speeds your time-to-market by allowing you to integrate it within your industrial design easily (SMD mounting) and efficiently.

10 x 10 x 0.9 mm (image karger than actual size)

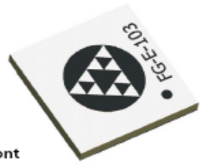

Front

Back

Patent Pending: WO0154225, WO0122528, PCT/EP01/10589, PCT/EP02/07837, US60/613394, US60/627653 and PCT/EP02/07836

Product Benefits

High performance/price ratio

Raises your device's competitiveness by increasing satellite sensitivity and decreasing your device's BoM cost.

Omnidirectional pattern

Optimises device usage due to a uniform radiation pattern.

Small Volume

Allows integration into space limited areas easily and efficiently.

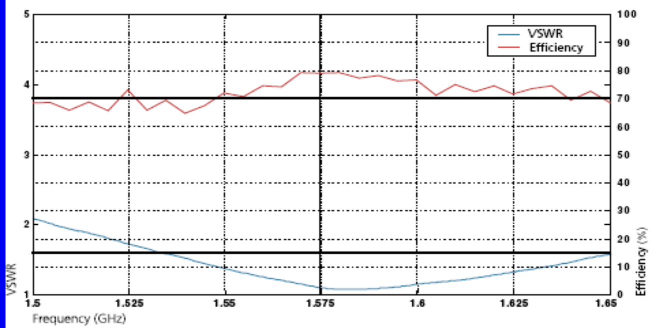

Frequency Range	1575 MHz
Efficiency	> 70 %
Peak Gain	> 1 dBi
VSWR	< 1.6:1
Weight	0.20 g
Temperature	-40 to +85 °C
Impedance	50 Ω unbalanced
Dimensions	10 x 10 x 0.9 mm

Measured results from a standard PCB of 70x30 mm

Please contact your sales representative at Richardson Electronics to obtain additional information on recommended configurations for different UWB devices.
Richardson Electronics: **www.rell.com** Fractus: **wireless@fractus.com** Reference: **DS_FR05-S1-E-0-103_v01**

Fractus® Compact Reach Xtend™ Chip Antenna — P/N: FR05-S1-N-0-102

The **Fractus Compact Reach Xtend Chip Antenna** for Bluetooth® and 802.11 b/g WLAN is a tiny rectangular 3D-shaped antenna suitable for headset, compact flash (CF), secure digital (SD) and other small PCB devices operating at 2.4 GHz where high performance and low-cost are mandatory. Its broad bandwidth ensures high quality signal reception and transmission across wireless devices and different plastic housing designs.

Taking advantage of the space-filling properties of fractals, this **small monopole** antenna is ideal for use within indoor (highly scattered) environments. The **Fractus Compact Reach Xtend Chip Antenna** speeds your time to market by allowing you to easily integrate it within your industrial design (SMD mounting).

7 x 3 x 2 mm (image larger than actual size)

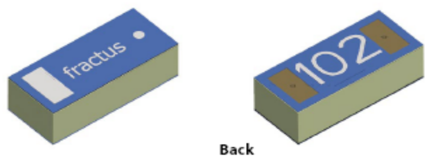

Front **Back**

Patent Pending: WO0154225, WO0122528, PCT/EP01/10589, PCT/EP02/07837, US60/613394, US60/627653 and PCT/EP02/07836

Product Benefits

Small form factor

Allows integration into space limited areas easily and efficiently with minimum clearance area.

Broad bandwidth

Ensures robust performance when considering different plastic housing and close body proximity.

Omnidirectional pattern

Optimises device usage due to a uniform radiation pattern.

Multi-mode support

Works for Bluetooth, and Wi-Fi 802.11b and g standards.

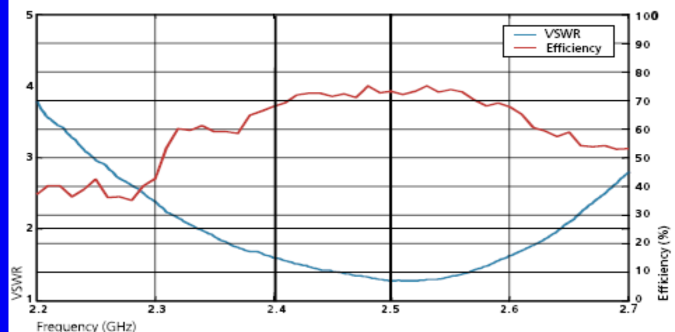

Frequency Range	2.4 - 2.5 GHz
Efficiency	> 70 %
Peak Gain	> 1 dBi
VSWR	< 2:1
Weight	0.20 g
Temperature	-40 to +85 °C
Impedance	50 Ω unbalanced
Dimensions	10 x 10 x 0.8 mm

Measured results from a standard PCB of 47x23 mm

Please contact your sales representative at Richardson Electronics to obtain additional information on recommended configurations for different UWB devices.
Richardson Electronics: **www.rell.com** Fractus: **wireless@fractus.com** Reference: **DS_FR05-S1-N-0-102_v01**

Fractus® EZConnect™ Zigbee™ Chip Antenna — P/N: FR05-S1-R-0-105

The Fractus **EZConnect Zigbee Chip Antenna** is a compact rectangular antenna suitable for smart home, security and other industrial devices using the 915 MHz ISM band, where low power consumption and cost are top of mind.Taking advantage of the space-filling properties of fractals, this **compact monopole** antenna is ideal for use within indoor (highly scattered) as well as outdoor environments.

The **Fractus EZConnect Zigbee Chip Antenna** speeds your time to market by allowing you to easily integrate it within your industrial design (SMD mounting).

18 x 7,3 x 1 mm (image larger than actual size)

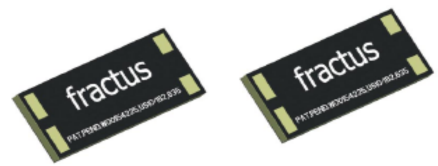

Front **Back**

Patent Pending: WO0154225, WO0122528, PCT/EP01/10589, PCT/EP02/07837, US60/613394, US60/627653 and PCT/EP02/07836

Product Benefits

Small form factor

Allows integration into space limited areas easily and effectively.

Broad bandwidth

Ensures robust performance in different PCB dimensions and plastic housing, without the need for a matching network.

High performance

Optimises power consumption and increases device range.

Omnidirectional pattern

Increases device robustness due to a uniform radiation pattern.

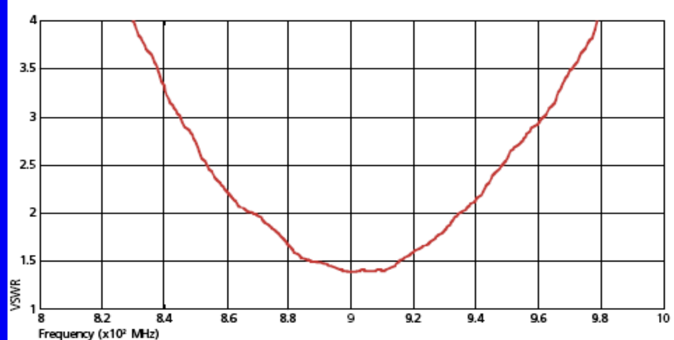

Frequency Range	902 - 928 MHz
Efficiency	> 40 %
Peak Gain	> 0 dBi
VSWR	< 2:1
Weight	0.20 g
Temperature	-40 to +85 °C
Impedance	50 Ω unbalanced
Dimensions	18 x 7,3 x 1 mm

Measured results from a standard PCB of 120x65 mm

Please contact your sales representative at Richardson Electronics to obtain additional information on recommended configurations for different UWB devices.
Richardson Electronics: **www.rell.com** Fractus: **wireless@fractus.com** Reference: **DS_FR05-S1-E-0-105_v01**

Customised Mobile Handset Antenna
Pat. Pending: WO012258, VS2002140615, WO0154225, VS10/182,635

Fractus Compact Dual-Band Reach XtendTM WLAM 802.11 a/b/g/j/n Chip Antenna 2.4 & 5GHz

FRACTAL ANTENNA SYSTEMS INC

Electronic Warfare

UAB™ Antenna

Extreme wideband and omnidirectional performance with superior gain. Operates with or without a ground plane over a 25:1 frequency range, from VHF to microwave. Compact form factor packaged in a 7.7 inch-diameter, 10 inch-high radome weighing 4.8 pounds. Up to 250W input power. VSWR less than 2:1.

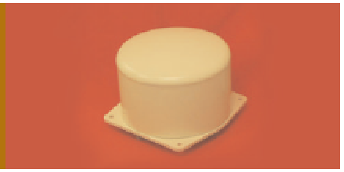

UAD™ Antenna

Extreme wideband performance with up to 250W power handling and superior gain. Operates over UHF to microwave. Low profile of 5.7 inches and easily concealable in a 7.7 inch-diameter radome. VSWR less than 2:1.

UGS™ Antenna

Single antenna integrated with an unattended ground sensor (UGS) providing superior omnidirectional long-range performance. Operates over high HF through VHF. Innovative raised phase center design minimizes ground losses, while improving radiation pattern and launch angle. Easily deployed in a compact, lightweight package measuring 2.5 inches in diameter and 3 feet in height.

RFsabre™

With outstanding lower frequency gain and less than 3:1 VSWR over a very wide frequency range, the RFsabre antenna delivers great performance in a distinctly compact form factor. The vehicle-mounted version can survive impacts with solid objects at speeds up to 25 MPH. Geared for security, communications, signal gathering, and high power transmit applications. New hanging or tripod mounted versions available.

TRANZTENNA™

Breakthrough performance in a wideband antenna from the fractal antenna innovators

Fractal antenna technology, implemented in transparent conductive film, makes covert capability possible with a mission-capable antenna system that operates over a huge frequency range.

- Outstanding gain
- Transparent
- Conformable
- Only 13 x 18 inches
- VSWR less than 3:1
- Inherently 50 Ohms
- Optional frequency lowering panels

Signal intelligence warfighters face a difficult challenge — the need to monitor communications over a very wide frequency range while remaining clandestine. Current electronic surveillance systems employ multiple antennas that are either large or noisy. Covertness and high performance are united in the Tranztenna™ optically transparent antenna: an extremely wideband antenna designed for vehicle or building window placement. This conformable, rugged, compact antenna is easy to transport and install in field operations. New missions to intercept and monitor enemy communications are possible with this breakthrough in transparent antenna technology.

Feature	Advantage	Benefit
Transparent	Visually unobtrusive	Covert use of antenna in vehicle or building window
Good Gain	Superior to ITO films	Excellent signal-to-noise ratio
Wideband	Operation over very wide frequency range	Instantaneously access most spectrum of interest
Compact Size	Effective use of small window apertures	Access to lower frequencies
Conformable	Flexible sheet	Easy transport and deployment

135 South Road
Bedford, MA 01730 USA
781-275-2300
www.fractenna.com

GPS / GSM Antenna

- **Detailed Product Description**
- Features:
- 1) Item no.: GS-205
- 2) Frequency: GPS 1,575MHz ± 3MHz
- 3) Band width: ±5MHz
- 4) Impedance: 50Ω
- 5) SWI: 1.5:1
- 6) Gain: >3dBi
- 7) Cable: RG-174
- 8) Frequency: GSM 890-960MHz, 1,710-1,990MHz
- 9) Impedance: 50Ω
- 10) SWI: <2
- 11) Gain: 2.15dBi
- 12) Cable: RG-174
- 13) Frequency: 76-110MHz (FM), 525-1,700kHz (AM)
- 14) Gain: +20dB (FM), +5dB (AM)
- 15) Impedance: 75 ohms
- 16) Cable: 3C-2V
- 17) Voltage: 10-14V
- 20) Fits for VW, GM, Audi, BWM and Peugeot

G-Antetech Industrial Co., Ltd

- **Detailed Product Description**
- Item no.: GS-208 Frequency:
- GPS 1,575MHz+/-3MHz
- Band width: +/-5MHz
- Impedance: 50Ω SWIR: 1.5:1
- Gain: >3dBi
- Cable: RG174
- Frequency: 76-110MHz (FM), 525-1,700MHz (AM)
- Gain: +20dB (FM), +5dB (AM)
- Impedance: 75Ω Cable: 3C-2V
- Voltage: 10-14V Cable length: 8"
- Dia. of installation hole: diameter 15mm

Shanghai Sky Year Technology Co., Ltd.

The only patented AM/FM roof mounted shark fin antenna that completely integrates GPS, GSM, AMPS/PCS and satellite radio frequencies

Data Compression

- A color full-screen GIF image of Mandelbrot Set occupies about 35 kilobytes
- Formula z = z^2 + c, 7 bytes! (99.98%)
- It could work for any other photos as well
- The goal is too find functions, each of which produces some part of the image.
- IFS (Iterated function system) is the key.

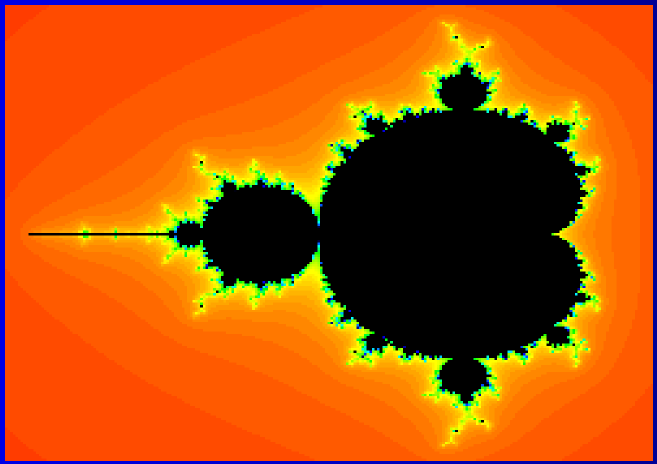

RF ID applications

- RFID tag antenna, dubbed Tagtenna antenna for 900 MHz.

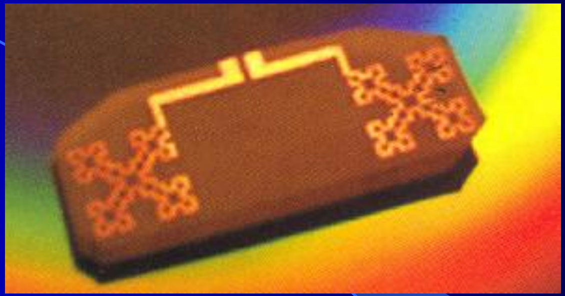

- Readtenna RFID antenna that is 1/3 the form factor area of a patch antenna of equal performance. This FEA is a microstrip patch based on a fractalised ground plane and a Sierpinski carpet fractal.

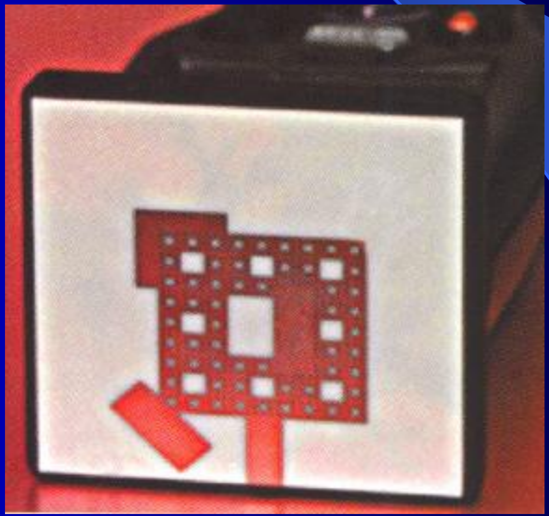

TagtennaTM and ReadtennaTM antennas are available in evaluation kits from Fractal Antenna Systems, Inc.
The antennas are protected by US *patents* 6140975, 6127977, *and* 6104349 *and pending patents* US *and foreign.*

Enhanced Read-out distance

In a recent study carried out by researchers at the Tampere University of Technology's Rauma Research Unit, in Finland, a fractal UHF RFID handheld reader antenna performed better than traditional antenna designs. The research findings were published in a paper entitled "Read Range Performance Comparison of Compact Reader Antennas for a Handheld UHF RFID Reader," in the April 2007 edition of the online magazine *IEEE Applications & Practices*.

How far can we scale down the fractal structures?
What is the smallest feature size of a microelectonic fractal object?

HARD LIMIT !!!
FRACTAL ELECTRODYNAMICS !!

Fractal electrodynamics

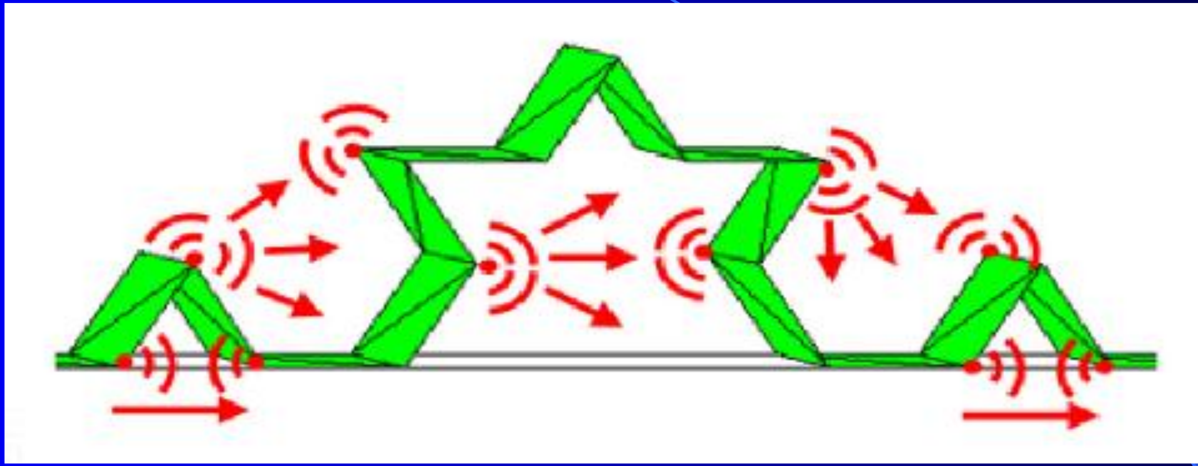

The angles radiate a spherical wave with phase center at the vertex. Each angle not only radiates, but also receives the signal radiated by other angles. As a consequence, part of the signal does not follow the wire path, but takes "shortcuts" that start at a radiating angle. The length of the path traveled by the signal is, therefore, shorter than the total wire length. The higher iteration number in the Koch antenna, the more angles it has and the closer to each other they are, so the more signal takes shortcuts and the less signal follows the whole curve path.

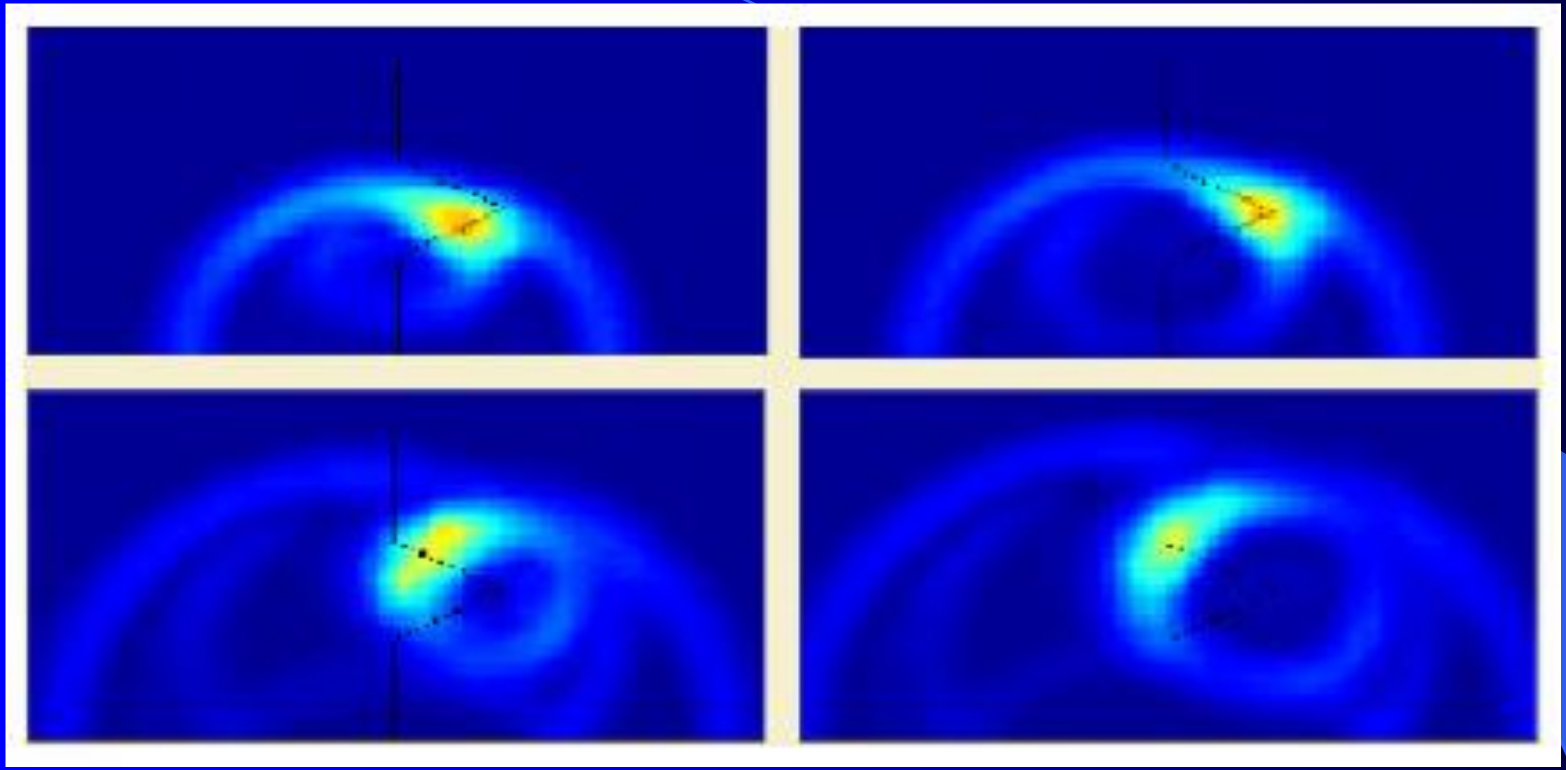

Near fields in the time domain in the vicinity of a single-iteration Koch monopole (K1) with short-pulse excitation. The sharp angles of the pre-fractal curve become the center of spherical wave radiation, which corroborates the coupling or shortcut effect hypothesis.

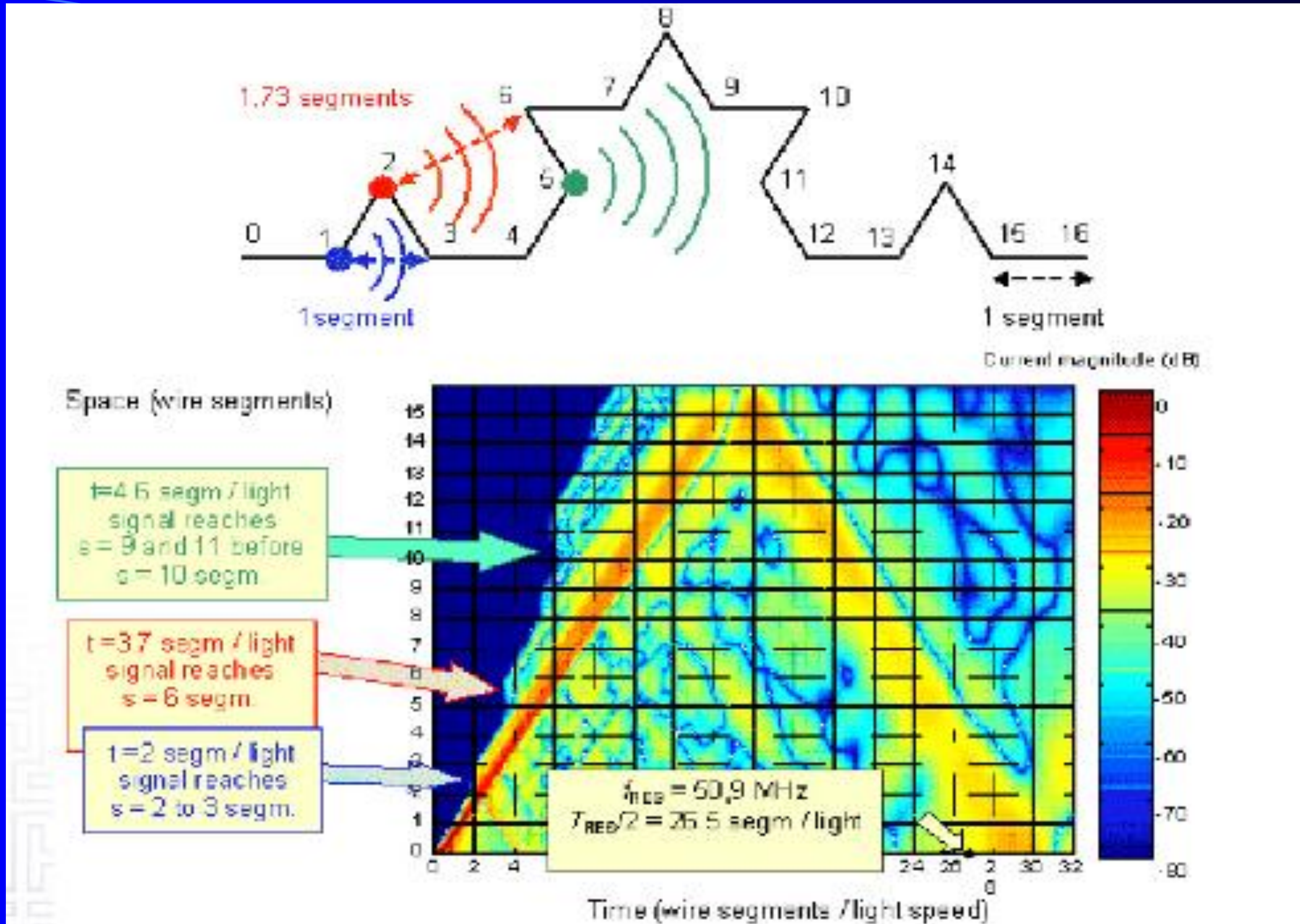

Figure 7: Space time-diagram for short-pulse excitation in a 1m-height K2 monopole. The antenna has been modeled as a thin wire using DOTIG code from University of Granada. The signal shortcuts from angles 1 to 3 (blue color), 2 to 6 (red color) and 5 to 9 (green color) can be clearly observed.

Entering nano and tera

If we cannot decrease the feature size what is the use of fractal geometries?

Change the fractal paradigm!

Do not build „artificial" fractals –

Use fractal nature of surfaces created in new technologies!

how to make nanonet transistors ?

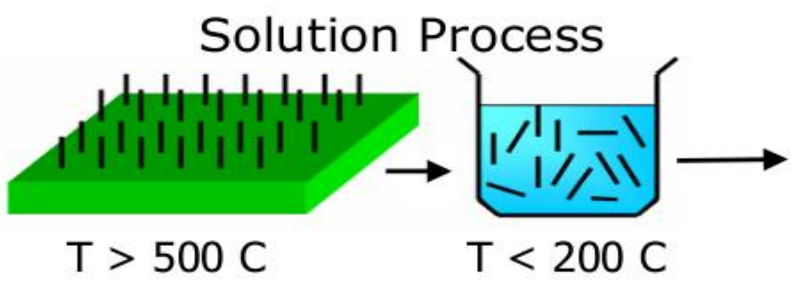

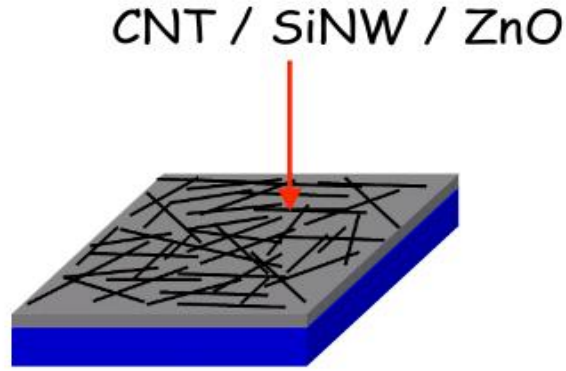

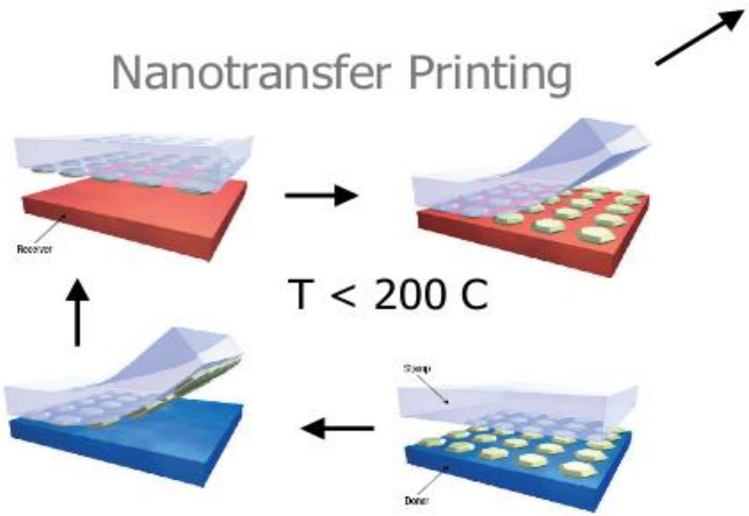

Advantages

- Highly crystalline CNT / SiNW by high temperature process
- Plastic, glass or organic substrate :
  Low temperature final step
- Transparent and conducting

- Rogers et al, Nature 2006

Short Channel nanonet transistors

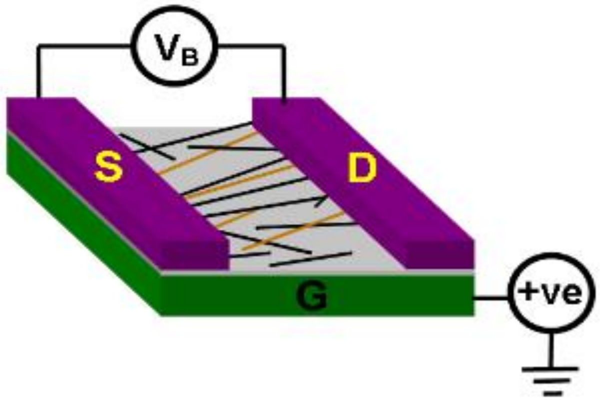

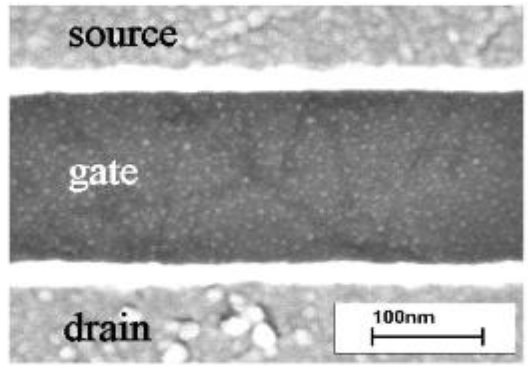

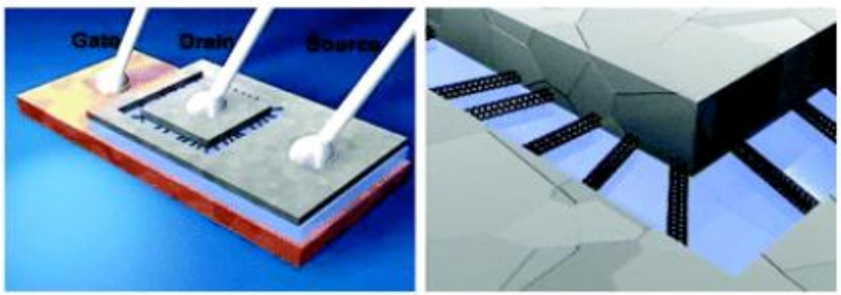

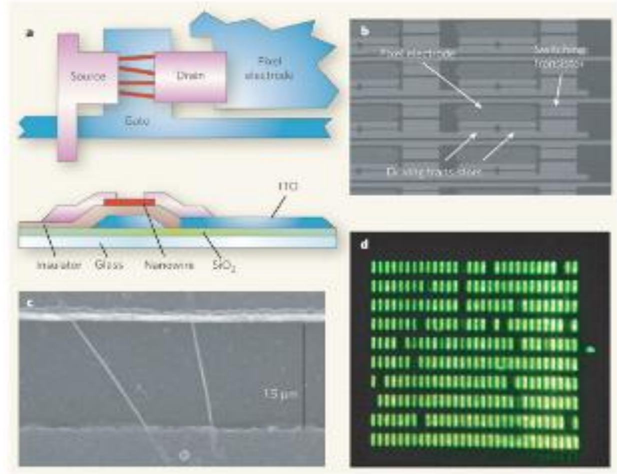

Seidel, NanoLetters, 2004.

Janes, Nature Nanotech, 2008.

Stick – fan model

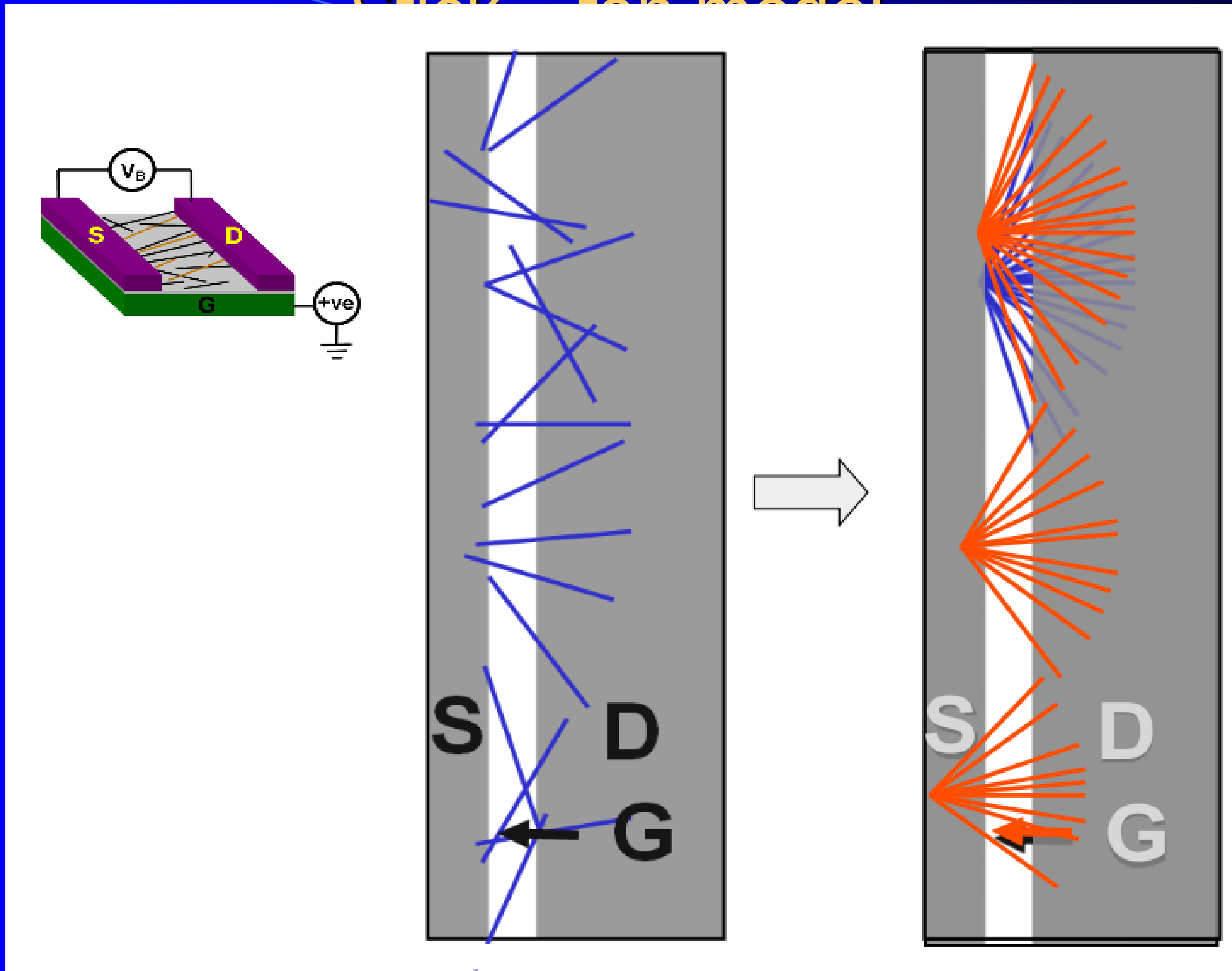

Long channel nanonet transistors

$$\sum_i \nabla^2\Phi_i + \frac{\rho_i}{\varepsilon} = \frac{d^2\Phi_i}{ds^2} + \frac{\rho_i}{\varepsilon} + \sum_{j\neq i}\frac{\Phi_j-\Phi_i}{\lambda_{ij}^2} - \frac{\Phi_i - V_G}{\lambda^2} = 0$$

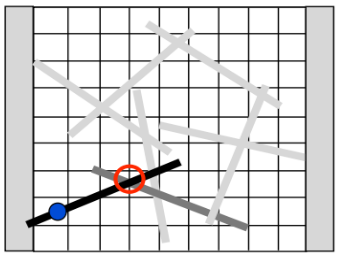

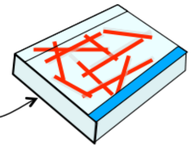

$$J_{n,i} = qn\mu E - qD\frac{dn}{ds}$$

$$\sum_i \frac{dJ_{n,i}}{ds} - \sum_{i\neq j} c_{ij}^n (n_i - n_j) = 0$$

- Analytical solution not possible
- Self consistent numerical DD-Poisson solver
- Solve for hundreds of configuration
- Solve for various biases

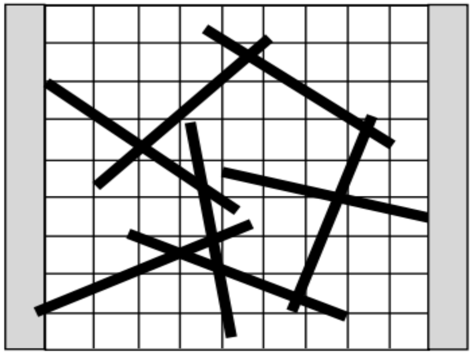

Simulator at www.nanohub.org as 'NanoNET'

the end of Ohm's law …

$$I_D = f(V_D, V_G) \times \xi\left(\frac{L_S}{L_C}, DL_S^{\,2}\right)$$

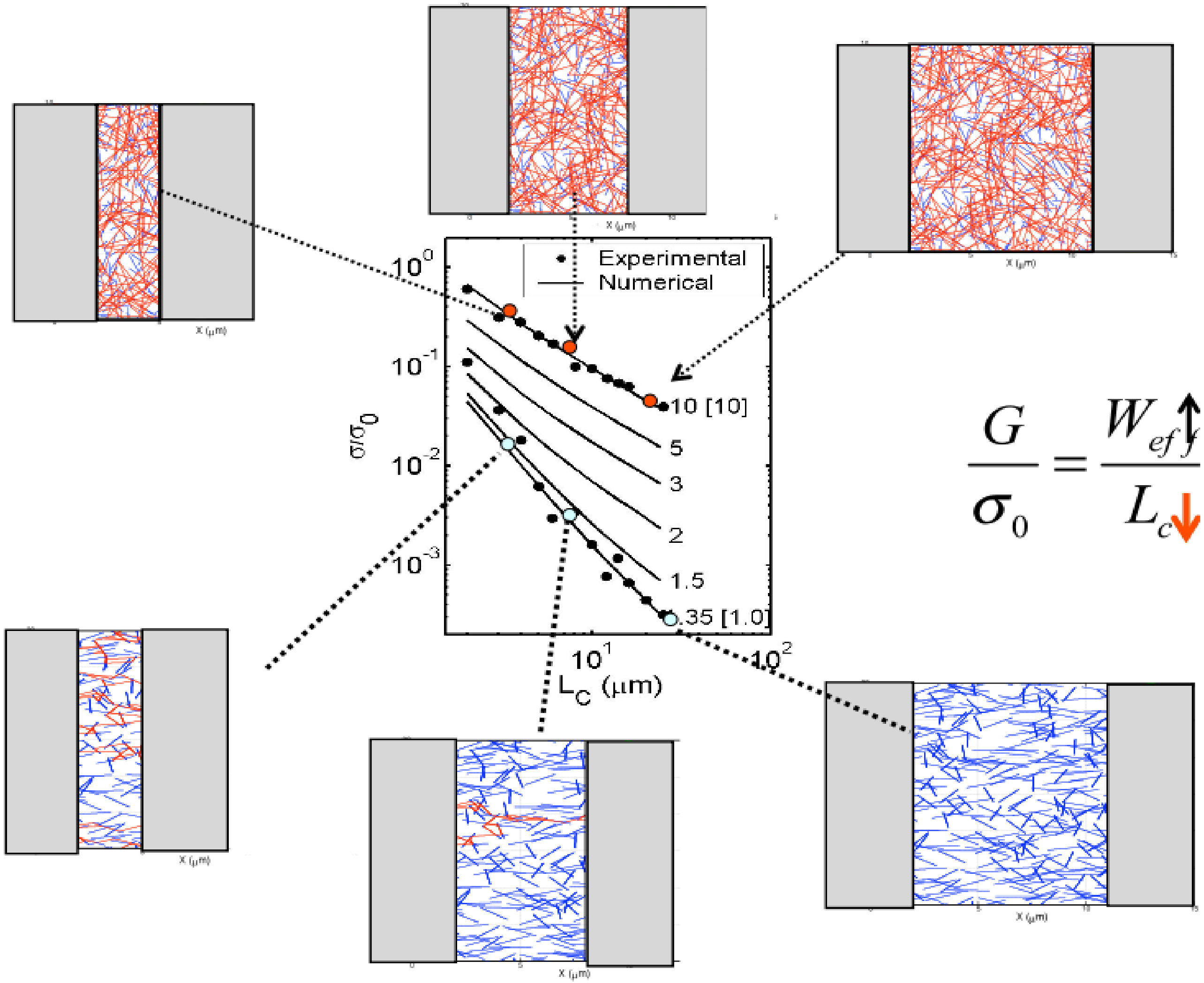

$$\frac{G}{\sigma_0} = \frac{W_{eff}}{L_c}$$

$$G \sim \sigma_{row} p^{L} \frac{W}{L}$$

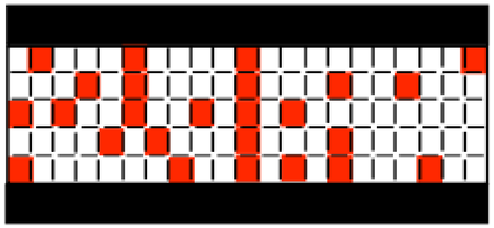

$$G \sim \sigma_{row} \frac{W}{L^{\alpha}}$$

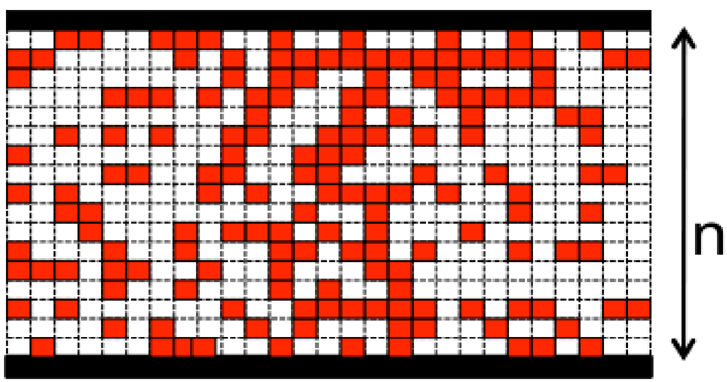

$$G = \frac{2q^2}{\pi^2 \hbar} D_C L_S \left[\sqrt{1 - \left(\frac{L_C}{L_S} \right)^2} - \frac{L_C}{L_S} \cos^{-1} \frac{L_C}{L_S} \right]$$

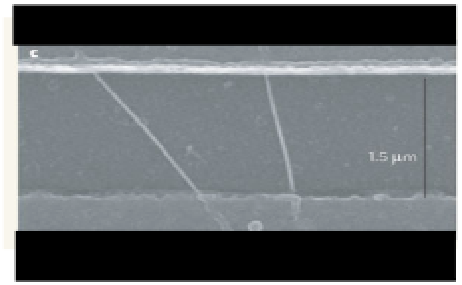

$$G \sim \frac{1}{L_S} \left(\frac{L_S}{L_C} \right)^{m(DL_S^2)}$$

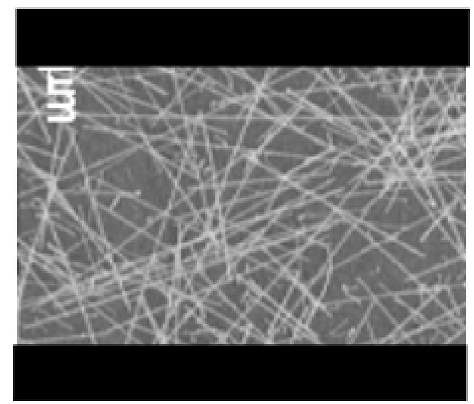

2D to 2D Cantor transform

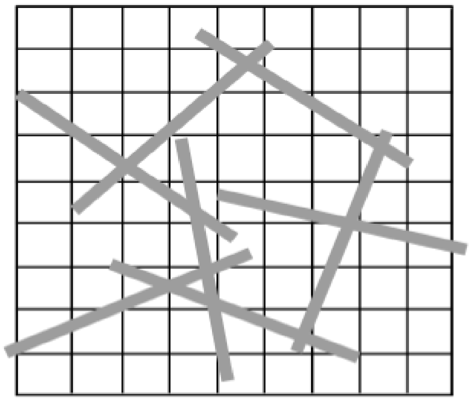

$D_{F,CT}= D_{F,stick}$

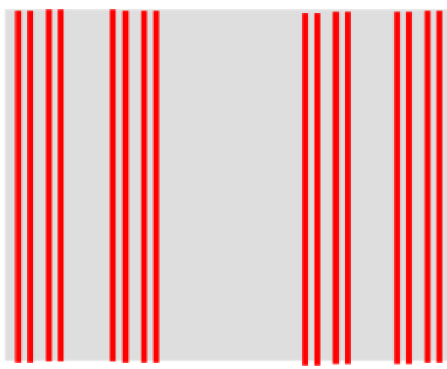

$D_{F,CT}=1+\log(m)/\log(n)$

For $D_{F,stick}=1.5$

Let m=2, solve for n:

$\log(n)=\log(2)/(D_{F,stick}-1)$

Result: n=4

Generation algorithm:

Take a line segment

Remove the fraction (n-2)/n

from its centre (result: $\frac{1}{2}$)

repeat …

After : Lectures of M. A. Alam
Electrical and Computer Engineering, Purdue University
2009 NCN@Purdue-Intel Summer School

Fractal analysis of quantum dots

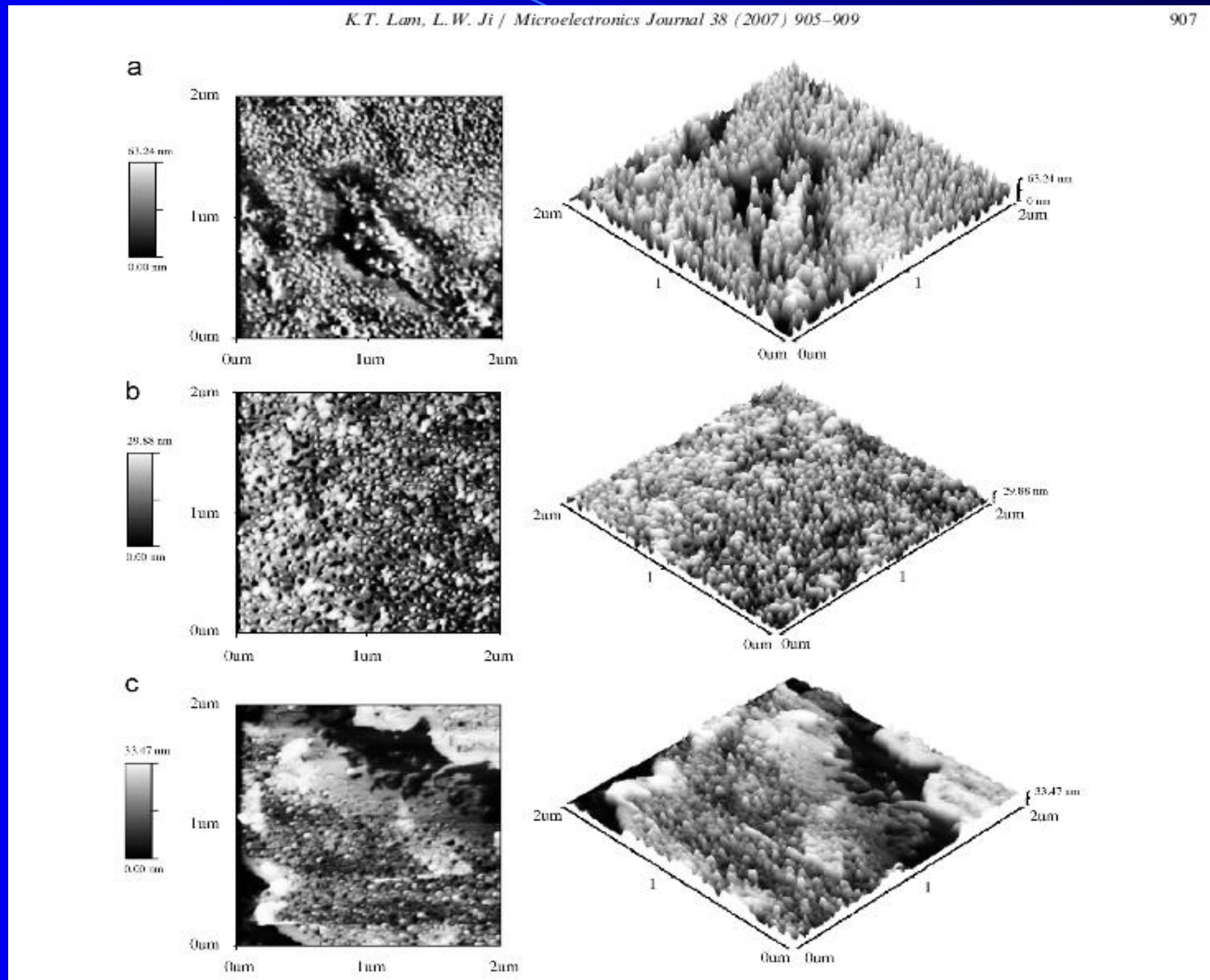

Fig. 1. 2000 × 2000 nm^2 AFM images of (a) sample A, (b) sample B (annealed at 750 °C) and (c) sample C (annealed at 800 °C), respectively.

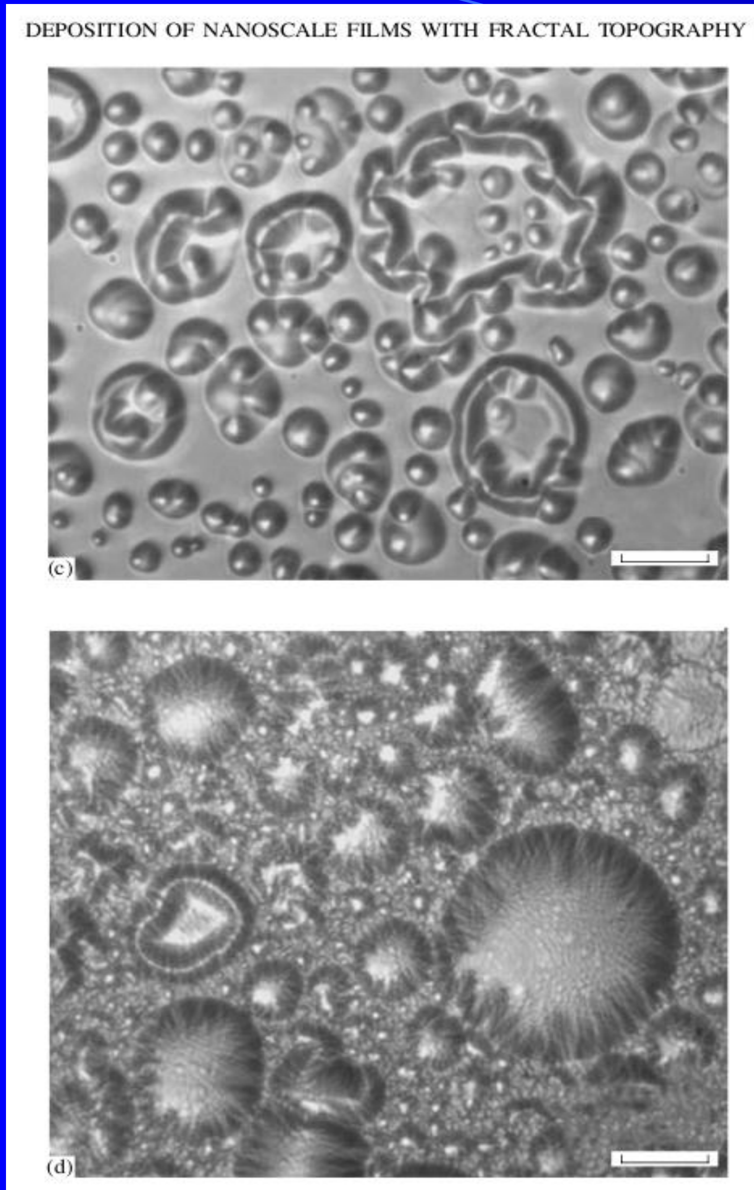
DEPOSITION OF NANOSCALE FILMS WITH FRACTAL TOPOGRAPHY
(c)
(d)

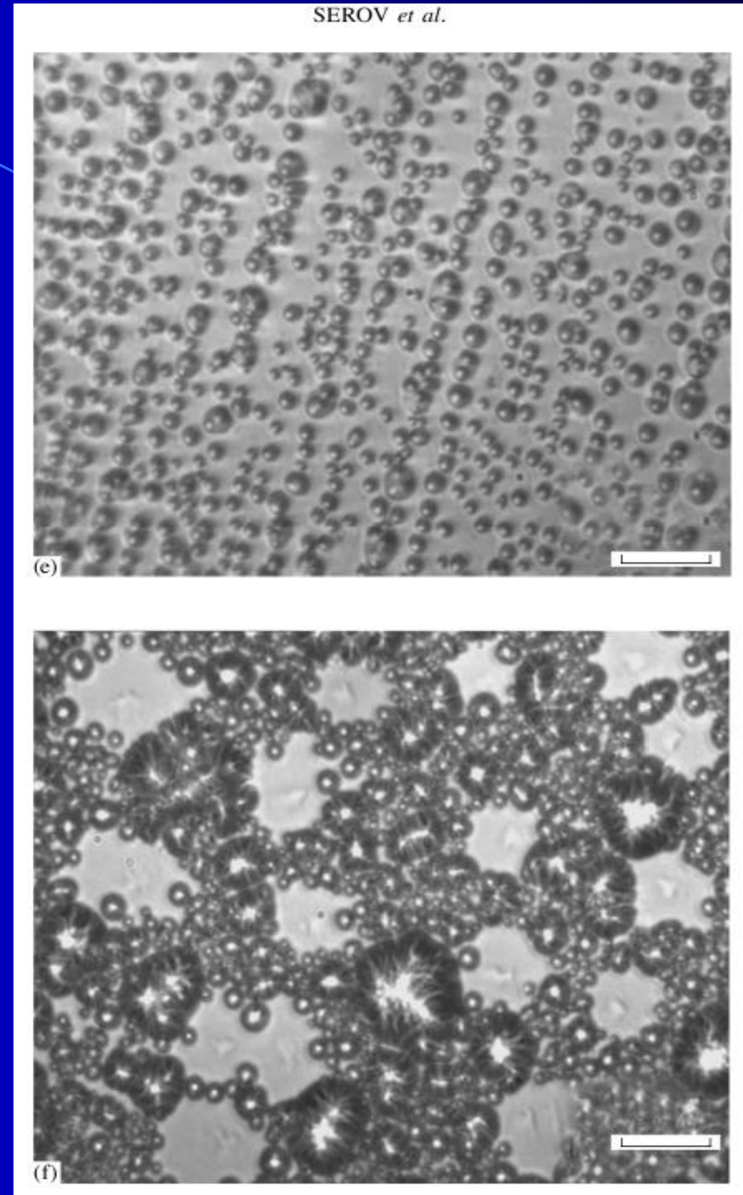
SEROV et al.
(e)
(f)

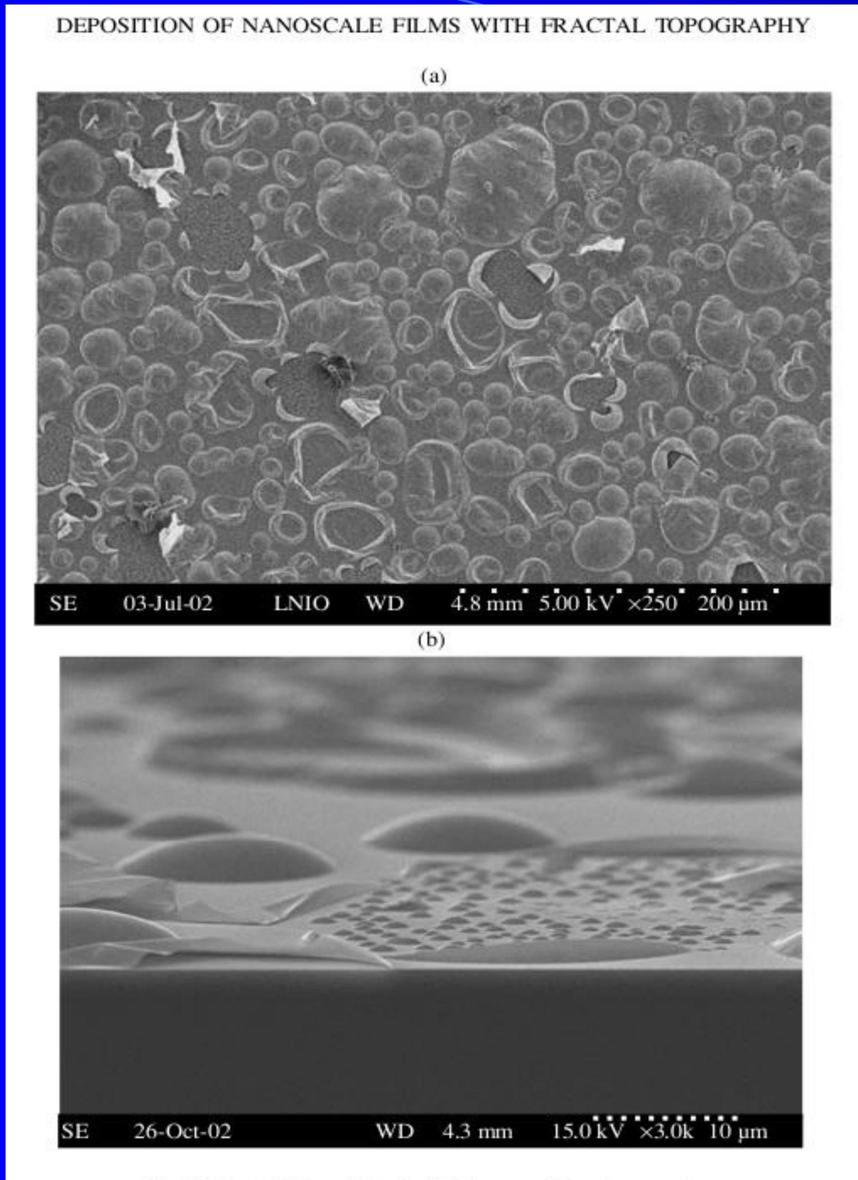
DEPOSITION OF NANOSCALE FILMS WITH FRACTAL TOPOGRAPHY
(a)
SE 03-Jul-02 LNIO WD 4.8 mm 5.00 kV ×250 200 μm
(b)
SE 26-Oct-02 WD 4.3 mm 15.0 kV ×3.0k 10 μm

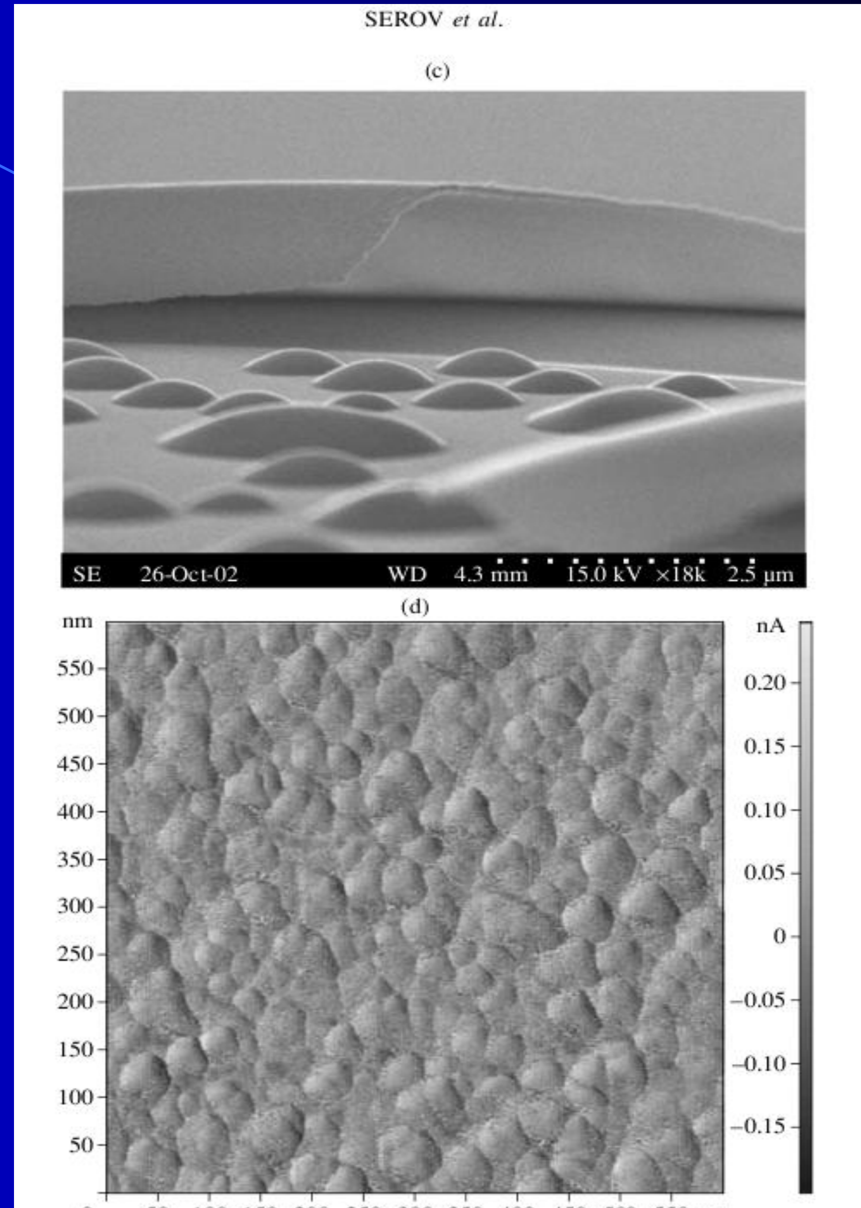
SEROV et al.
(c)
SE 26-Oct-02 WD 4.3 mm 15.0 kV ×18k 2.5 μm
(d)
nm
550
500
450
400
350
300
250
200
150
100
50
nA
0.20
0.15
0.10
0.05
0
−0.05
−0.10
−0.15

One of very few descriptors is

FRACTAL DIMENSION !!

nature nanotechnology

LETTERS

CORRECTED ONLINE: 31 MARCH 2009
PUBLISHED ONLINE: 15 MARCH 2009 | DOI: 10.1038/NNANO.2009.37

Nanotubular metal–insulator–metal capacitor arrays for energy storage

Parag Banerjee[1,2], Israel Perez[1,2], Laurent Henn-Lecordier[1,2], Sang Bok Lee[3,4]* and Gary W. Rubloff[1,2,5]*

NATURE NANOTECHNOLOGY DOI: 10.1038/NNANO.2009.37

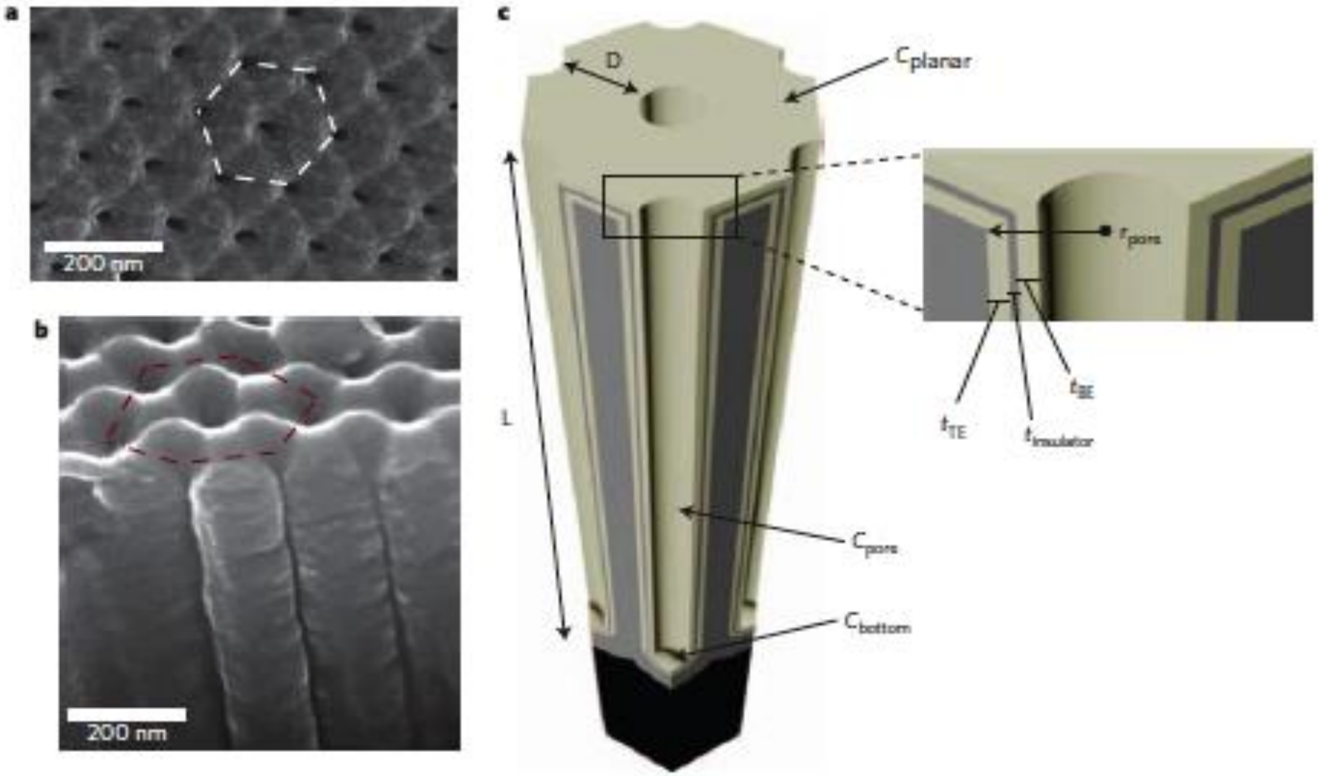

Figure 3 | Relationship between MIM nanotubular structure and the parameters used to calculate total capacitance. a, Plan-view SEM of an AAO MIM structure showing the hexagonal unit cell. **b,** Cross-section of the sample in **a**. **c,** Schematic of a unit cell of an AAO MIM capacitor defining the various parameters used to compute total capacitance of the structure. Here, t_{TE} is the thickness of the top electrode (TE), $t_{insulator}$ is the thickness of the insulating film, t_{BE} is the thickness of the bottom electrode (BE), r_{pore} is the radius of the pore, D is the interpore edge-to-edge distance and L is the depth of the pores. The contribution to total capacitance comes from the sum of the top planar part C_{planar}, the cylindrical region of the pore C_{pore}, and the bottom part of the pore C_{bottom}, next to the barrier layer.

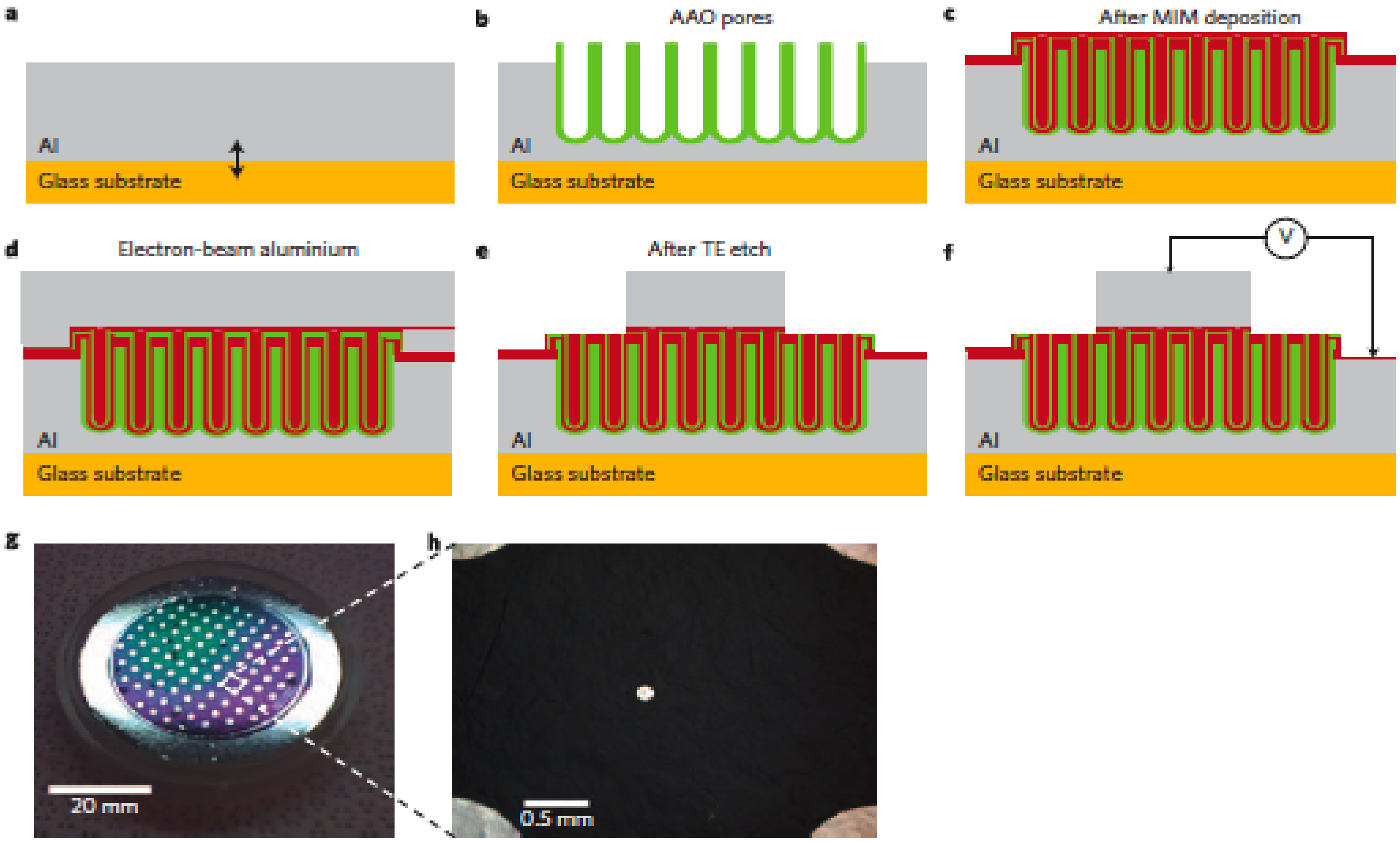

Figure 4 | Process sequence to prepare MIM capacitors. a, Al foil is anodically bonded to a glass substrate. **b,** AAO pore formation. **c,** MIM deposition via ALD processes. **d,** Electron-beam Al is deposited on top. **e,** Photolithography, masking and etching of the Al electrode, then the top electrode (TE) TiN, to define the capacitor area. **f,** Electrical testing using the Al foil (which is in contact with the bottom electrode TiN) as a back contact and electron-beam Al as the top contact. **g,** Two-inch wafer with capacitors of different areas defined on the surface. **h,** A blown-up image of an actual 'dot' capacitor tested. Each such dot capacitor is 125 μm wide and contains ~1×10^6 nanocapacitors.

Fractal capacitors in nano structures

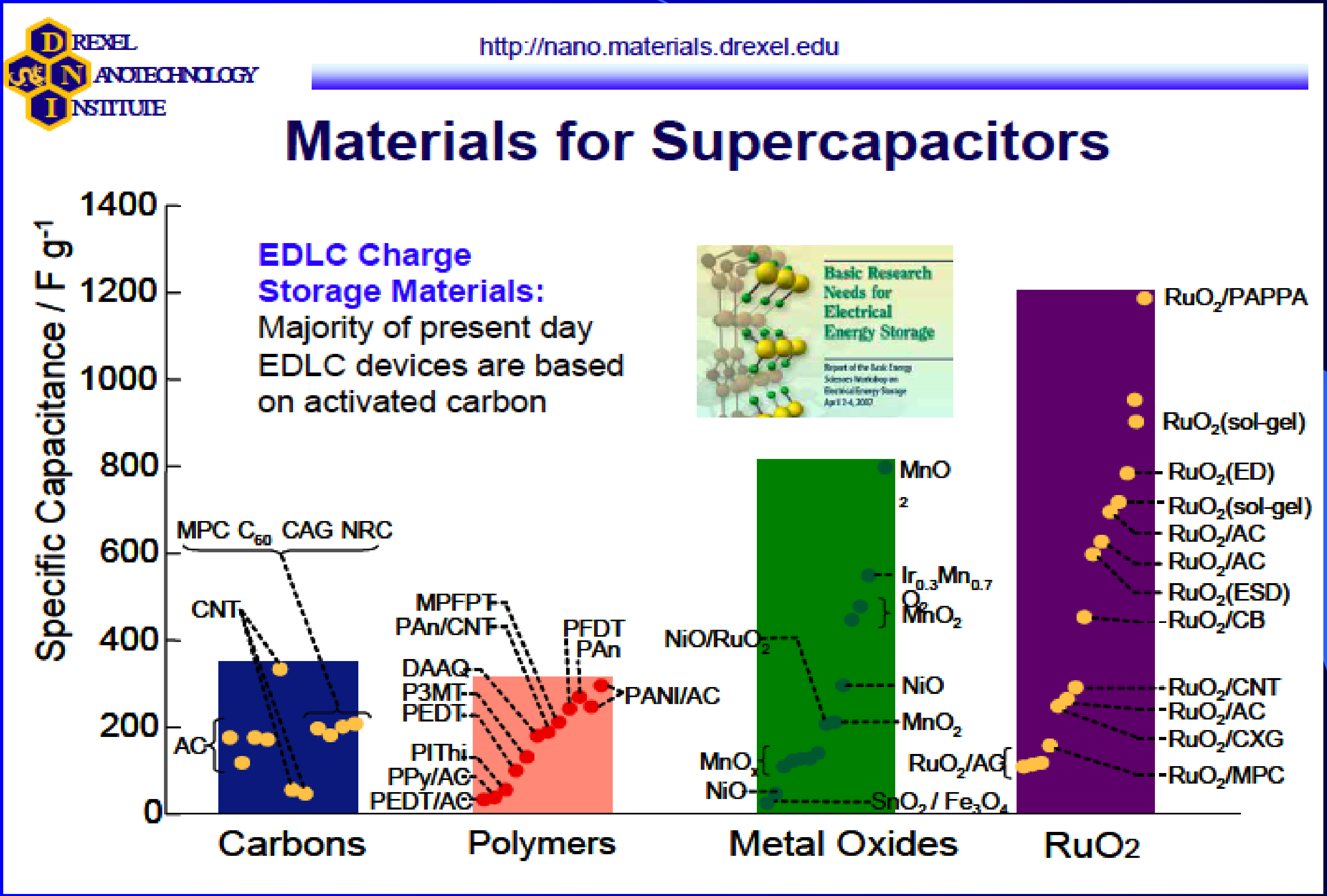

Size Matters

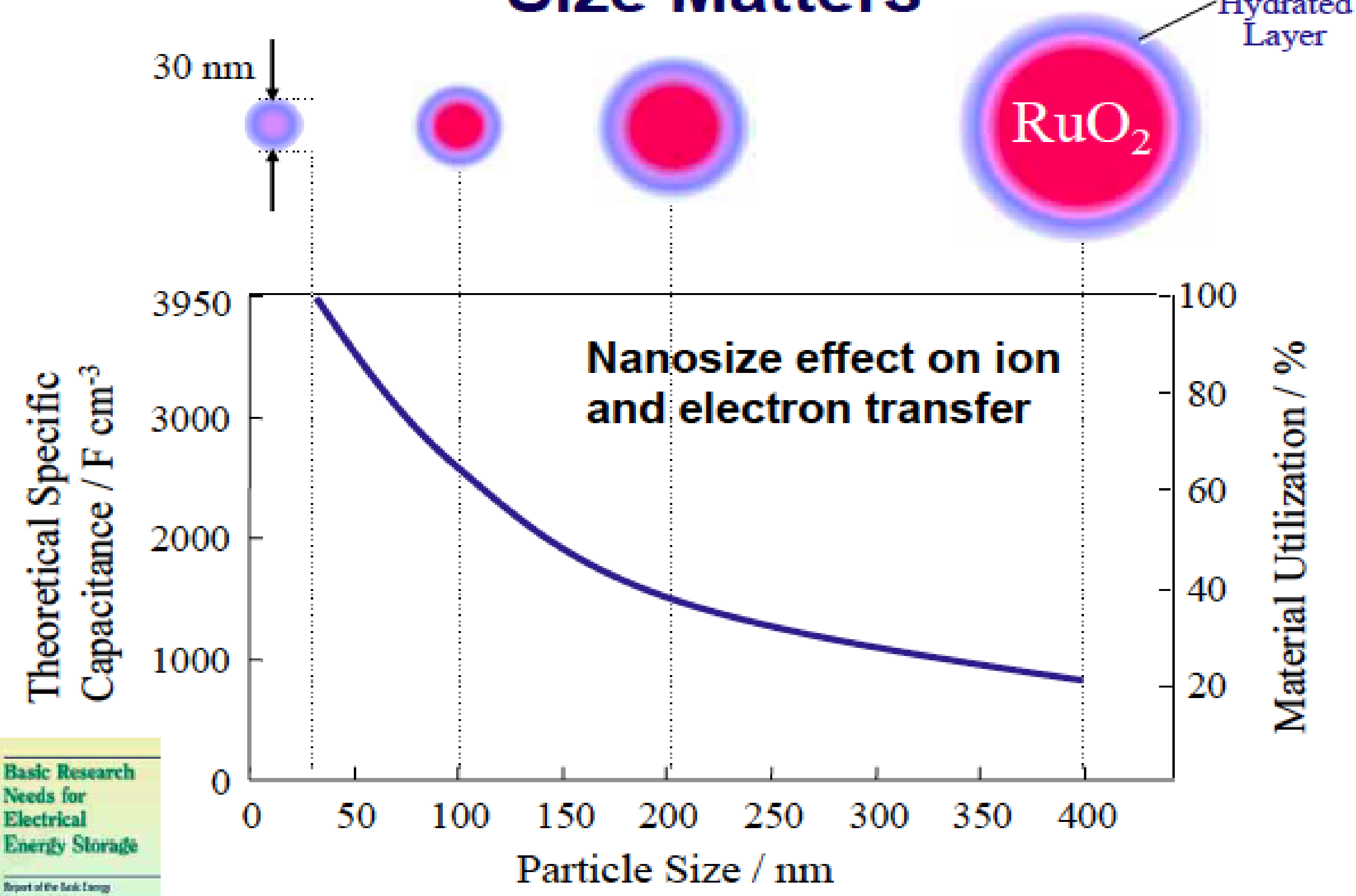

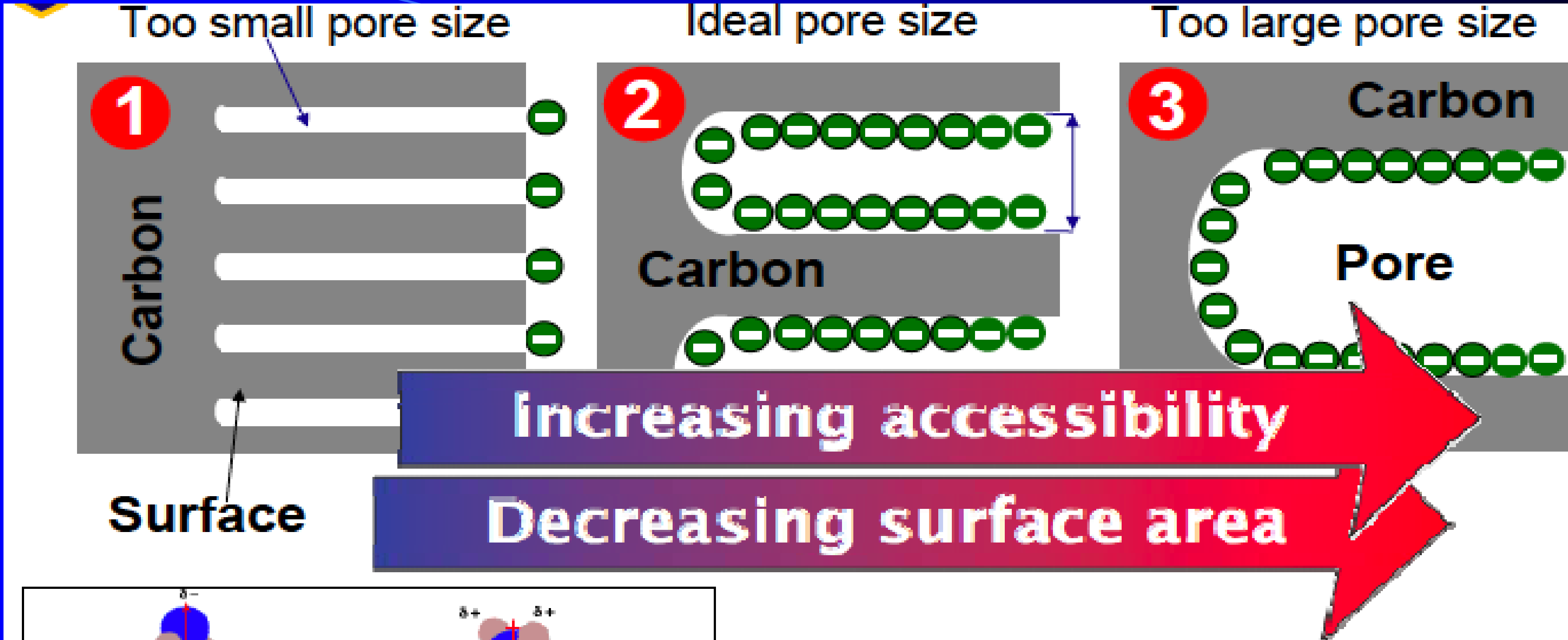

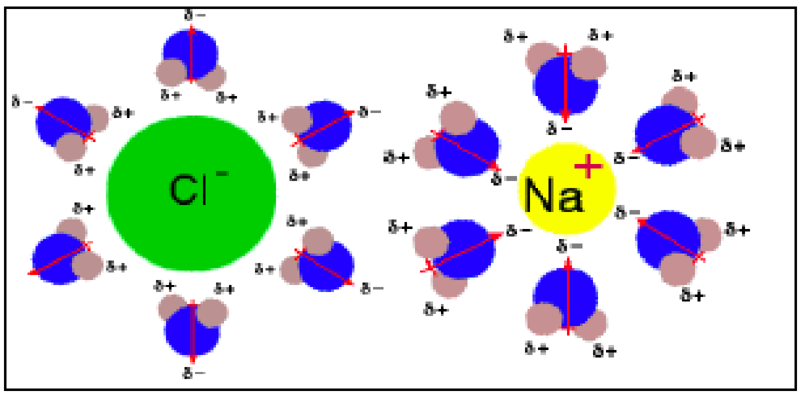

Conventional wisdom says increasing surface area is only good insomuch as the pores are large enough to accommodate the ion and its solvation shell

M. Endo *et al.*, *Carbon* 40, 2613 (2002).

M. Hahn *et al.*, *Electrochemical and Solid-State Letters* 7, A33 (2004).

Double cylinder capacitor

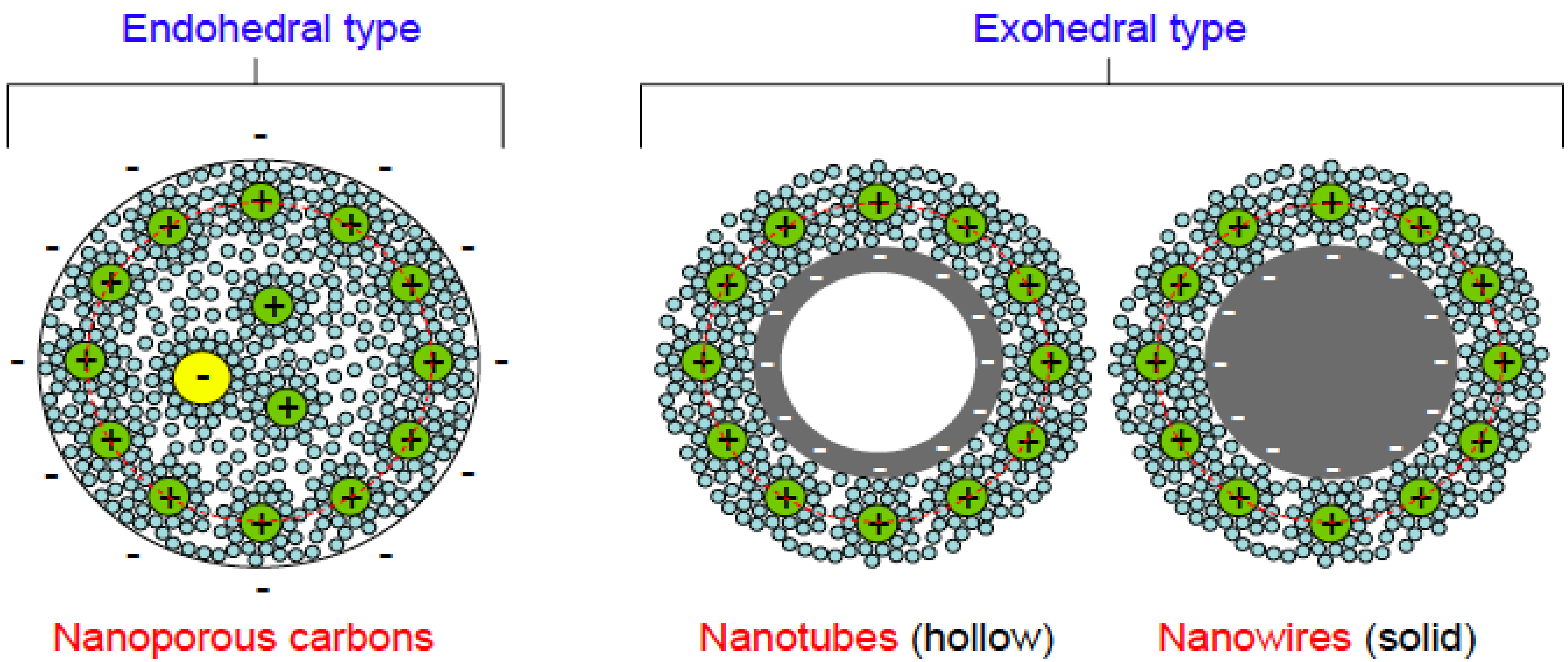

With double layer formed in the pores, it should be a double cylinder capacitor, not a parallel plate capacitor.

Huang, J.; Sumpter, B. G.; Meunier, V. ***Angew. Chem. Int. Ed***. 2008, *47*, 520.

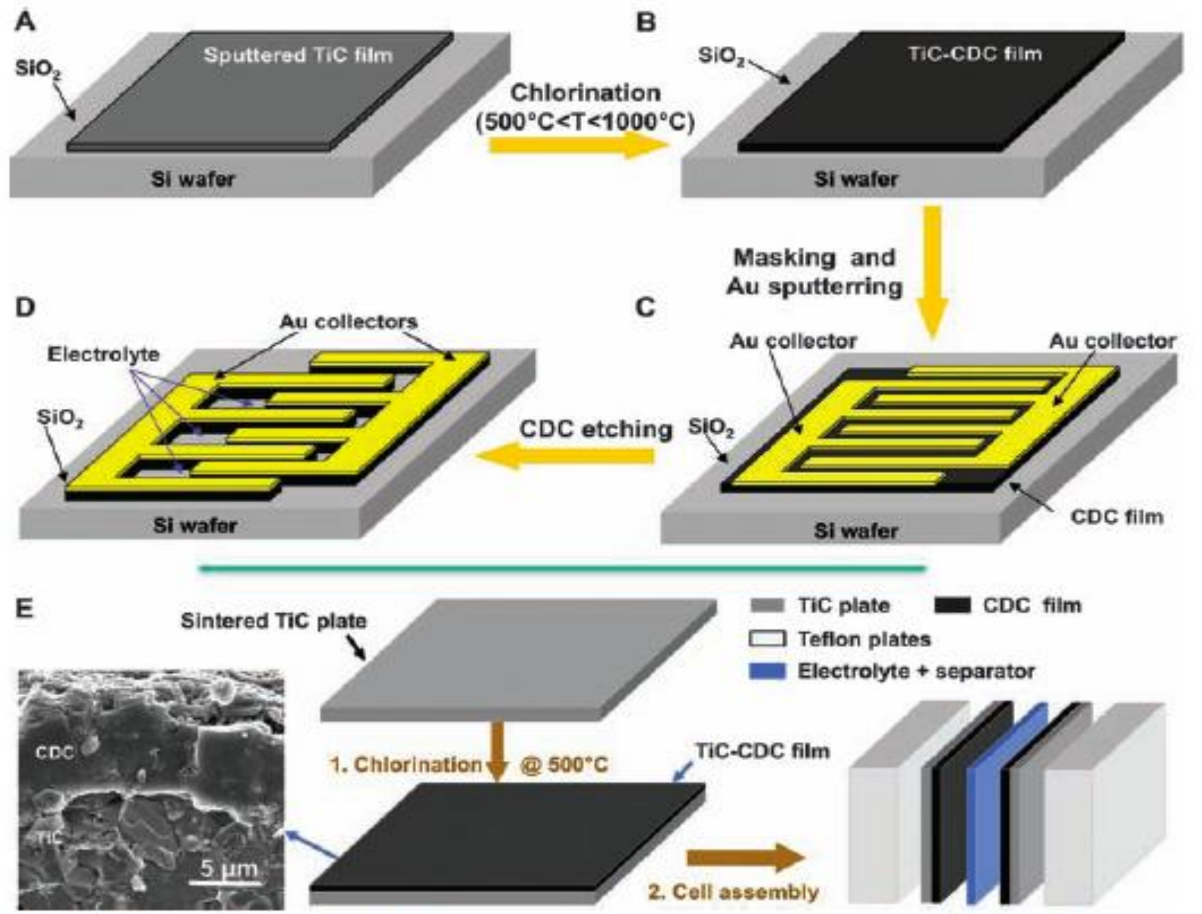

Fig. 1. (**A** to **D**) Schematic of the fabrication of a micro-supercapacitor integrated onto a silicon chip based on the bulk CDC film process. Standard photolithography techniques can be used for fabricating CDC capacitor electrodes (oxidative etching in oxygen plasma) and deposition of gold current collectors. (**E**) CDC synthesis and electrochemical test cell preparation schematic. Ti is extracted from TiC as $TiCl_4$, forming a porous carbon film. Two TiC plates with the same CDC coating thickness ranging from 1 to 200 µm are placed face to face and separated by a polymer fabric soaked with the electrolyte. SEM micrograph shows a representative image of a CDC/TiC interface, with a good film adhesion and a glassy film fracture surface typical of amorphous carbon.

23 APRIL 2010 VOL 328 SCIENCE

LETTERS

NATURE NANOTECHNOLOGY DOI: 10.1038/NNANO.2010.162

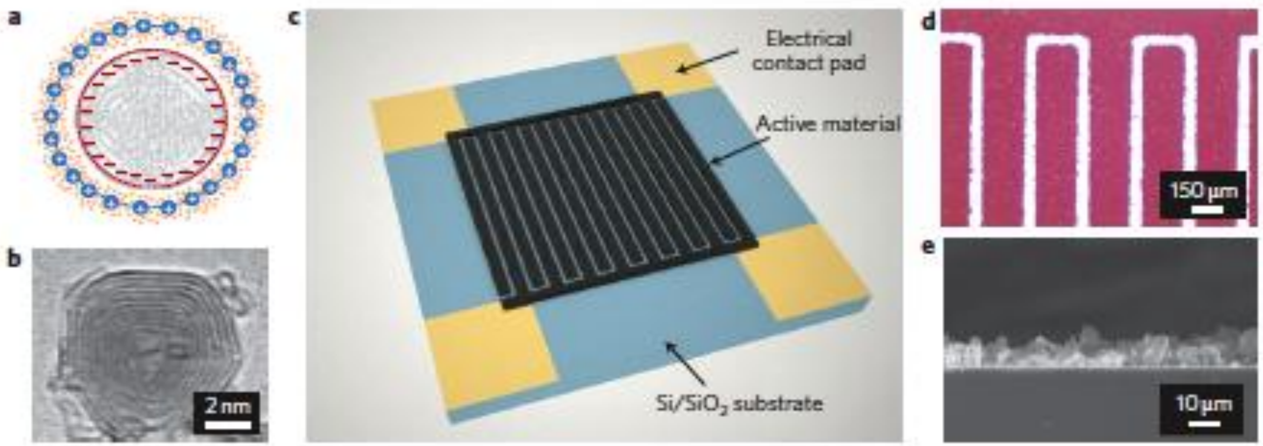

Figure 1 | Design of the interdigital microsupercapacitor with OLC electrodes. **a**, Cross-section of a charged zero-dimensional OLC (grey) capacitor, consisting of two layers of charges (blue and pink) forming the inner and outer spheres, respectively. **b**, Transmission electron microscopy image of a carbon onion produced at 1,800 °C. Lattice spacing between the bent graphitic layers in the onions is close to 0.35 nm. **c**, Schematic of the microdevice (25 mm^2). Two gold current collectors made of 16 interdigital fingers were deposited by evaporation on an oxidized silicon substrate and patterned using a conventional photolithography/etching process. Carbon onions (active material) were then deposited by electrophoretic deposition onto the gold current collectors. **d**, Optical image of the interdigital fingers with 100-µm spacing. **e**, Scanning electron microscope image of the cross-section of the carbon onion electrode. A volumetric power density of 1 kW cm^{-3} was obtained with a deposited layer thickness in the micrometre range, not the nanometre range.

nature nanotechnology

SUPPLEMENTARY INFORMATION

DOI: 10.1038/NNANO.2010.162

Ultrahigh-power micrometre-sized supercapacitors based on onion-like carbon

David Pech, Magali Brunet, Hugo Durou, Peihua Huang, Vadym Mochalin, Yury Gogotsi, Pierre-Louis Taberna and Patrice Simon

cnrs

LAAS

Laboratoire d'Analyse et d'Architecture des Systèmes

INSTITUT CARNOT

CIRIMAT

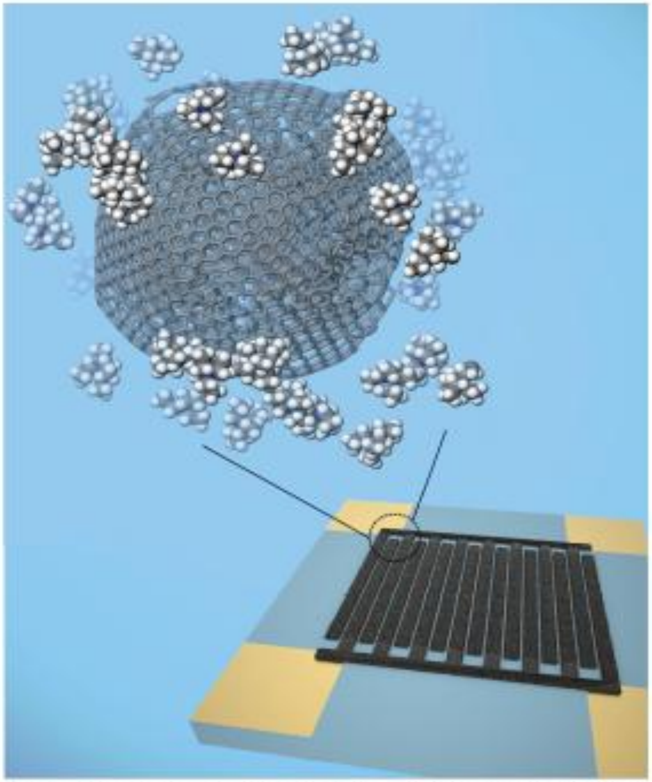

Micro supercondensateur constitué de nano oignons de carbone déposé « pur » sur des microélectrodes en or en forme de doigts interdigités fabriquées sur lame de silicium

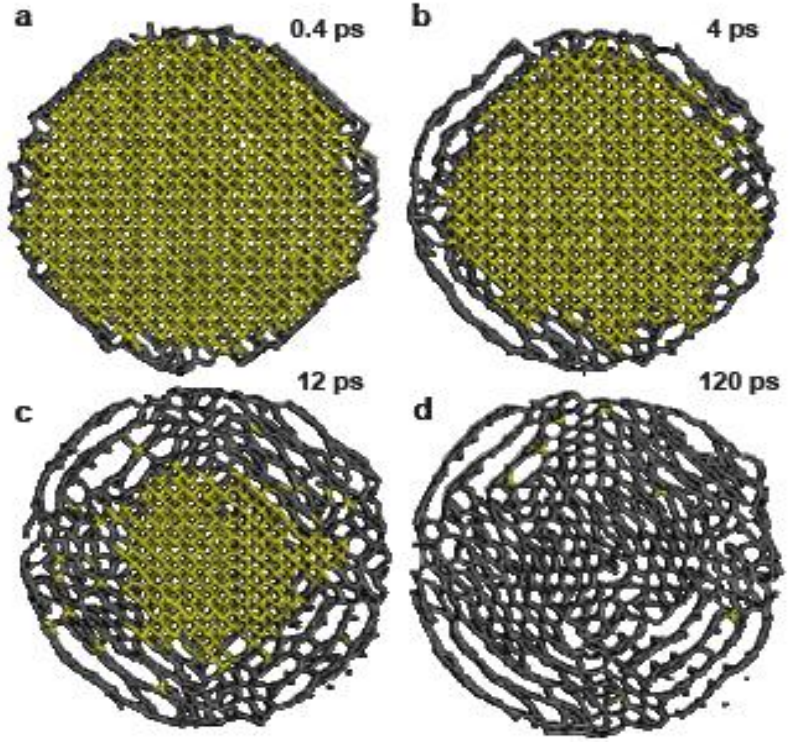

Supplementary Figure S1. Onion-like carbon. **a-d,** Molecular dynamics simulation of evolution of diamond into OLC for a nanodiamond crystal of 4 nm in diameter. 0.6 nm thick slices through the center of the particle are shown for four different times starting from the initial stage (diamond) to the fully formed graphitic onion.

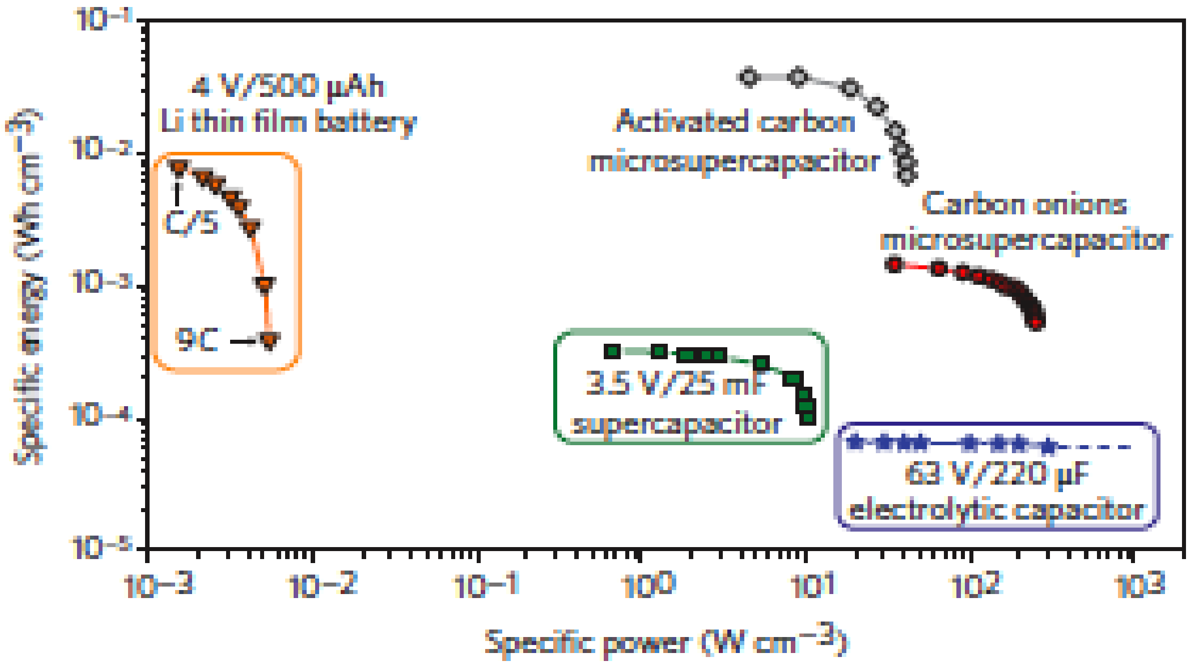

Figure 4 | Comparison, in a Ragone plot, of the specific energy and power density (per cm^3 of stack) of typical electrolytic capacitors, supercapacitors and batteries with the microdevices. All the devices (macro and micro) were tested under the same dynamic conditions. A very high energy density was obtained with the AC-based microsupercapacitor, whereas ultrahigh power density was obtained with the OLC-based microsupercapacitor.

What is THz?

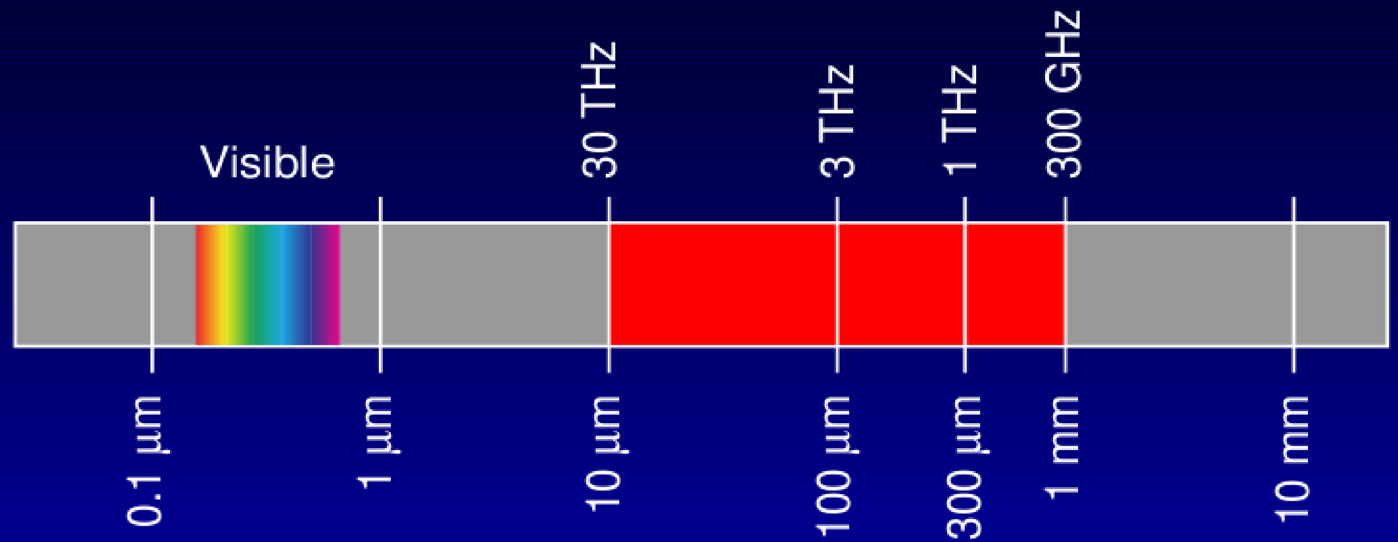

Go-between for Microwave and Optics

- $1\text{THz} = 10^{12}\text{Hz}$
- $\lambda = 300\mu\text{m}$ in vacuum
- $\Delta E = 4.1\text{meV}$

Sierpinski Gasket – Isolated Antenna

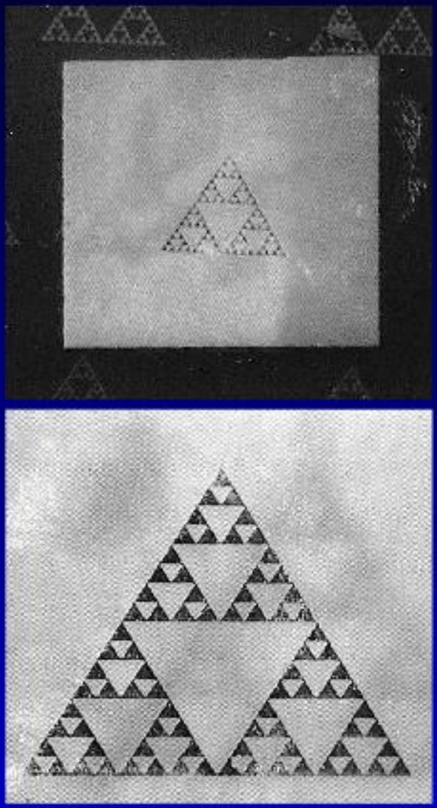

Thin SiN_x film
(CEM2)

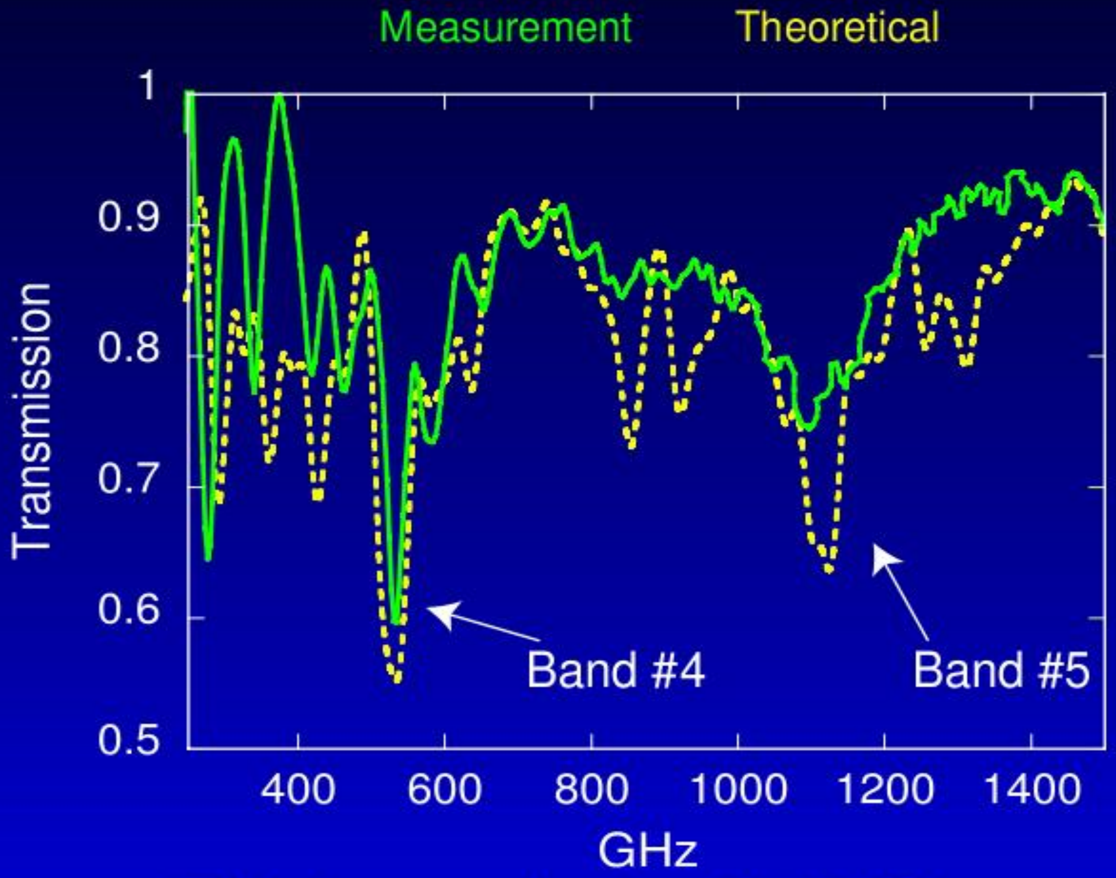

THz transmission (LAHC)

Towards THz Integrated Sources

After:
THz fractal antennas for electrical and optical semiconductor emitters and receptors

L. CHUSSEAU, C. GAUBERT, A. GIANI, D. GASQUET, F. GARET†, F. AQUISTAPACE†, L. DUVILLARET†, J.-L. COUTAZ† and W. KNAP‡
CEM2, UMR n5507 CNRS, Universitee Montpellier II, FRANCE
†LAHC, Universit ęe de Savoie, FRANCE
‡GES, UMR n5650 au CNRS, Universite Montpellier II, France

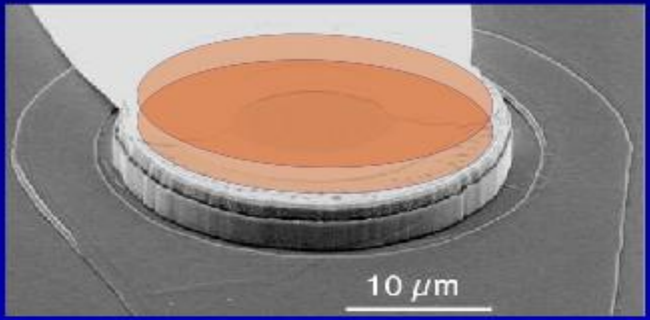

LT GaAs

Coupled Cavity VCSEL

Towards THz Integrated Sources

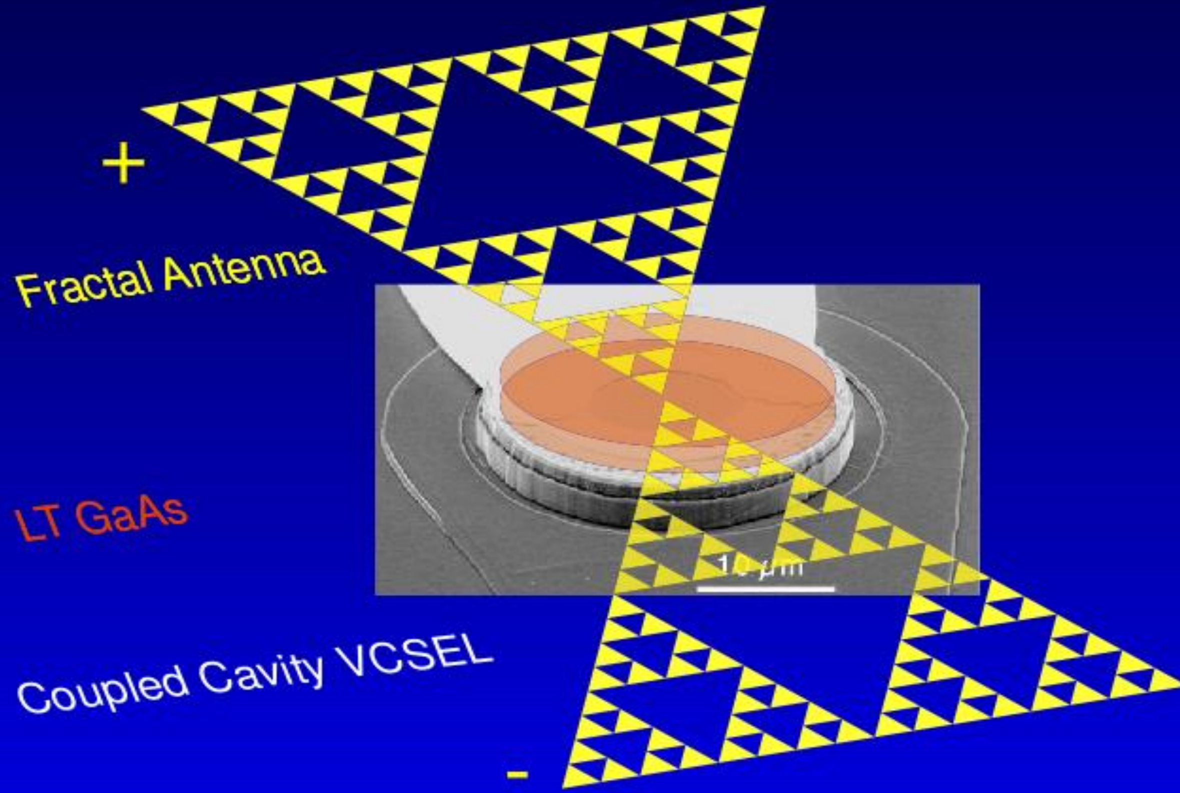

Towards THz Integrated Sources

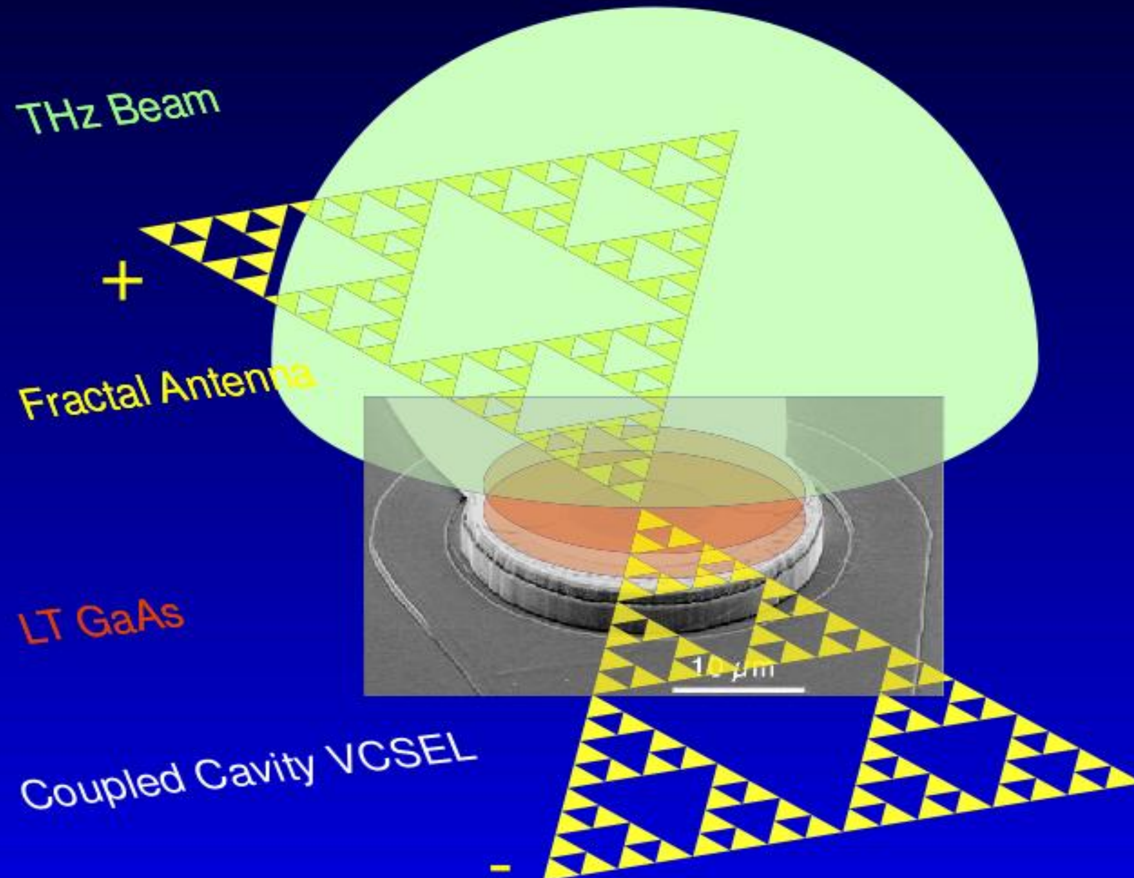

APPLICATIONS

Encoding images

Fractal from Iterative Function System

- IFS
  - Multiple Reduction Copy Machine

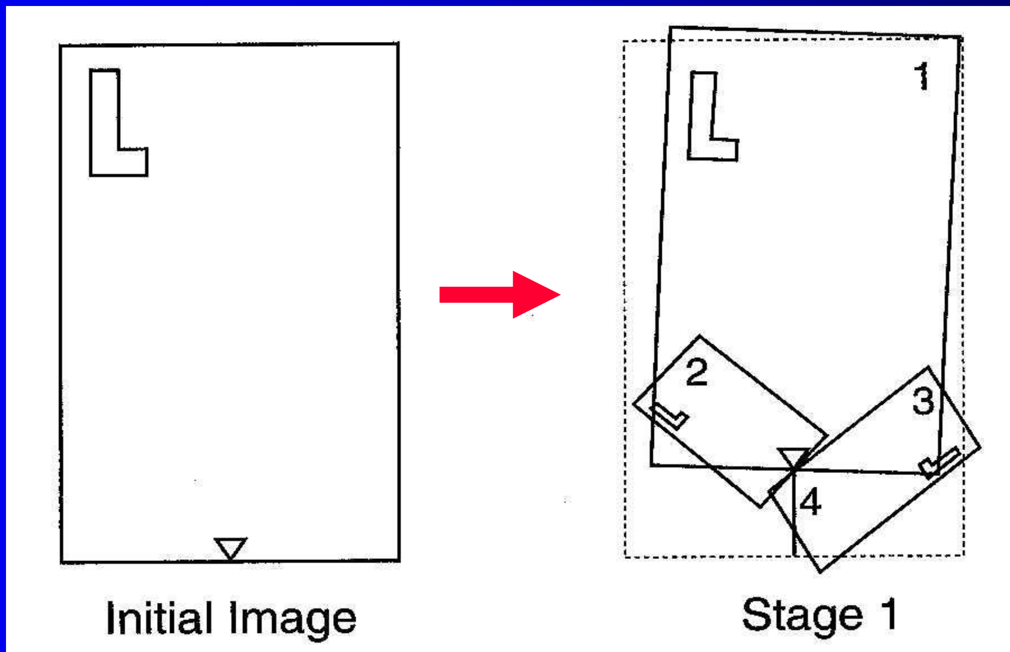

Blueprint for Barnsley's fern

MRCM (IFS machine)

- Repeat the copying process $x_{n+1}=W(x_n)$

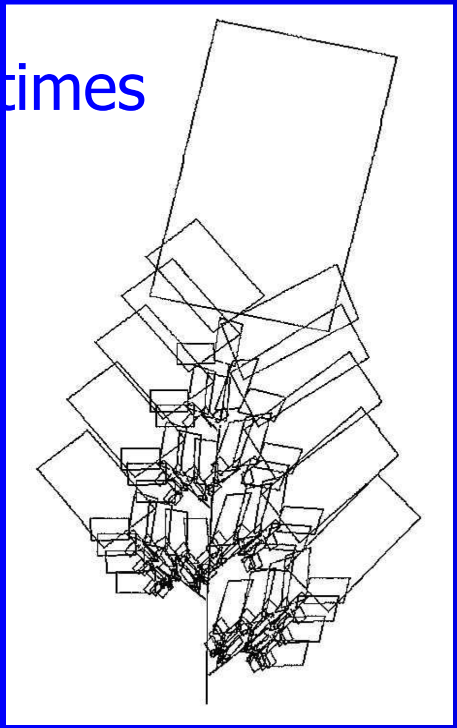

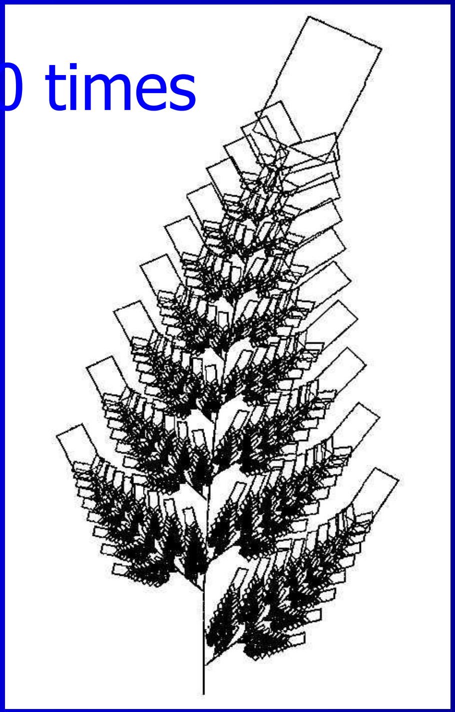

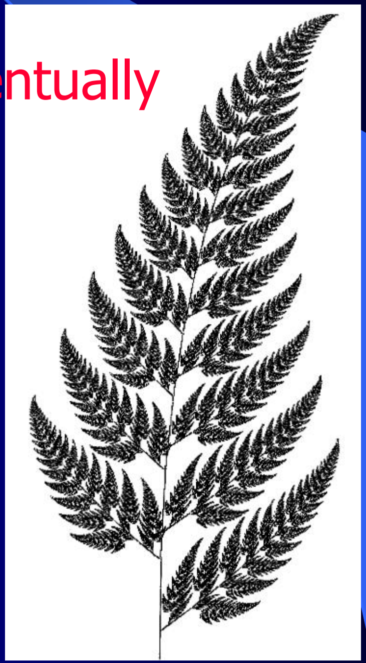

Very high compression ratio

- The whole fern is compressed to four set of numbers

Translation		rotation		scaling	
e	f	ϕ	ψ	r	s
0	1.6	-2.5	-2.5	0.85	0.85
0	1.6	49	49	0.3	0.34
0	0.44	120	-50	0.3	0.37
0	0	0	0	0	0.16

- If each number needs 32 bits to represent, then we need 32x24 bits for the coding. *If the picture is mxn pixels,*
- *the compression rate = mxn/32x24 !!   VERY HIGH!*

Question: how long does decoding take?

- Suppose
  - The initial rectangle is 500x200 pixels
  - reduction factor = 0.85
- We want the object to shrink to one pixel in N steps.
  - $500 * 0.85^N = 1$
- Thus, $N \approx 39$.
- In each step, 4 times more rectangles are drawn. So, we need to draw
  - $1 + 4 + 4^2 + 4^3 + 4^4 + \ldots + 4^{39} = (4^{39}-1)/3$ objects
  - i.e., ≈ **3×10^{23}** objects
- Suppose the computer draws 1 million rectangles per second. We need about 3×10^{17} sec or 10^{10} years to complete!

Problems

- How to decode in reasonably short time with reasonably good resolution?

  Deterministic (brute-force) approach
  Chaos approach
  Adaptive cut approach

- How to encode an image?

  Similarity method
  - No efficient or general approach

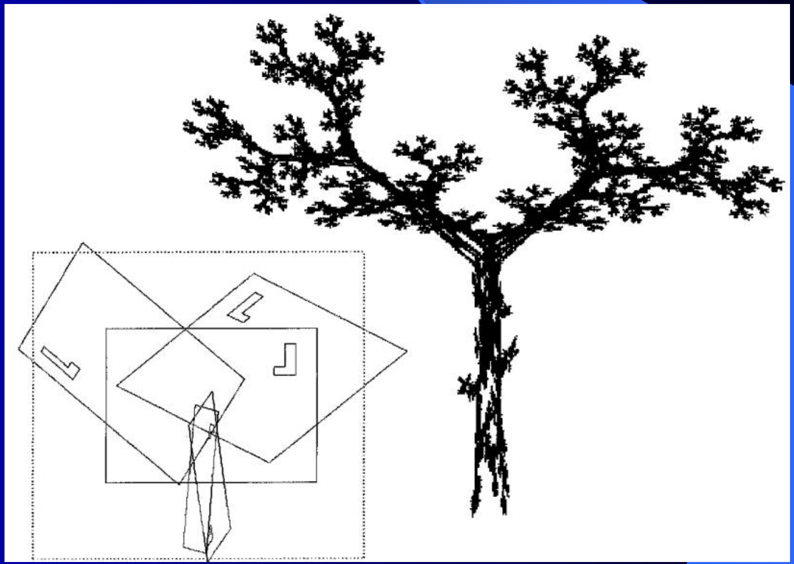

Decoding

- IFS machine: $y = w_1(x) \cup w_2(x) \cup w_3(x)$
- ***Chaos approach:***
  - Iterate randomly, with weighted probability for each transformation
- ***Adaptive cut approach:***
  - Stop iterating when neighboring points are close enough.

Decoding

IFS
262,144

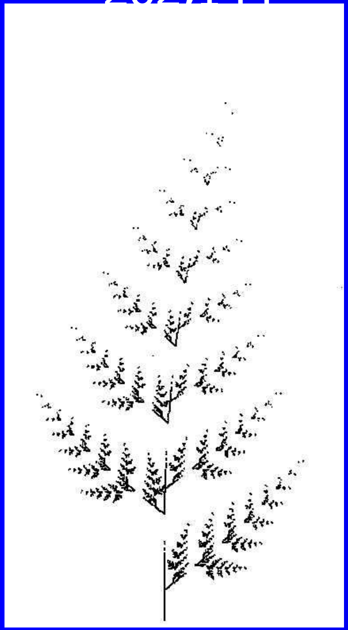

Chaos (equal prob)
100,000

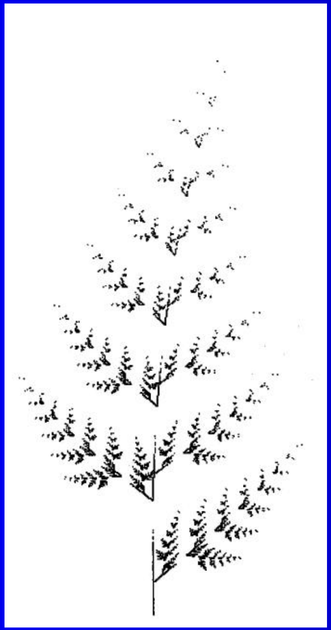

Chaos (weighted prob)
100,000

Adaptive cut
198,541

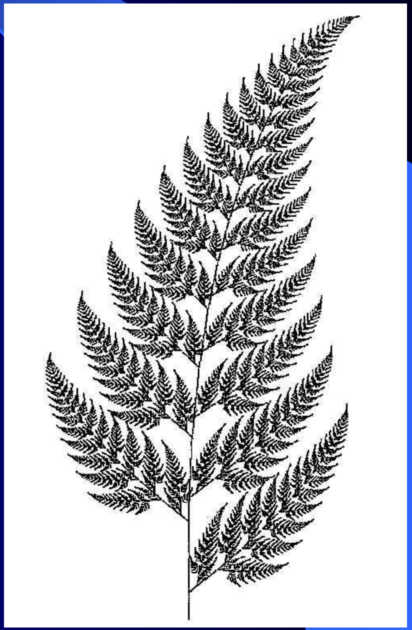

Example

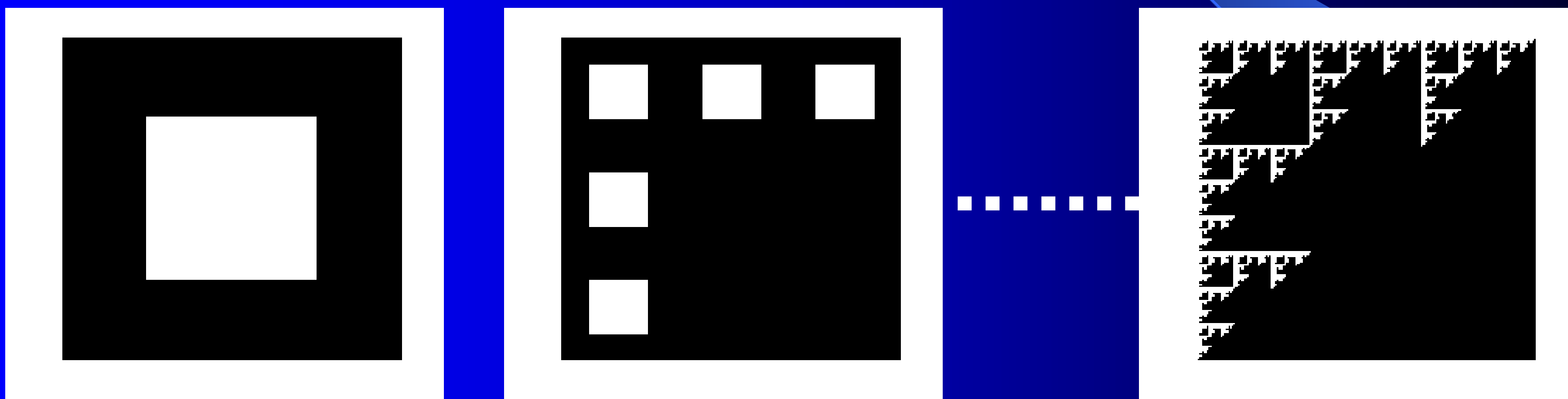

Examples

The Transformation | Attractor | Zoom in

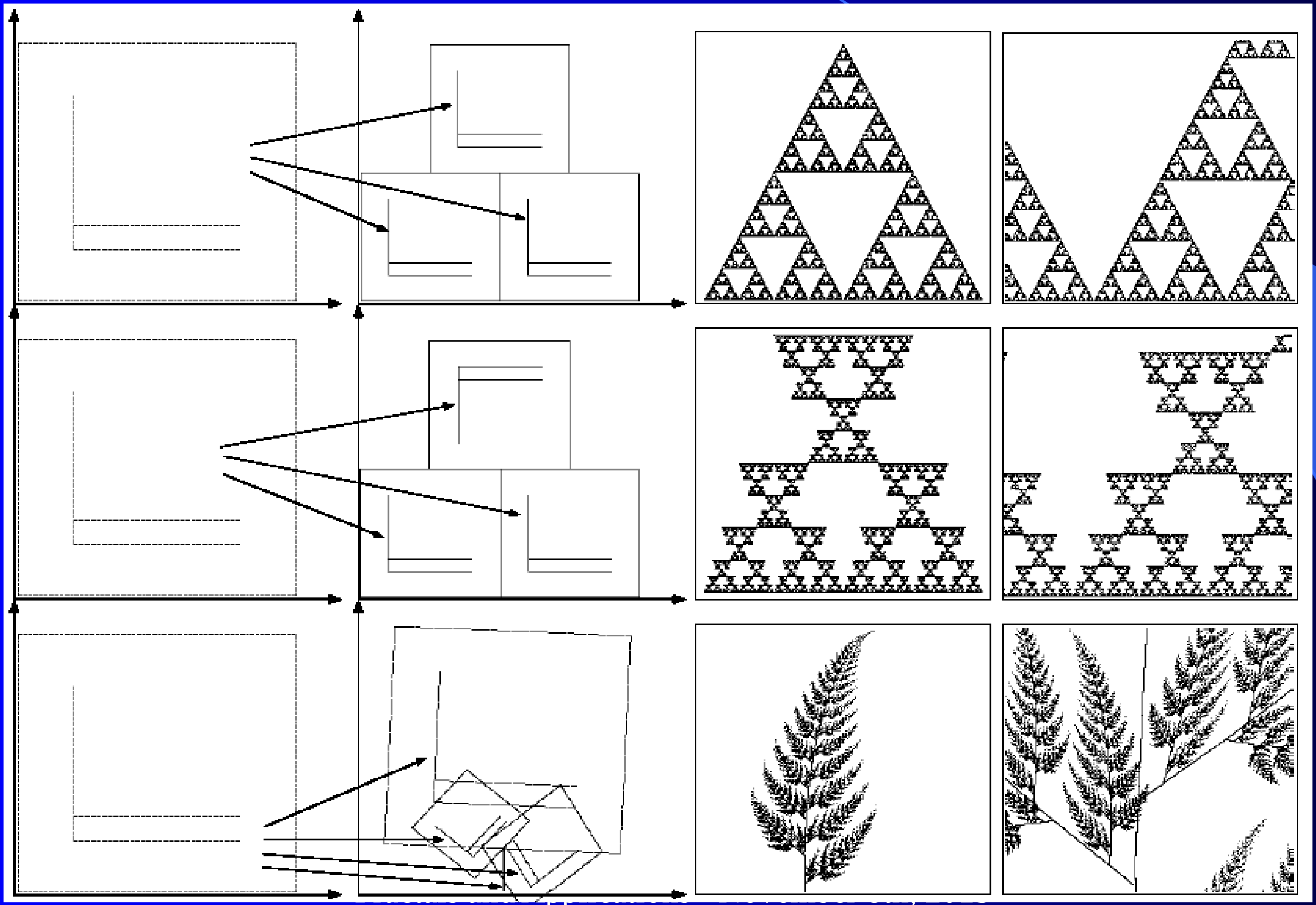

Contractive Mapping

Let (X,d) be a metric space.

A map w: $X \rightarrow X$ *is* ***contractive***

if there exists a constant $s \in [0, 1)$,

such that $\forall\ x, y \in X$:

$$d(w(x), w(y)) \leq s\, d(x, y)$$

s is called the ***contraction factor*** of w.

An Example of Contractive Mapping

- Let d be the Euclidean distance.
  Let $w(x) = x/2$
  Then it is easy to see that $s = 1/2$,
  Therefore w is a contractive mapping.

Contractive Mapping Theorem

- If w is a contractive mapping then there exists a unique x^* such that

$$w(x^*) = x^*$$

and for any $x \in X$,

$$\lim_{n \to \infty} d(w^{(n)}(x), x^*) = 0$$

Contractive Mapping

Proving the uniqueness of the fixed point by contradiction:

Assume the fixed point is not unique.
Let x^* and y^* be the two fixed points

Since w is contractive, $d(w(x^*), w(y^*)) \leq s\, d(x^*, y^*)$
But x^*, y^* are fixed points, so LHS = $d(x^*, y^*)$.
This is a contradiction because $s < 1$.

Iterated Function System

- An IFS consists of
  - a complete metric space (X, d)
  - a set of contractive mappings w_n defined on X.

i.e. $\{X, w_n: n=1,\ldots,N\}$

Hausdorff Distance

$$h(A,B) = \max(d(A,B), d(B,A))$$

$$d(A,B) = \max_a \min_b d(a,b)$$

For a metric space

$$h(A,B) = 0 \quad \text{iff} \;\; A = B$$

$$h(A,B) = h(B,A)$$

$$h(A,B) + h(B,C) \geq h(A,C)$$

Definition of Fractal Transform

- Let $(H(X), h)$ denote the metric space, s.t.
  - $H(X)$ consists of nonempty compact subsets of X
  - h is the Hausdorff Distance
- The fractal transform associated with an IFS is defined as $W: H(X) \rightarrow H(X)$

for all $B \in H(X)$

The Contraction Mapping Theorem for Fractal Transform

- If w_i are contractive with the contraction factor s_i. Then W is also contractive with contraction factor

$$s = \max_i s_i$$

- W is contractive, by contraction mapping theorem, there exists a unique fixed point A i.e.

- A is called the ***attractor*** of the IFS.

Fractal Transform

- For all $B \in \mathrm{H}(X)$, $\lim_{n\to\infty} W^{(n)}(B) = A$
- What does this say about coding?
- Encode an image I by with the IFS of I
- Decode the image by $I = \lim_{n\to\infty} W^{(n)}(J)$ where J is any random image.

Example

- w_i's are usually chosen to be affine transformations

Example

- Consider an IFS of the form $\{R^2; w_1, w_2, w_3\}$

Example (cont.)

- A is completely described by W and is independent of B

Fractal Encoding

- Problem definition:

  Given the image I,
  Find an IFS s.t. its attractor is I.

- Several methods have been adopted
- Not solved in general case.
- The *Collage Theorem* provides a guideline.

The Collage Theorem

- For a set C and a contractive transform W with attractor A, there exists $s \in [0, 1)$,

- IOW, to make C and A close, it is sufficient to make C and $W(C)$ close.
- $W(C)$ is called the *collage* of C.

Proving Collage Theorem

because A is an attractor

by def. of contractive transform

The Collage theorem

- In terms of each mapping w_i,

- w_i can be found by partitioning C into parts C_i, s.t. each part is approximated by the contractive transformation w_i of the whole set C.

Local Iterated Function Systems

- Intuitions:
  - Natural images generally do not contain parts that are affine transforms of the whole image.
  - Different parts of the image may become similar under certain affine transformation.

Local Iterated Function Systems

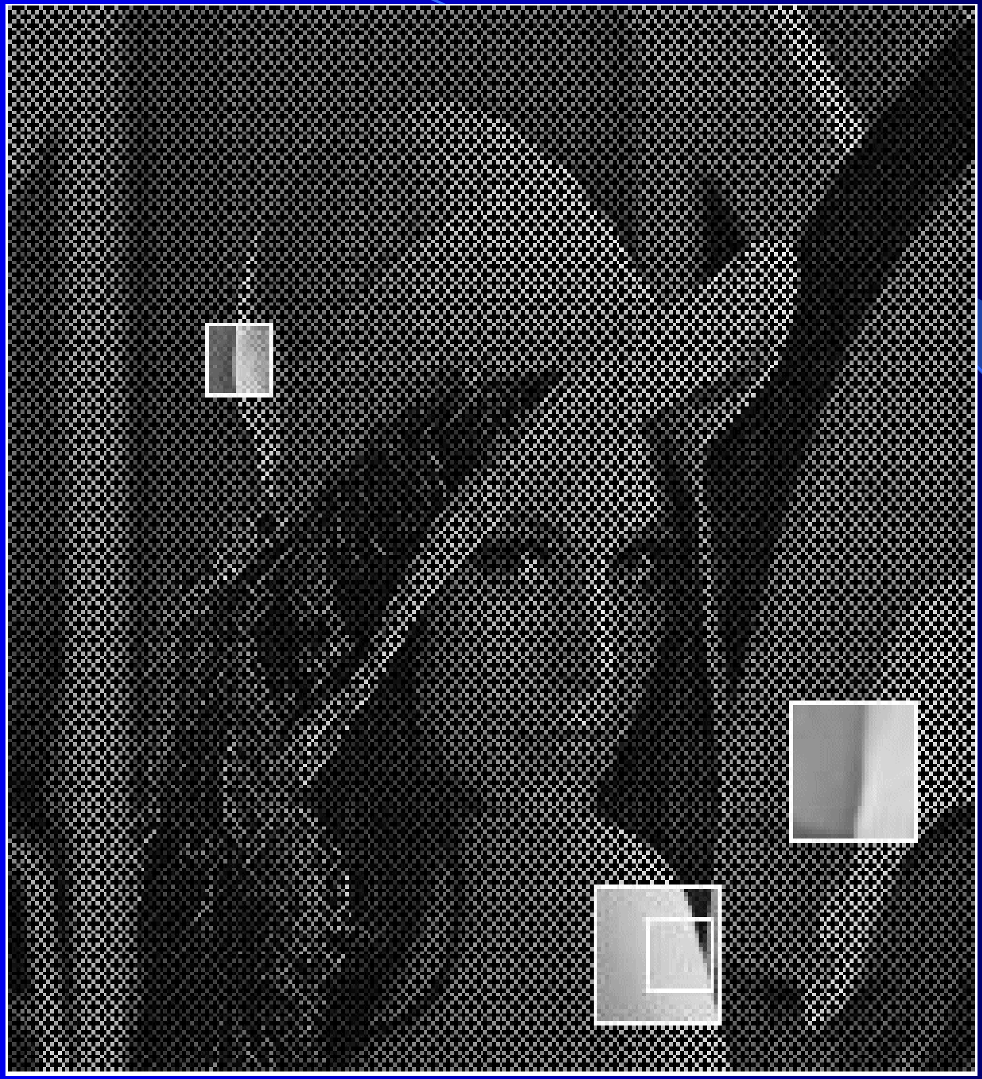

Local Iterated Function Systems

- IFS
  - approximates each part of the image by a transformed version of the *whole* image
- local IFS
  - approximates each part of the image by a transformed version of the *another part* of the image

Implementation Issues

- How to segment the image?
- What transformations to use?
- How to find the parameters of the transformations?
- Where to find the matching segments?

Encoding Images

- Given an image f
- How to find $w_1, w_2, \ldots, w_N$ s.t. f is the fixed point of W?

- Partition f into N range blocks R_i
- Find the domain blocks D_i and $w_i(.)$
- that minimize the distance $d(R_i, w_i(D_i))$, $i = 1, \ldots, N$
  - The best matching domain D_i is said to *cover* the range R_i

Machine Problem 3

- Original Image 128 x 128
- Range blocks 4 x 4 ➔ 1024 blocks (*non-overlapping*)
- Domain blocks 8 x 8 ➔ 121 x 121
  =14641 (*overlapping*)
- Need to compare 14641 squares with each of the 1024 range blocks
- Since the size of domain block is 4 times the size of range block, we need to down-sample.

Machine Problem 3

- w_i include
  - translation and down-sampling
  - adjust contrast a and brightness b

Encoding Images = Finding w_i

Search for best Spatial Transformation

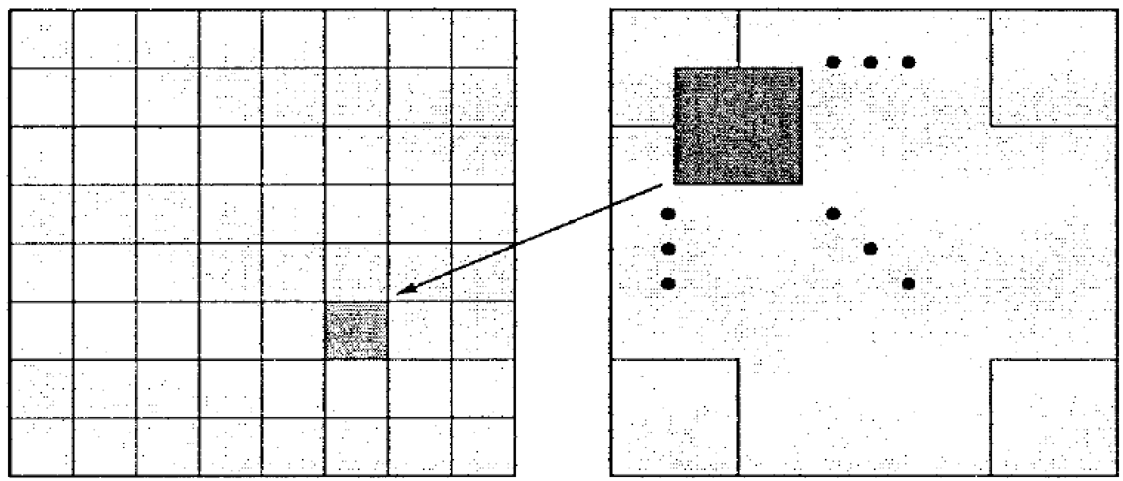

Partition Scheme
(Range Blocks)

Virtual Codebook
(Domain Blocks)

Search for best Grayscale Transformation

a = $\{0, 0.2, 0.4, 0.6, 0.8\}$

```
b=mean(range1D) - a*mean(p);
```

Things you can do for extra credits

- Add rotation and flip
  - Eight types of spatial transformations:
  - 1 ---> Rotate counterclockwise 0 degree.
  - 2 ---> Rotate counterclockwise 0 degree and flip.
  - 3 ---> Rotate counterclockwise 90 degree.
  - 4 ---> Rotate counterclockwise 90 degree and flip.
  - 5 ---> Rotate counterclockwise 180 degree.
  - 6 ---> Rotate counterclockwise 180 degree and flip.
  - 7 ---> Rotate counterclockwise 270 degree.
  - 8 ---> Rotate counterclockwise 270 degree and flip.

Things you can do for extra credits

- Solve both a and b analytically
  - Minimize

$$error = \sum_{i=1}^{n} (a \cdot p_i + b - q_i)^2$$

  - By setting the partial derivatives to zero therefore

$$a = \frac{n^2(\sum_{i=1}^{n} p_i q_i) - (\sum_{i=1}^{n} p_i)(\sum_{i=1}^{n} q_i)}{n^2 \sum_{i=1}^{n} p_i^2 - (\sum_{i=1}^{n} p_i)^2}$$

$$b = \frac{1}{n}\left[\sum_{i=1}^{n} q_i - a \sum_{i=1}^{n} p_i\right]$$

Results

- Left: original
- Right: after first iteration

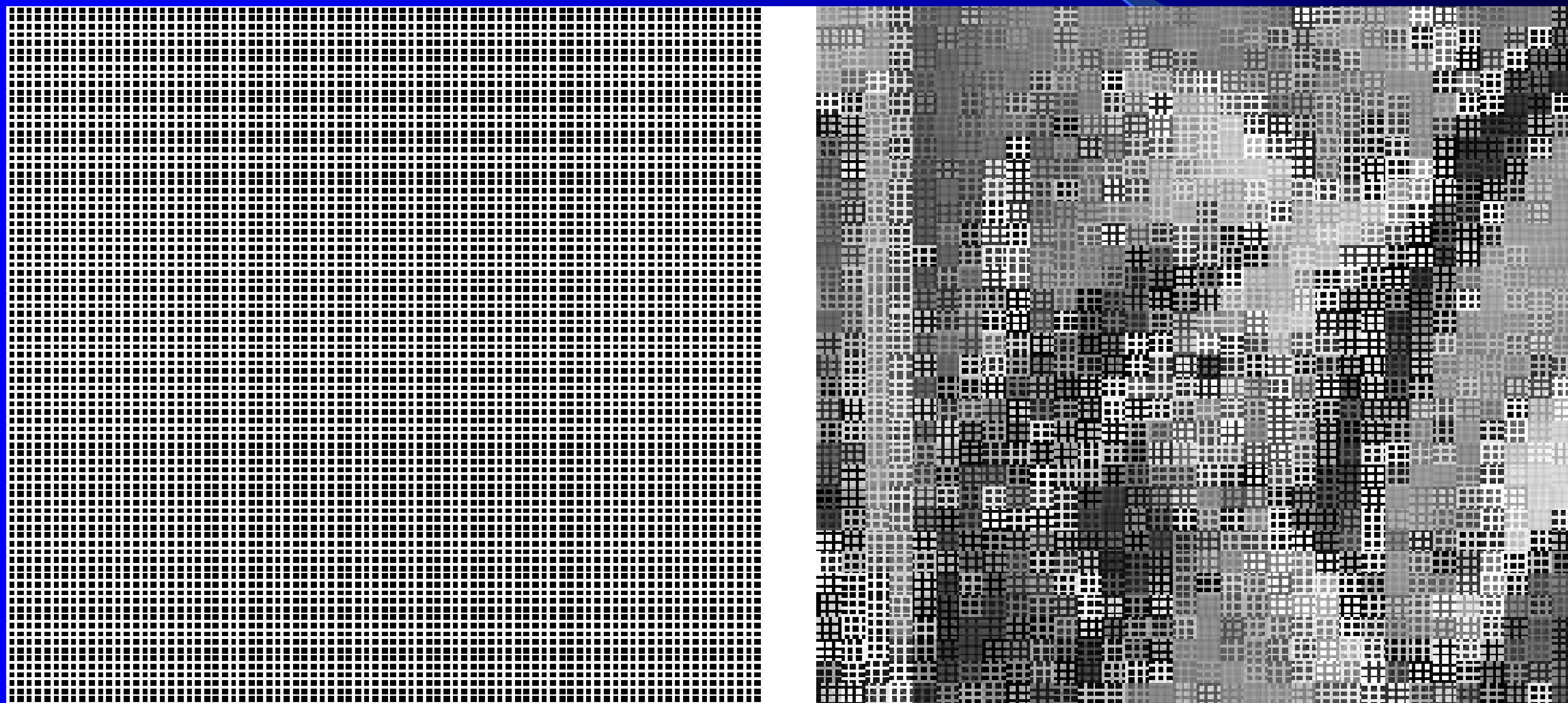

Results

- Left: after the second iteration
- Right: After the tenth iteration

Other Ways to Partition the Image

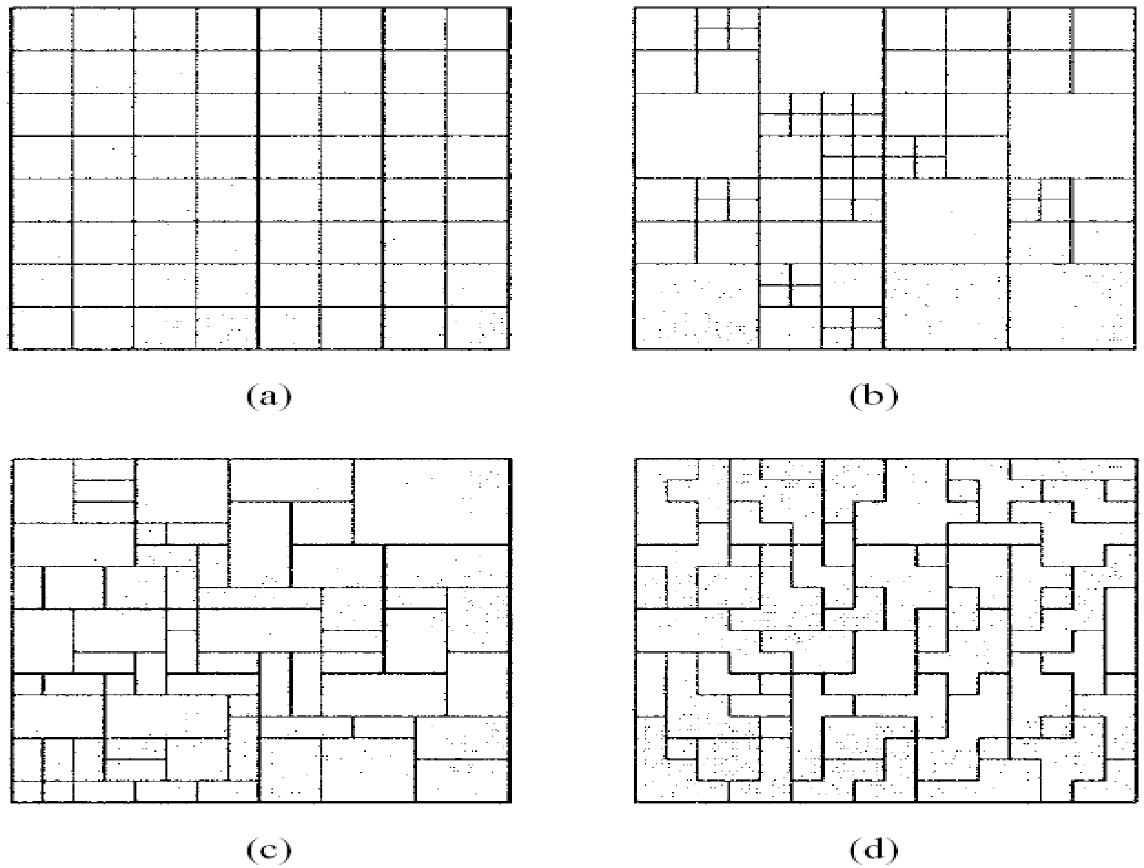

Fig. 2. Right-angled range partition schemes. (a) Fixed block size. (b) Quadtree. (c) Horizontal-vertical. (d) Irregular partition.

Other Ways to Partition the Image

- Motivation:
  - Different regions should be covered by different sizes of range blocks.
- Quadtree partitioning
  - Divide a square into 4 equally sized sub-squares.
  - Repeat divisions recursively until the squares are small enough.

An Example of Quadtree Partitioning

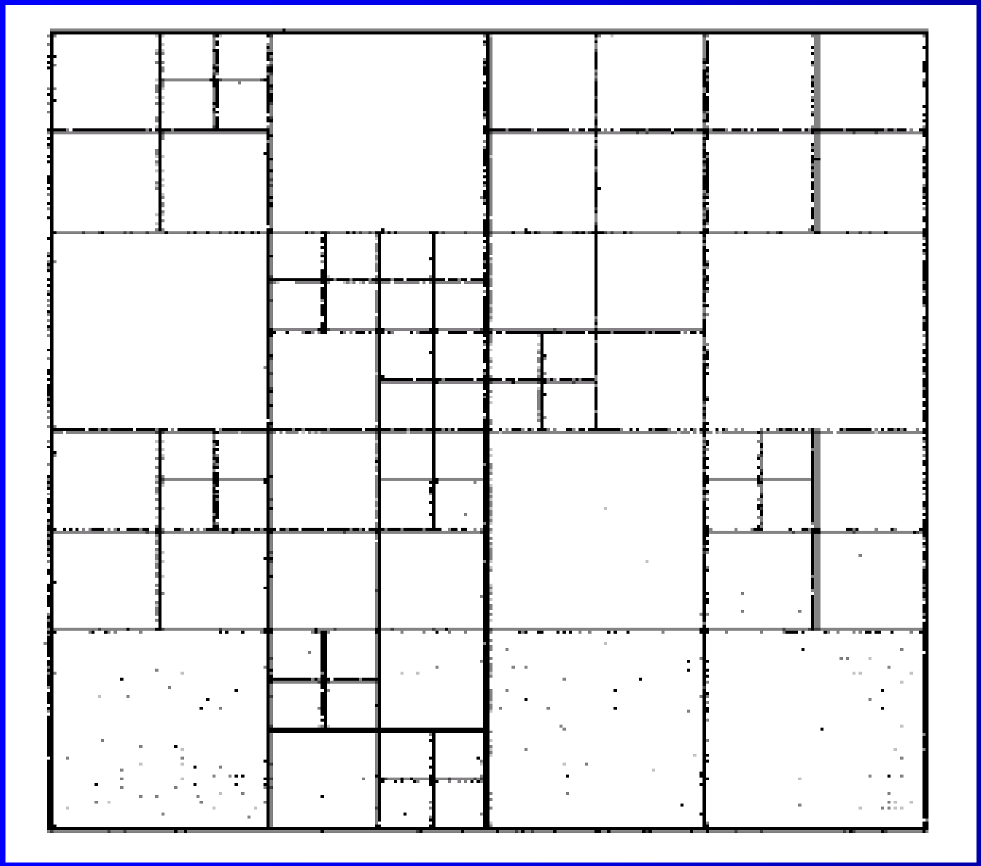

Other Ways to Partition the Image

- Motivation:
  - Use rectangular instead of square
- HV-Partitioning
  - A rectangular image is recursively partitioned either horizontally or vertically to form two new rectangles.
  - More flexibility than Quadtree
  - Can make the partitions share certain similar structures.

An Example of HV-Partitions

- HV-Partitions

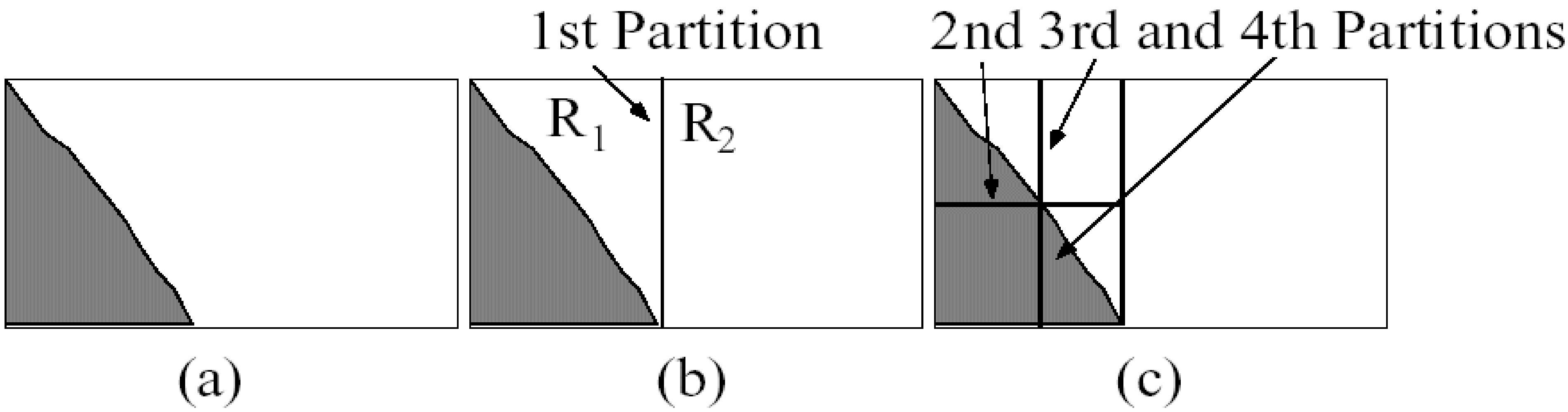

Figure 11. The HV scheme attempts to create self similar rectangles at different scales.

Results Using HV-Partitions

Other Ways to Partition the Image

- Triangular partitioning
  - A rectangular image is divided diagonally into two triangles.
  - Each triangle is recursively subdivided into 4 triangles by joining 3 partitioning points on the sides of the original triangle.

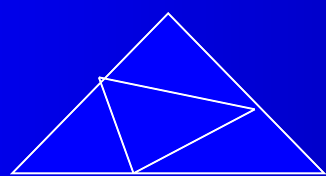

  - More flexible: triangles can have self-similarities.
  - The artifacts do not run horizontally and vertically.

Comparing Different Ways to Partition an Image

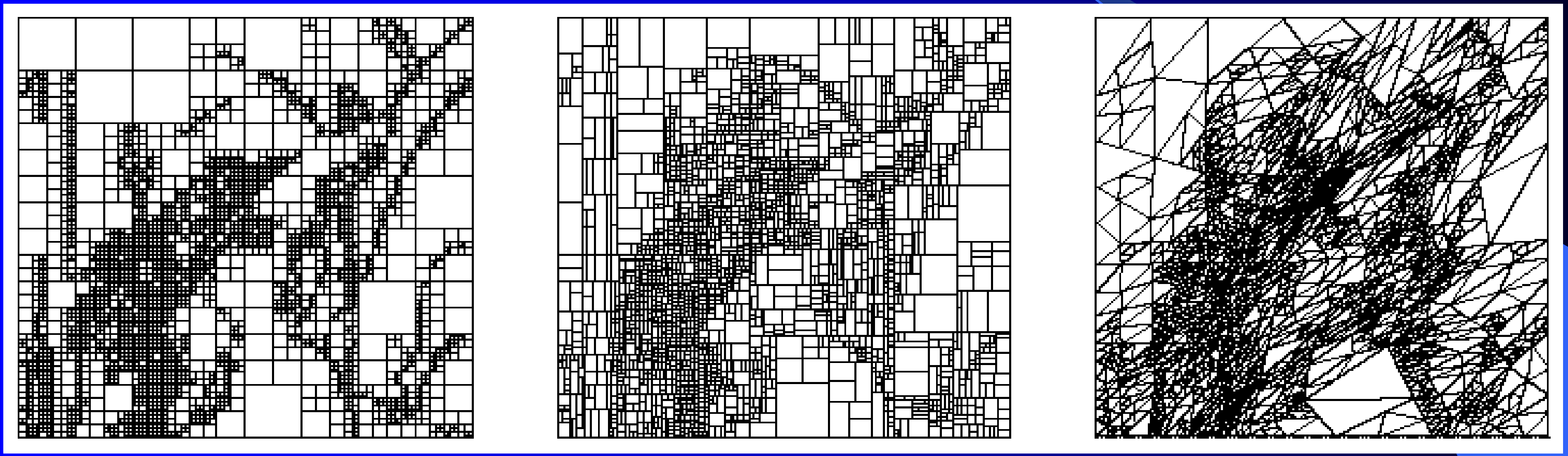

quad tree
5008 squares

HV-partition
2910 rectangles

triangular partition
2954 triangles

Fractal Zoom

- Resolution Independence
  - Decoded image can have higher resolution than the original image.
- The additional resolution is generated because the domain block is larger than its range block.
- Assumption: details of the domain block is also similar to details of the range block,
  - although details of the range block are not given in the original image.

Fractal Zoom

- Left: Decoding at 4 times its encoding size
- Right: Original image enlarged to 4 times the size

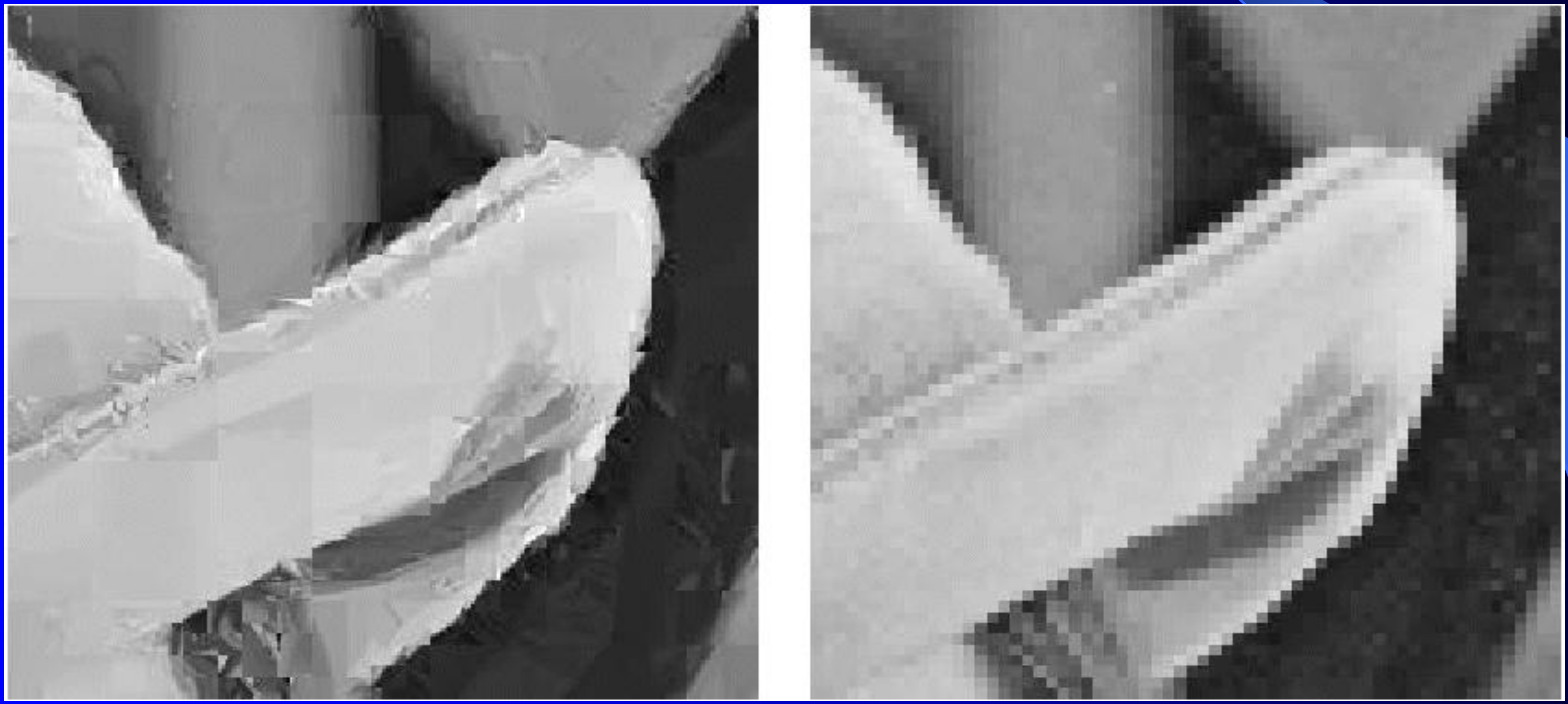

Fractal Zoom

Fractal Zoom

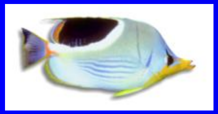

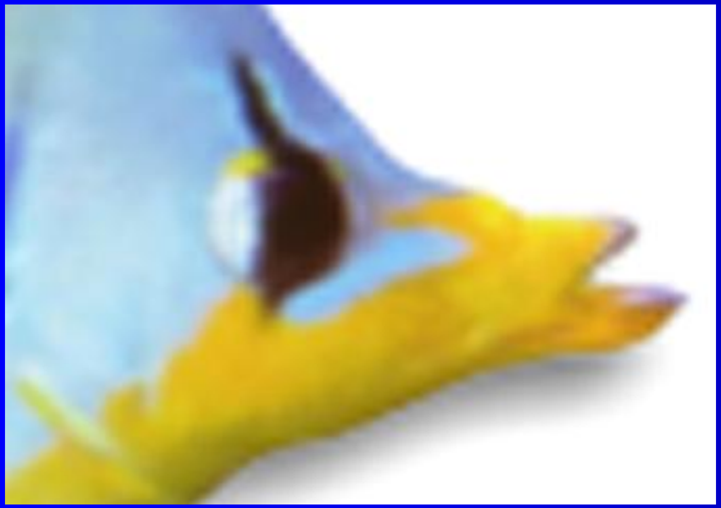

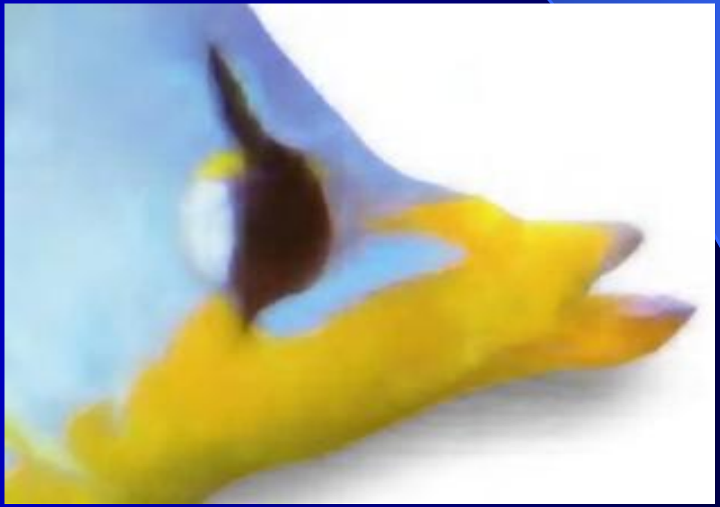

Vertical vs. Lateral Flux

- Lateral flux increases the total amount of capacitance.

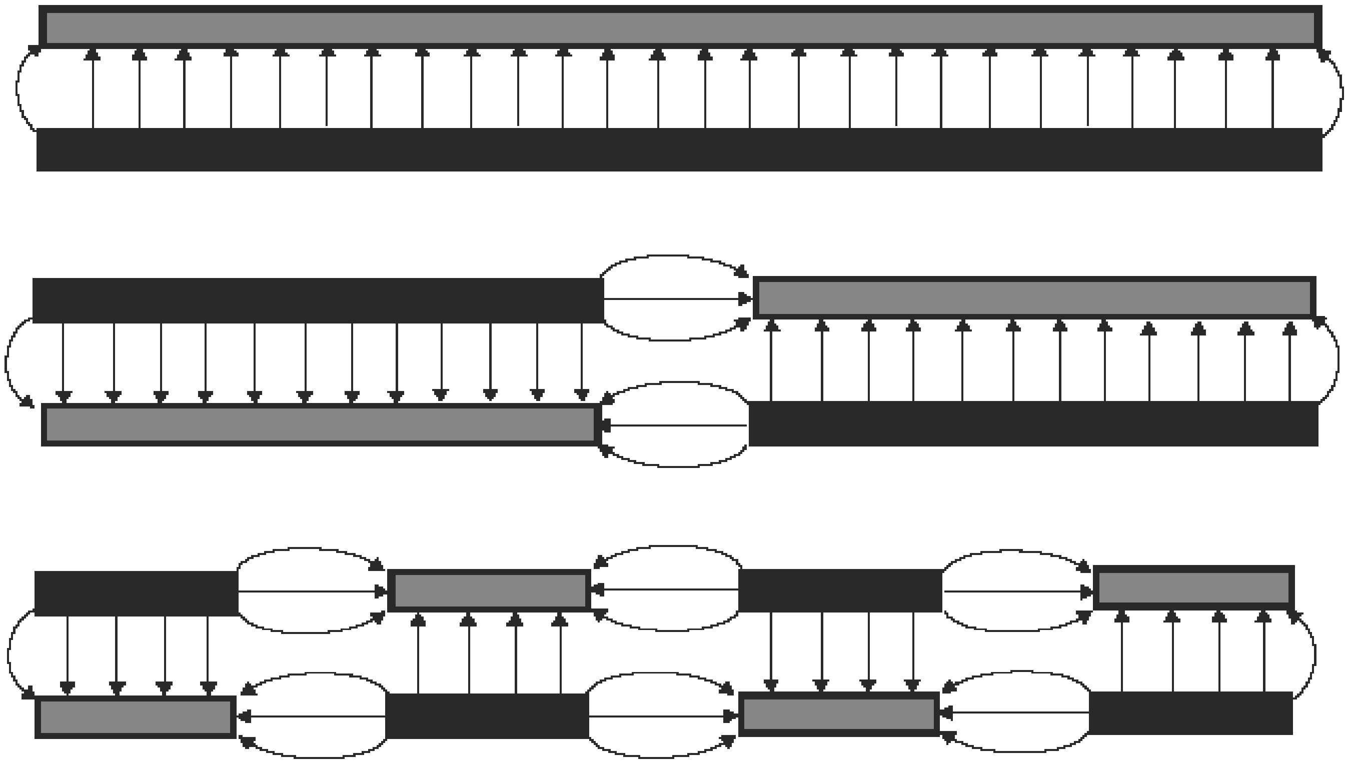

Scaling

- Unlike conventional parallel-plate structures, the capacitance per unit area increases as the process technologies scale.

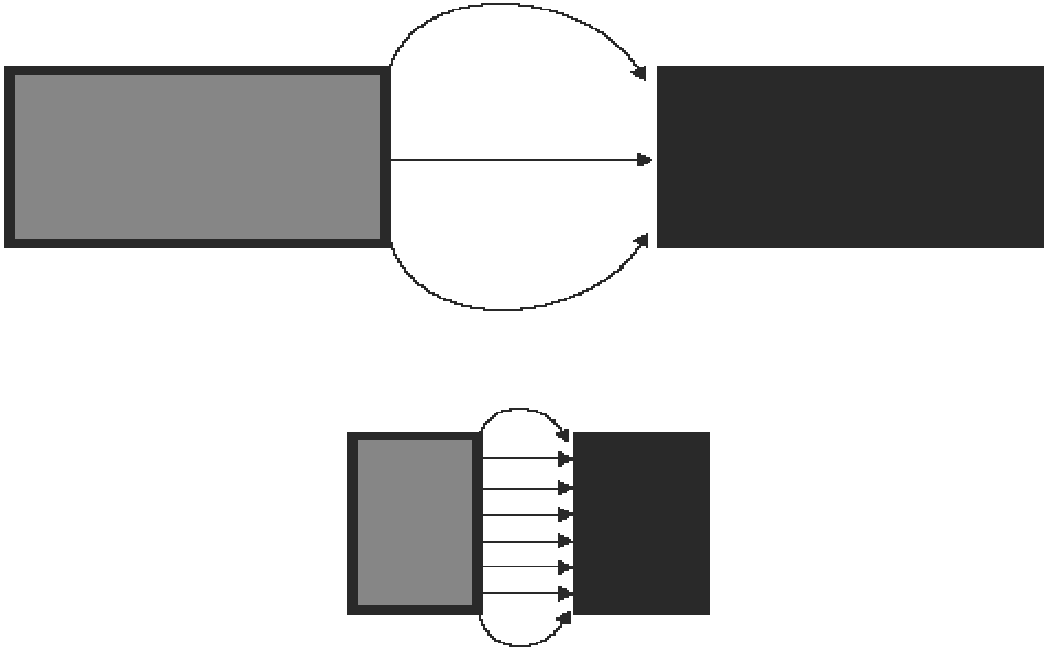

Manhattan capacitor structures

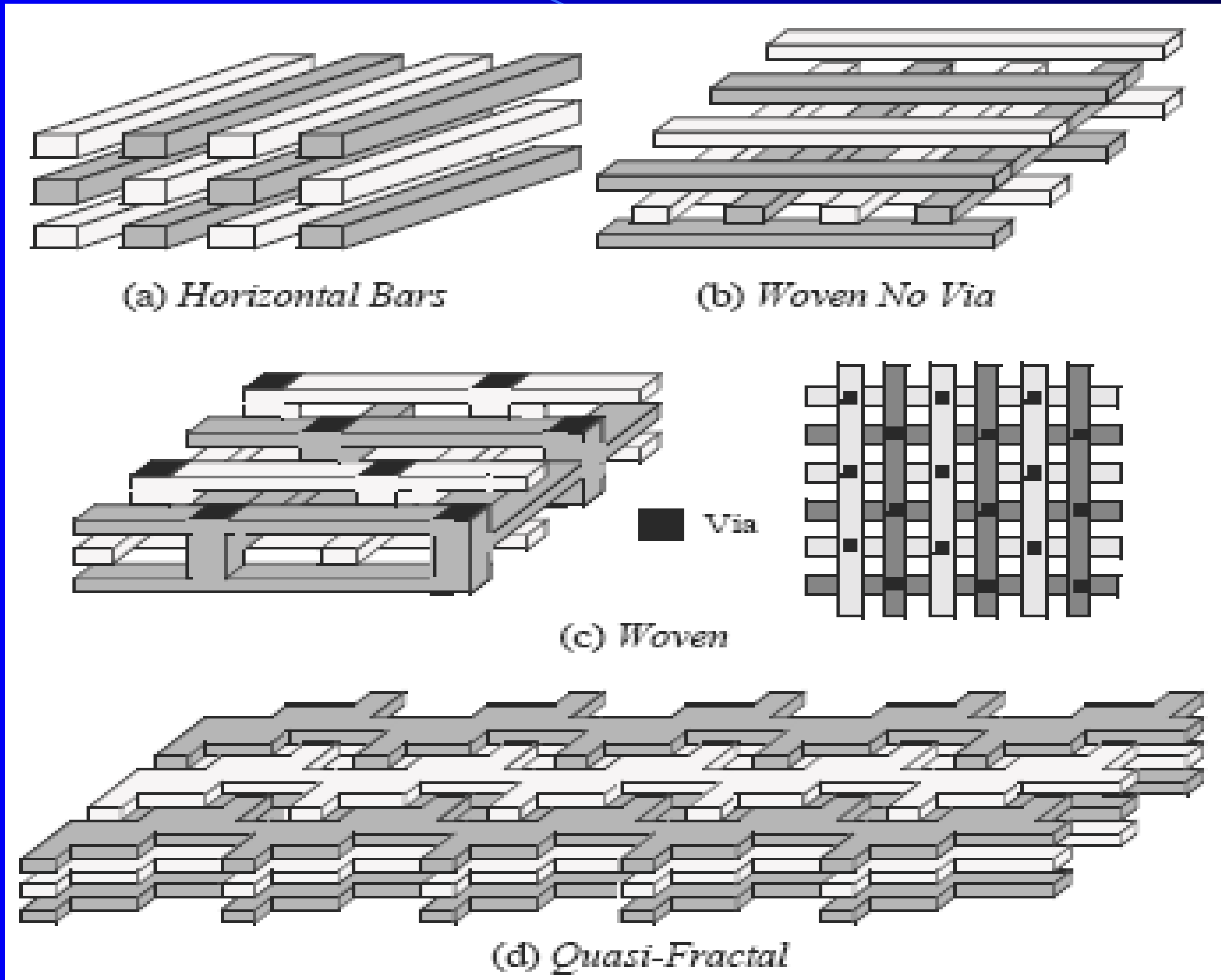

Fractal Capacitor

- Quasi fractal geometries can be utilized to increase capacitance per unit area.

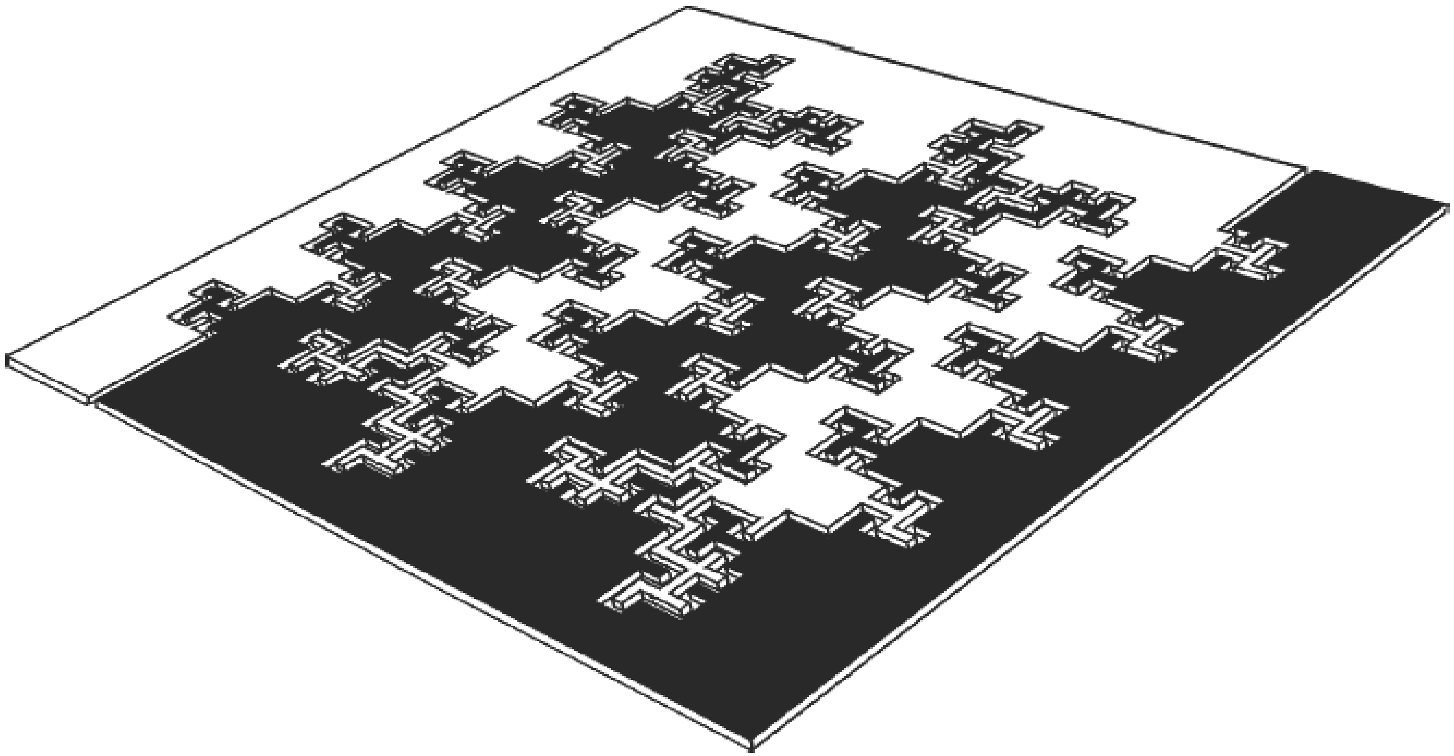

3-D representation of a fractal capacitor using a single metal layer.

Capacitance Estimation

$$C_{lateral} = K \frac{(\sqrt{A})^{D}}{(w+s)^{D-1}} \times t$$

- *w*: Minimum width of the metal.
- *s*: Minimum spacing between two adjacent strips.
- *A*: Area of the fractal capacitance.
- *t*: Thickness of the metal layers.
- *K*: Proportionality factor that depends on the family of fractals being used.
- *D*: Fractal dimension.

Boost Factor *vs.* Lateral Spacing

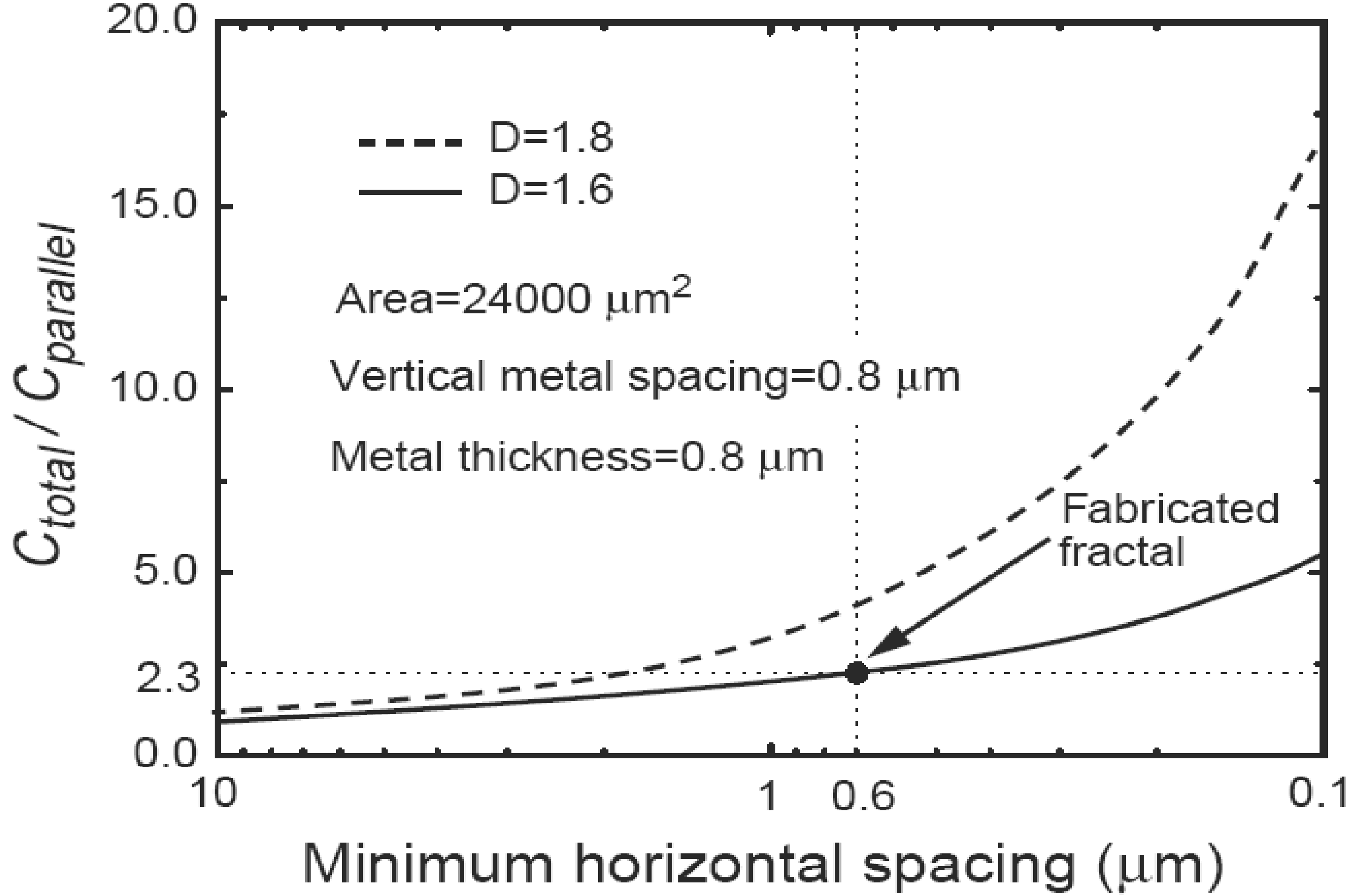

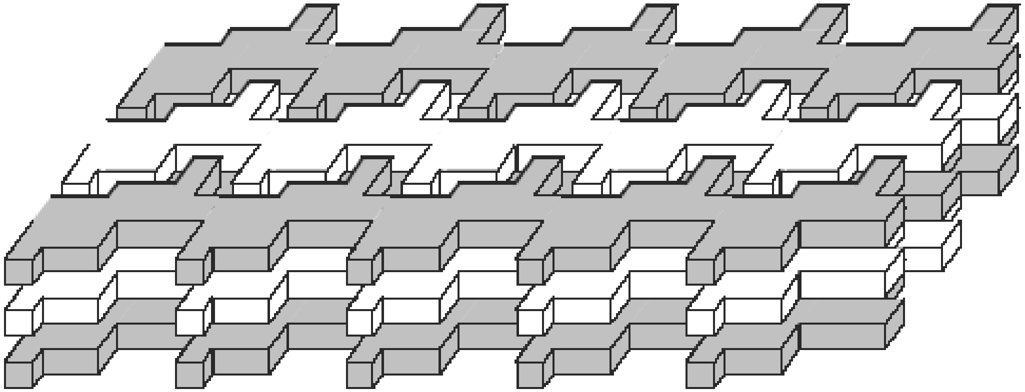

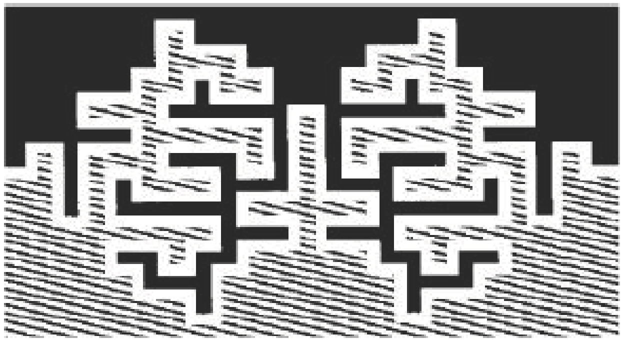

- Quasi-fractal structures maximize periphery to increase field usage,
- Have strong vertical *and* lateral components,
- Time consuming to generate and simulate,
- Look beautiful !

[Samavati, Hajimiri, Shahani, Nasserbakht, and Lee, ISSCC 1998]

Capacitance density comparison

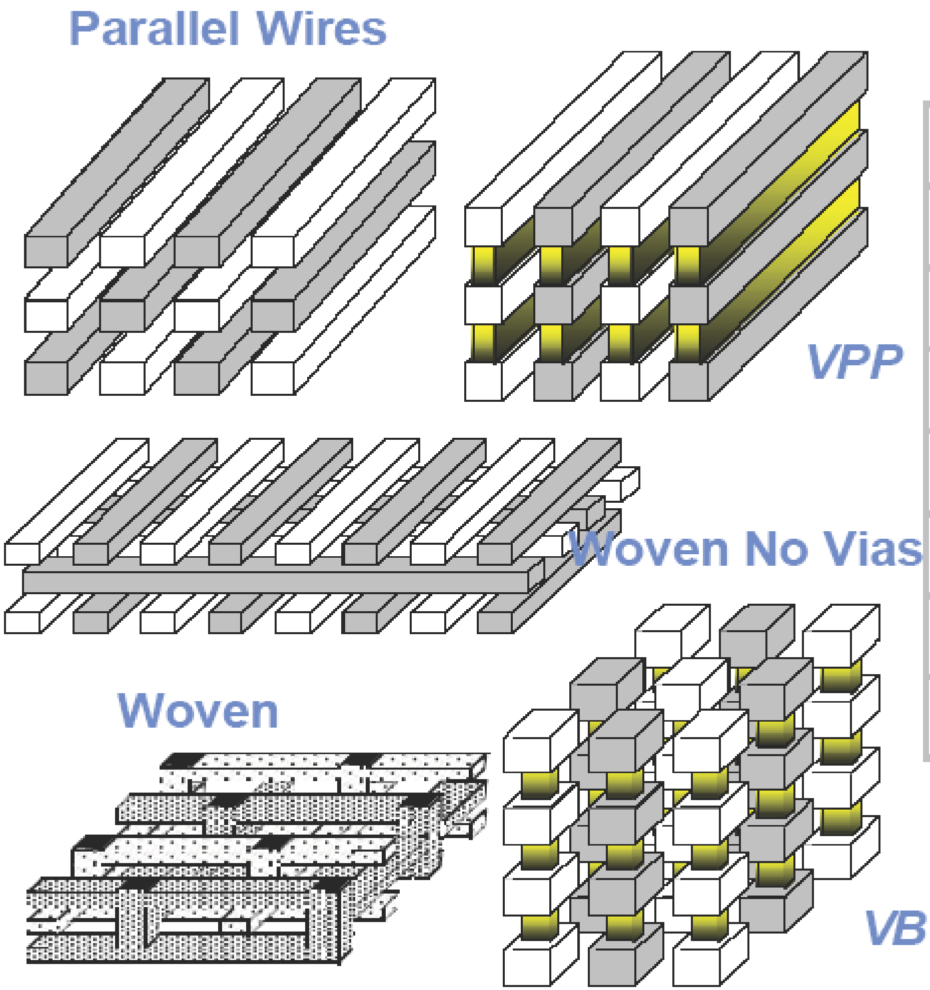

	% TL1	% TL2
Woven	37.0%	52.7%
Woven no Vias	28.3%	40.3%
Parallel Wires	28.3%	40.3%
Quasi-Fractal	17.9%	25.5%
Horizontal PP	0.8%	1.1%
Vertical PP	49.6%	70.7%
Vertical Bars	63.7%	90.8%

[Aparicio and Hajimiri, JSSC March 2002]

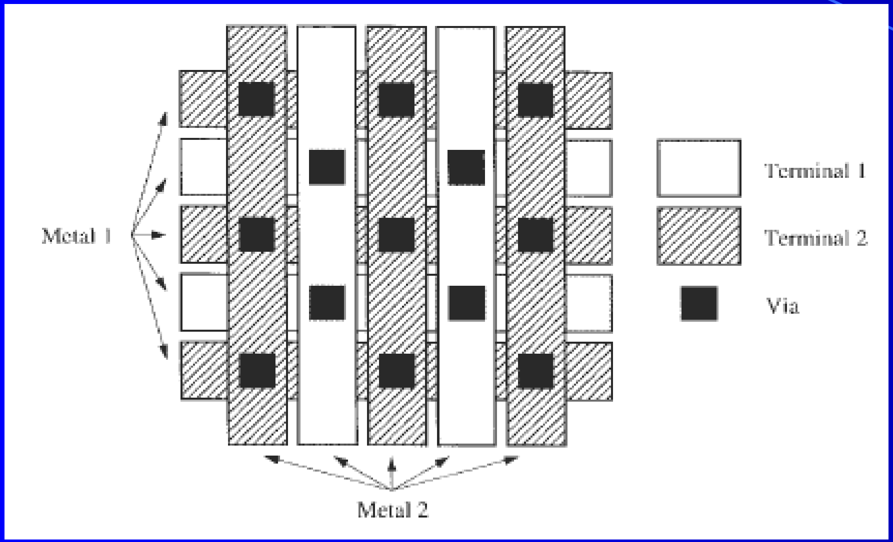
Terminal 1
Terminal 2
Via
Metal 1
Metal 2

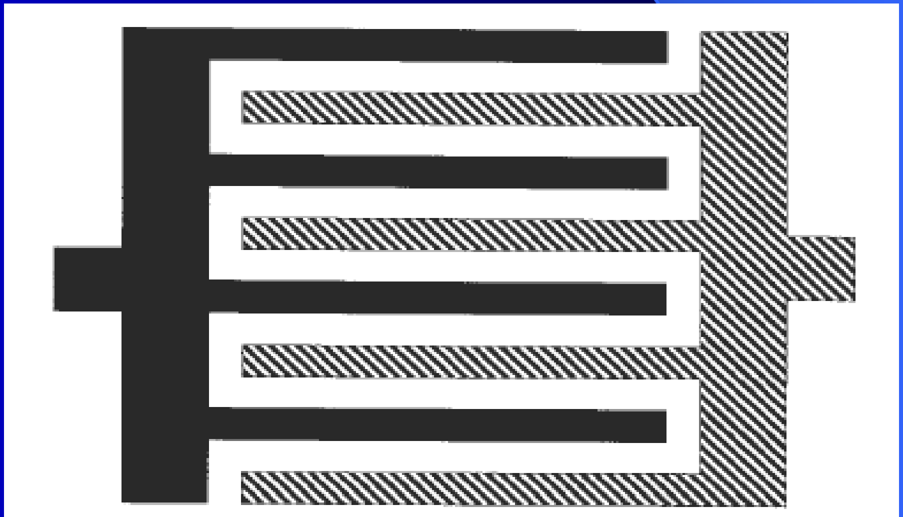

Measurement Summary

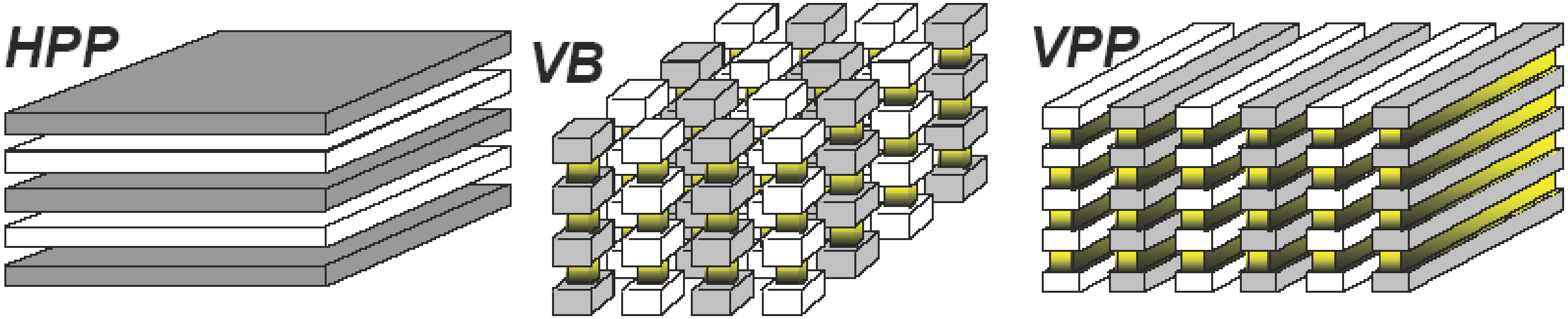

	HPP	VB	VPP	MIM 0.18μ
Average Cap. [pF]	1.095	1.076	1.013	1.057
Cap. Density [aF/μm^2]	203.6	1281.3	1512.2	1100
Cap. Enhancement	1	6.29	7.43	5.40
f_{res} [GHz]	21	37.1	40 <	11
Q (Measured) @1GHz	63.8	48.7	83.2	95

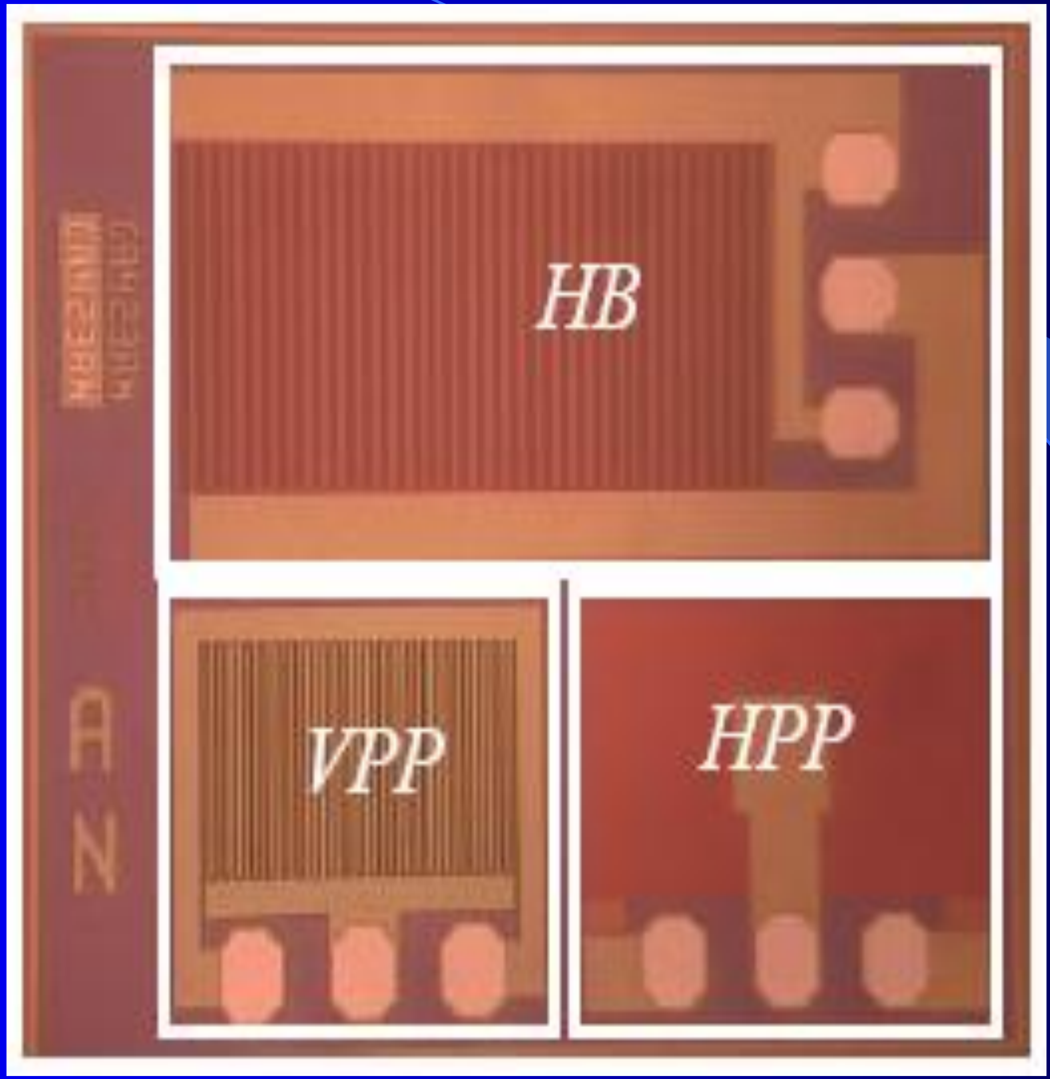
HB
VPP
HPP